

5-2017

A Mathematical Model of Remyelination in Multiple Sclerosis

Matthew J. McGuinness
College of William and Mary

Follow this and additional works at: <https://scholarworks.wm.edu/honorstheses>



Part of the [Computational Neuroscience Commons](#), and the [Nervous System Diseases Commons](#)

Recommended Citation

McGuinness, Matthew J., "A Mathematical Model of Remyelination in Multiple Sclerosis" (2017). *Undergraduate Honors Theses*. Paper 1114.
<https://scholarworks.wm.edu/honorstheses/1114>

This Honors Thesis is brought to you for free and open access by the Theses, Dissertations, & Master Projects at W&M ScholarWorks. It has been accepted for inclusion in Undergraduate Honors Theses by an authorized administrator of W&M ScholarWorks. For more information, please contact scholarworks@wm.edu.

A Mathematical Model of Remyelination in Multiple Sclerosis

A thesis submitted in partial fulfillment of the requirement
for the degree of Bachelor of Science in Neuroscience from
The College of William and Mary

by

Matthew Joseph McGuinness

Accepted for _____

Prof. Randolph Coleman, Director

Prof. Christine Porter

Prof. Sarah Day

Williamsburg, VA

May 1, 2017

Abstract

This project presents a mathematical model of the biochemical pathways involved in remyelination during multiple sclerosis. The model examines several major factors involved in remyelination and their expression over a course of time. This model also highlights processes which are targets for pharmaceutical treatment improving remyelination. The treatments examined include current treatments, drugs being examined for clinical trial, and theoretical treatments. Construction of the model is rooted in Biochemical Systems Theory (BST), which has been successfully applied in the past to examine the biochemistry of neurodegenerative disease. The model uses MATLAB as a means of coding the biochemical pathways into a system of ordinary differential equations (ODEs) producing a qualitative output. Use of MATLAB allows for a variety of treatment states, including use of drug cocktails or delayed onset of treatment.

1. Introduction

Multiple sclerosis (MS) is a neurodegenerative disorder characterized by substantial loss of the myelin sheath in the central nervous system (CNS), resulting in physical symptoms of pain, weakness, rigidity, and muscle paralysis. The loss of the myelin sheath, and the resulting symptoms of MS, begin with the death of oligodendrocytes (OL), cells whose primary purpose is the formation and maintenance of the myelin sheath. Loss of the myelin sheath can lead to oxidative stress of neurons and neurodegeneration. Despite this destruction, the CNS is able to regenerate certain amounts of myelin due to the presence of oligodendrocyte progenitor cells (OPCs), which may migrate to the site of MS lesions and differentiate into myelin forming oligodendrocytes, alleviating certain symptoms of the disease (Podbielska et al., 2013). The promotion of this differentiation involves receiving signals from neurons, immune cells, and

other glia. Once differentiated, cells will produce the components of myelin, including lipids and myelin proteins. This paper presents a mathematical model detailing the impact of signals received by OPCs and the downstream effect these signals have on transcription and translation of differentiation markers, as well as the resulting transcription and translation of myelin proteins.

Research into the causes of MS has led to multiple hypotheses about its origin, with emphasis on the roles of inflammation and the immune response as primary sources of demyelination.

Multiple sclerosis is therefore the most common autoimmune disorder affecting the CNS (Stadelmann, 2011). Patients with MS frequently present a relapsing-remitting course, in which subsequent immune and inflammatory attacks can cause further severe symptoms (Compston & Coles, 2002). Most pharmaceutical treatments focus on reducing the severity or frequency of immune system attack. Of these, the most well-known are the β -interferons (Podbielska et al., 2013). However, these treatments do not fully resist the disease and its symptoms, and research has shifted to searching for pharmaceutical targets which may promote remyelination (Kremer, Küry, & Dutta, 2015).

The model presented here utilizes Biochemical Systems Theory (BST), a mathematical modeling framework established by Savageu in 1969. BST has been utilized successfully to analyze a variety of neurodegenerative diseases including multiple sclerosis (Broome & Coleman, 2011; Braatz & Coleman, 2015). Ordinary differential equations (ODE) are used to model concentrations of species and reaction rates, in order to represent the progression of multiple sclerosis over time. The baseline model includes a healthy state and a disease state, and compares the success of remyelination in both states. The healthy state represents a system in which no demyelination takes place, while the disease state examines remyelination in the

presence of inflammatory demyelinating signals. The disease state is created by adding a trigger point, in this case demyelination, or by modifying concentrations of certain species to reflect evidence found in current research. In addition, various treatment states are presented. The treatment states mimic the mechanism of action of a known or theoretical treatment for MS, and are utilized both beginning at the onset of the disease and partway through progression, representing a delay in treatment during diagnosis. The treatments examined target key reactions in the pathology of MS, and aim to provide insight into their potential success outside of a BST model.

2. Methods

2.1 Pathways of OPC Differentiation

This section describes major pathways and contributing signals involved in the differentiation of oligodendrocyte progenitors into myelin generating oligodendrocytes. These pathways were represented visually using the program CellDesigner. In the accompanying models, arrows indicate transitions between species. Formation of complexes was considered reversible unless otherwise indicated. Modulation of reactions is represented with an open circle for catalysis and a hard edge for inhibition. A full version of the model may be found in the Appendix.

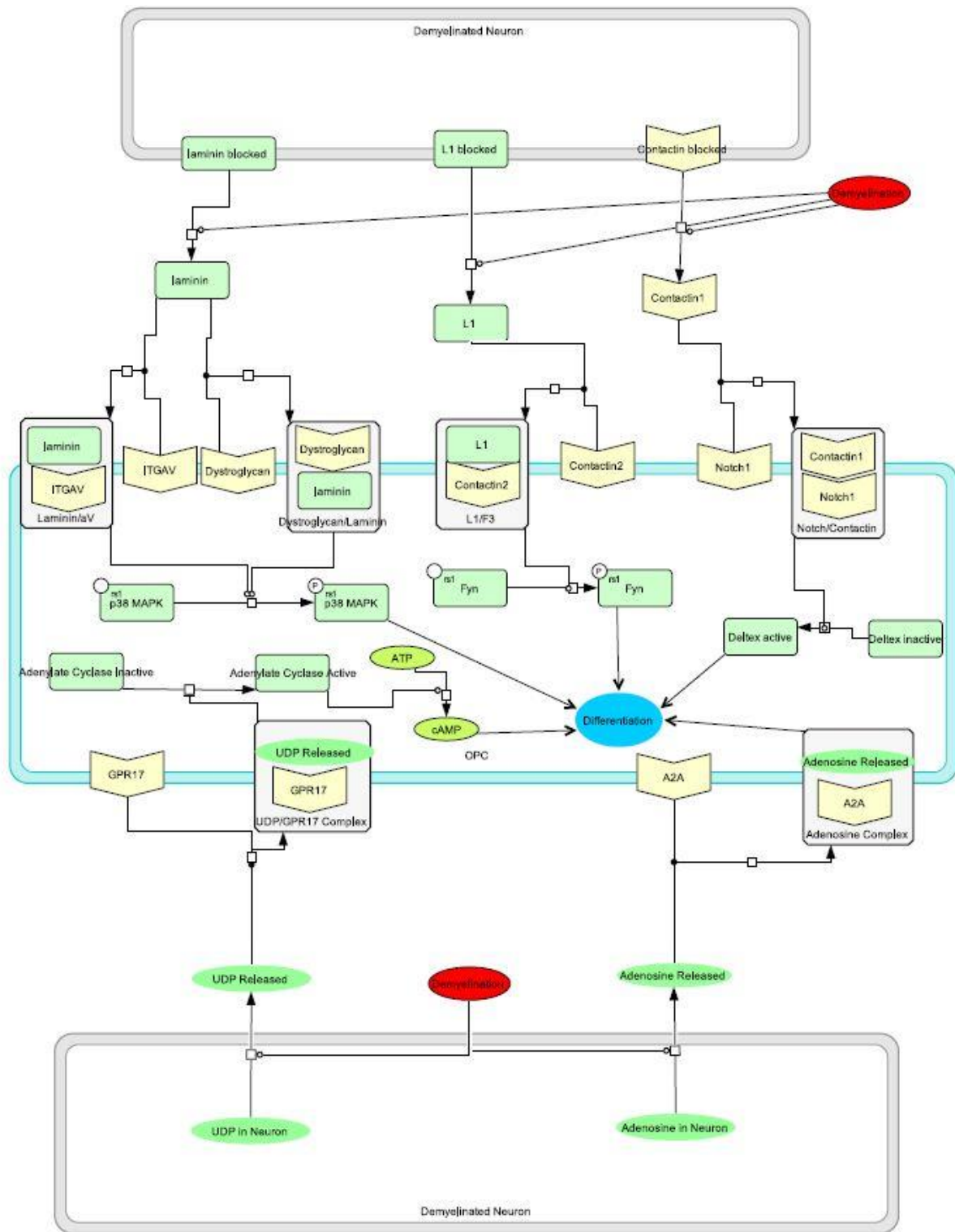
2.1.1 Important Markers of OPC Differentiation

This section focuses on a variety of contributors to differentiation of oligodendrocyte progenitors and the overall promotion of that differentiation. However, differentiation is not a step-by-step process, but a gradual transition that can be generally marked by increased expression of certain proteins. Among the most important of these are: oligodendrocyte transcription factor 2 (Olig2), Homeobox protein Nkx2.2, platelet derived growth factor receptor alpha (PDGFR α), neural/glial antigen 2 (NG2), oligodendrocyte marker 1 (O1), and oligodendrocyte marker 4 (O4) (Hu, Du, &

Zhang, 2009). These markers not only act as useful tools for researchers, but some play active roles in the processes outlined below.

2.1.2 Neuronal Contribution

The destruction of the myelin sheath reveals several proteins and receptors expressed by neurons that are not previously active or involved in signaling. These proteins may bind to receptors on other cells, most notably on OPCs, as shown in Model 1. Laminin proteins are expressed by the neuron, and upon removal of the myelin sheath may bind to different receptors. Laminins bind the Integrin alpha-V (ITGAV) receptor and activates p38 mitogen-activated protein kinase (p38 MAPK) signaling, promoting OPC differentiation (Podbielska et al, 2013; Zhao et al., 2009). Laminins may also bind the dystroglycan receptor, activating p38 MAPK signaling (Galvin, Eyermann, & Colognato, 2010). L1 cell adhesion molecule (L1) from the neuron binds to Contactin 2 on the OPC and activate the selective phosphorylation of Fyn kinase, promoting differentiation (Podbielska et al., 2013). Contactin 1 of the neuron will also be revealed and activate a Notch signaling pathway which activates deltex 1 in the OPC, encouraging differentiation (Podbielska et al., 2013). Neurodegeneration will also lead to a release of purinergic signals from neurons. Adenosine has been shown to activate OPC differentiation, while uridine diphosphate (UDP), acting at the cysteinyl leukotriene receptor (GPR17), inhibits adenylate cyclase causing downstream inhibition of differentiation (Fumagalli, Lecca, & Abbracchio, 2016).



Model 1: Signals from demyelinated neurons affecting OPC differentiation

2.1.3 Astrocytic Contribution

Another chief source of intercellular signals related to OPC differentiation comes from a second type of glial cell, astrocytes. Model 2 shows all major products of astrocytes important in this differentiation. The first product, endothelin 1 (ET-1) shows increased expression in astrocytes following demyelination and in turn stimulates astrocytic expression of Jagged1 (Hammond et al., 2014). Jagged1 activates a Notch signaling pathway in the OPC which inhibits differentiation, but promotes OPC migration to the site of lesion (Brosnan & John, 2009).

A second signal produced by the astrocyte which activates signals for OPCs is ciliary neurotrophic factor (CNTF). Interleukin-1 beta (IL-1 β), which is present in lesions following demyelination, is found to increase astrocytic expression of CNTF, and CNTF in turn promotes astrocytic expression of fibroblast growth factor 2 (FGF-2) as well as expression of fibroblast growth factor receptor 1 (FGFR1) by the OPC (Moore et al., 2011; Albrecht et al., 2003). Directly on the OPC, CNTF activates glycoprotein 130 receptor tyrosine kinase (gp130), promoting Janus kinase 2 (JAK2) and signal transducer and activator of transcription 3 (STAT3) signaling and OPC differentiation (Steelman et al., 2016). FGF-2 has been shown to inhibit OPC differentiation upon binding FGFR1 on the OPC (Murtie et al., 2005).

A third signal, Tenascin C (TnC), is expressed by the astrocyte and acts on the OPC. TnC binds to ITGAV, activating p38 MAPK signaling (Zhao et al., 2009). Another signal, platelet derived growth factor (PDGF) is expressed to module OPC differentiation. Acting as a receptor tyrosine kinase, the PDGFR α expressed by the OPC inhibits differentiation by promoting the cell proliferation pathways, while also encouraging differentiation through the activation of protein kinase B (Akt) pathways (Murtie et al., 2005; McKinnon, Waldrin, & Kiel, 2005). The presence of tumor necrosis factor alpha (TNF α) in lesions following demyelination activates nuclear

factor kappa-light-chain-enhancer of activated B cells (NF- κ B) in the astrocyte, which promotes the expression of two more signaling molecules: CXCL12 and LIF (Patel et al., 2012; Fischer et al., 2014.) C-X-C motif chemokine 12 (CXCL12) inhibits differentiation upon binding the C-X-C motif chemokine receptor 4 (CXCR4) receptor on the OPC (Patel et al., 2012). Leukemia inhibitory factor (LIF), similar to CNTF, binds gp130 and promotes JAK/STAT signaling leading to differentiation (Steelman et al., 2016).

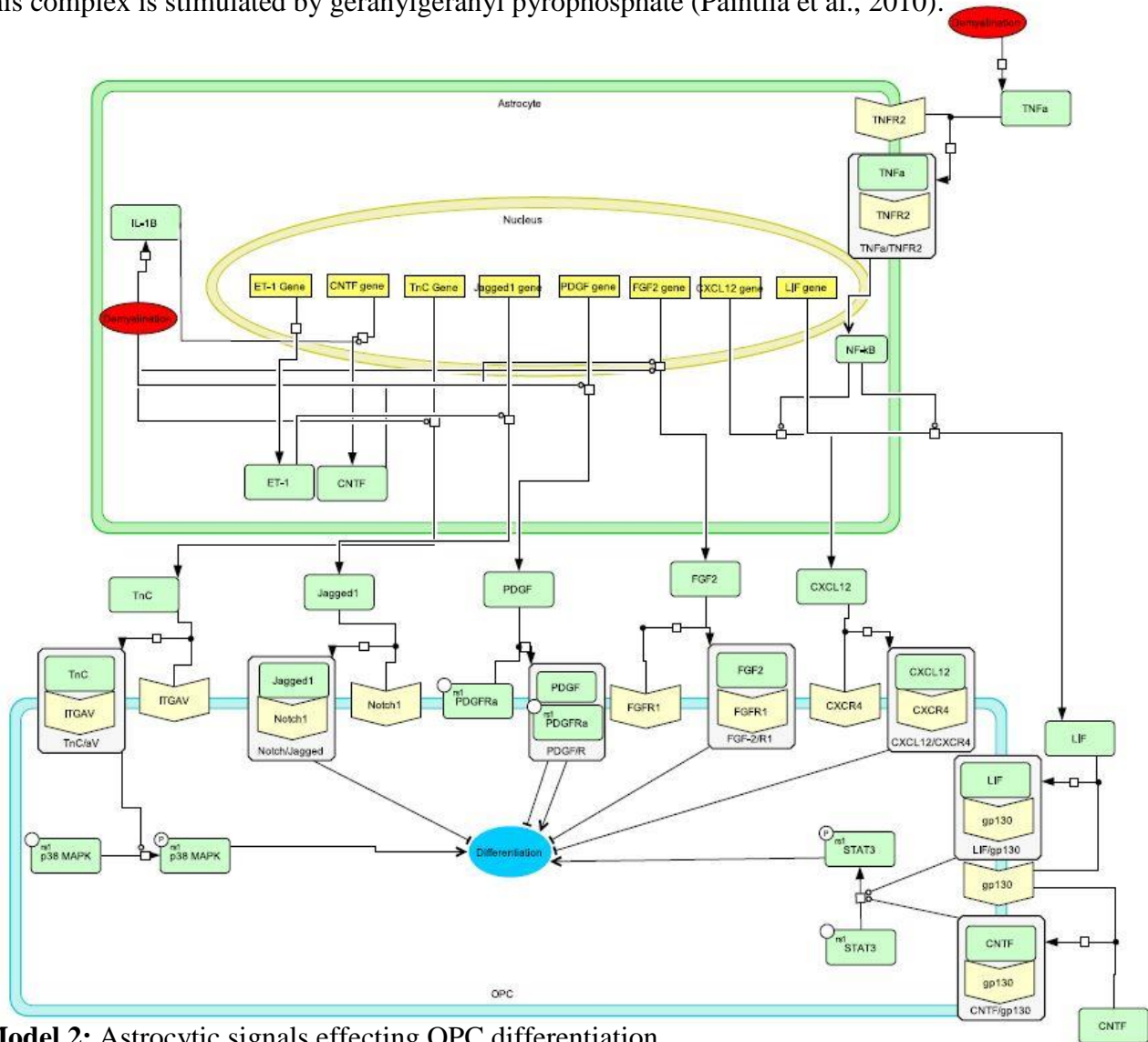
2.1.4 Immune Contribution

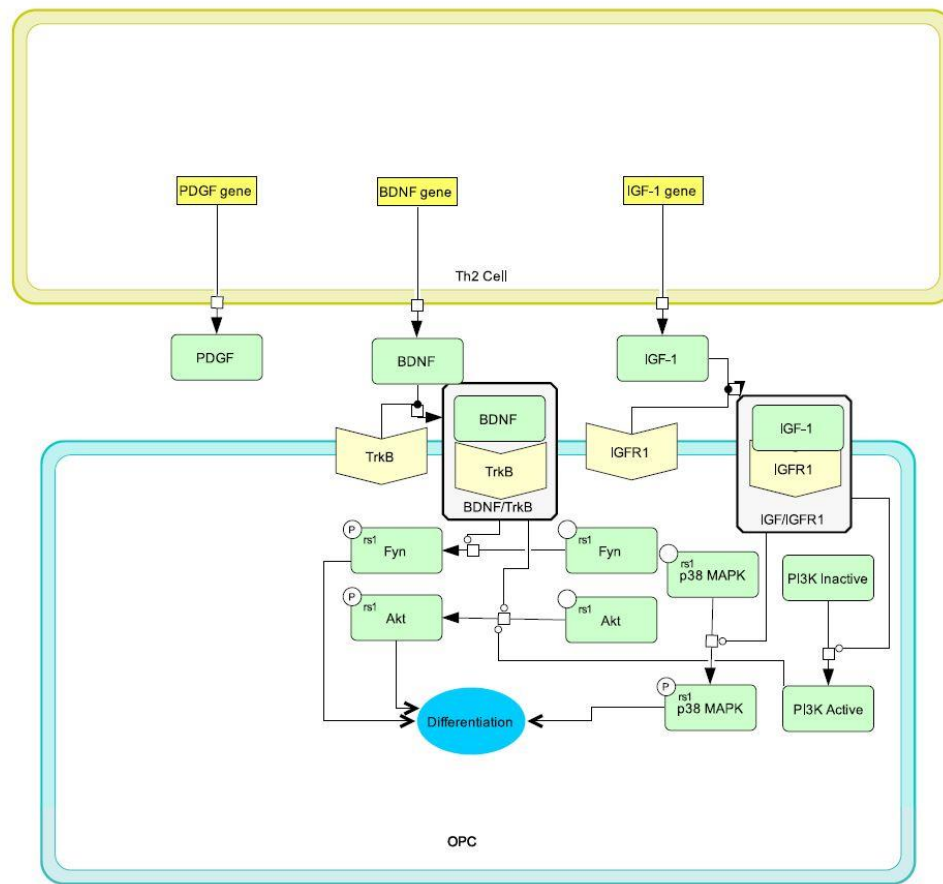
Model 3 outlines signals received by the OPC from a T helper 2 cell. The role of the immune system in MS has become increasingly more clear, and these signals demonstrate the immune system's minor role in remyelination. PDGF is released from these Th2 helpers and is able to act on the OPC through the same mechanism as when released by an astrocyte (Skihar et al., 2009). Brain derived neurotrophic factor (BDNF) is released and acts on the OPC at the tropomyosin receptor kinase B (TrkB) to promote differentiation by activating Fyn kinase and Akt (Skihar et al., 2009; Peckham et al., 2016). Insulin-like growth factor 1 (IGF-1) released by the Th2 helper cell binds the insulin-like growth factor receptor 1 (IGFR1) on the OPC to activate the p38 MAPK pathway and activate phosphoinositide 3-kinase (PI3K), which further activates Akt (Mason et al., 2003).

2.1.5 LINGO-1 Receptor Activation

An important neuronal contributor worthy of mentioning independent of other signals is the leucine rich repeat and immunoglobulin-like domain-containing protein 1 (LINGO-1) (Model 4). Like other neuronal signals, it is able to interact with the OPC upon significant demyelination. LINGO-1 has been shown to inhibit axonal regeneration in multiple CNS disorders (Podbielska et al., 2013). In MS, it has been repeatedly shown to inhibit OPC differentiation, and is a major

target for potential pharmaceutical treatment (Jepson et al., 2012; Mi, Pepinsky, & Cadavid, 2013). LINGO-1 binds to the receptor tyrosine-protein kinase erbB-2 (Erb2) on the OPC and exerts two main effects. The first is an inhibition of the binding of BDNF to TrkB (Mi, Pepinsky, & Cadavid, 2013). The second is an activation of Ras homolog gene family member A (RhoA) signaling, which has been shown to interact with Rho-associated protein kinase (ROCK) and inhibit p38 MAPK signals, as well as stop inhibit the transcription of phosphatase and tensin homolog (PTEN) (Baer et al., 2009; Paintlia et al., 2010; Jepson et al., 2012). The formation of this complex is stimulated by geranylgeranyl pyrophosphate (Paintlia et al., 2010).



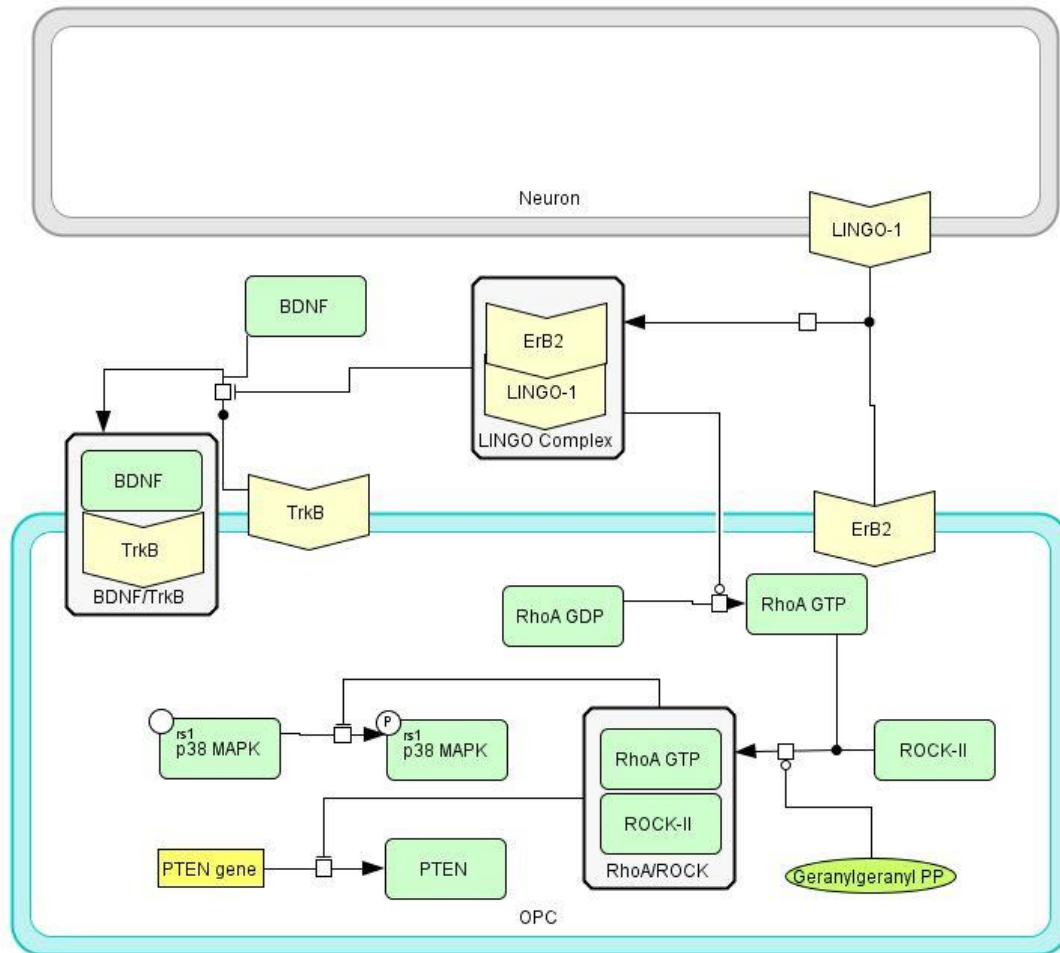


Model 3: Th2 Helper cell signals effecting OPC differentiation

2.1.6 Role of Muscarinic Acetylcholine Receptors

Neurodegeneration may lead to release of neurotransmitter in the site of lesions. For this reason, muscarinic acetylcholine receptors expressed by OPCs play a major role in the differentiation of OPCs, as well as in remyelination itself. Model 5 shows the processes effected by the binding of acetylcholine to different muscarinic receptor subtypes. Expression of PDFR α and Notch1 is increased by binding at the M3 and M4 receptors (De Angelis et al., 2011). Transcription of myelin basic protein (MBP), a major component of the myelin sheath, is upregulated by binding at the M1 and M3 subtypes (De Angelis et al., 2011). Formation of cyclic adenosine

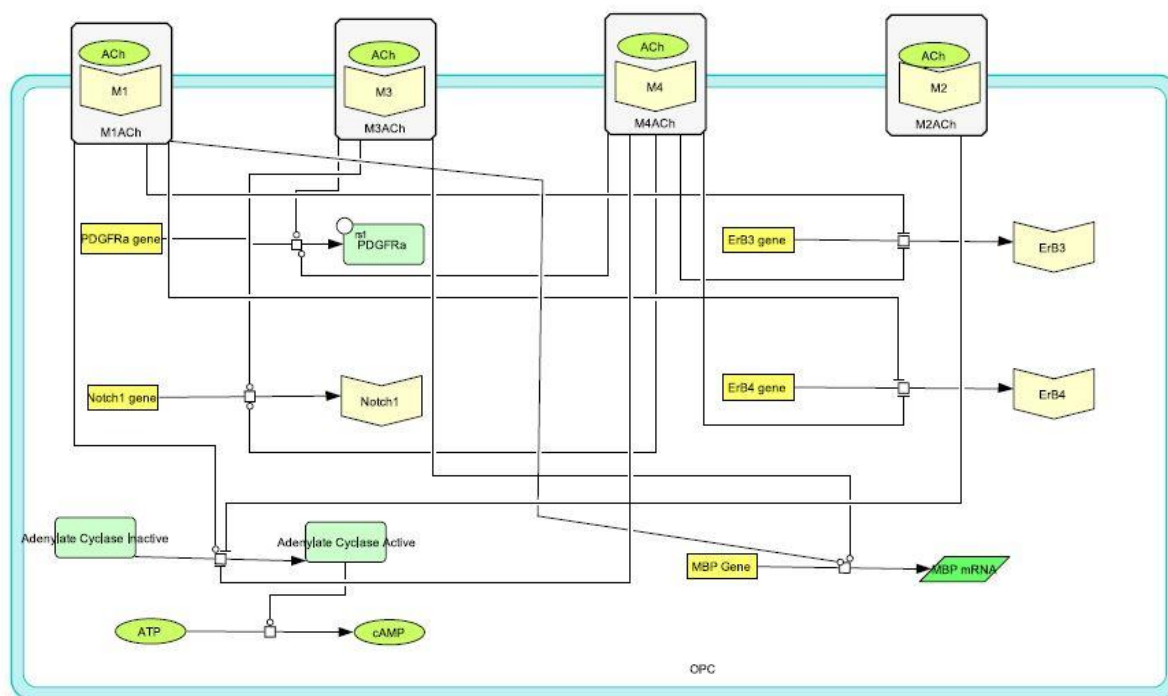
monophosphate (cAMP) is upregulated by binding at the M1 subtype through activation of adenylate cyclase, but inhibited by binding at the M2 and M4 receptors (De Angelis et al., 2011).



Model 4: LINGO-1 Signaling on the OPC

cAMP activates protein kinase A (PKA) which phosphorylates extracellular signal-regulated kinases (ERK) to encourage differentiation (Medina-Rodriguez et al., 2013). Binding of acetylcholine at the M1 and M4 receptors inhibits expression of receptor tyrosine-protein kinase erbB-3 (ErB3) and receptor tyrosine-protein kinase erbB-4 (ErB4) which activate PI3K in the presence of neuregulin 1 (NRG1) type III, a growth factor (De Angelis et al., 2011; Taveggia et

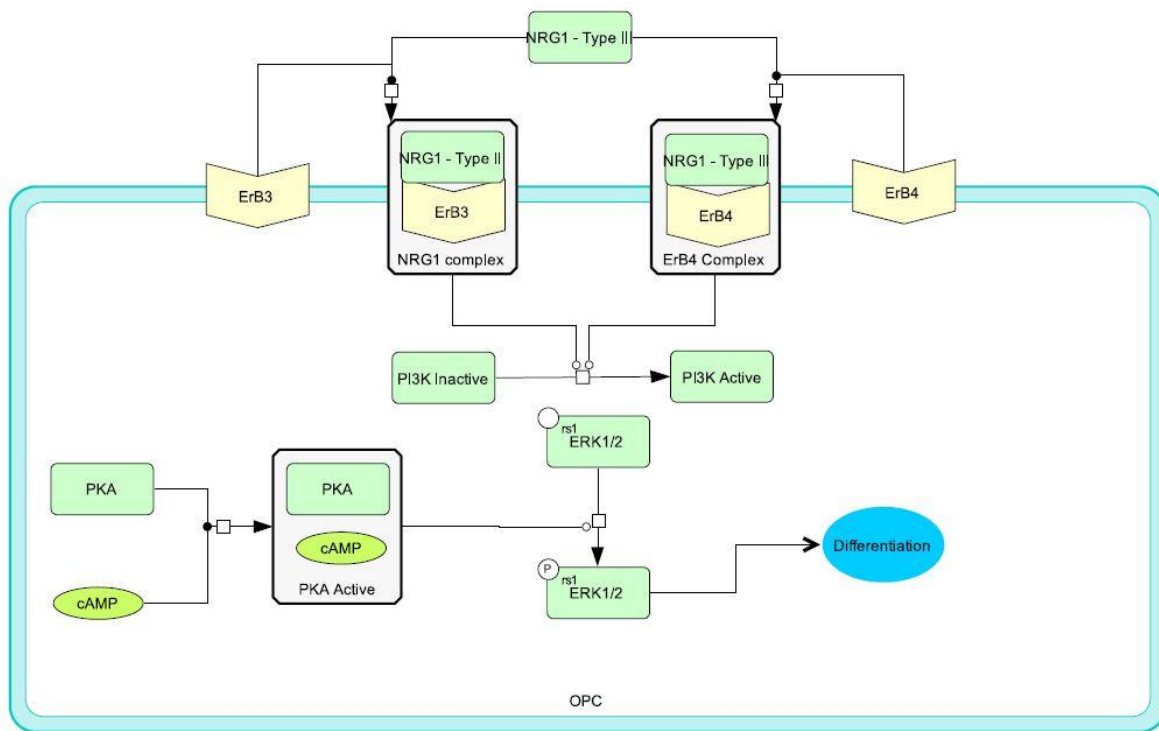
al., 2008). Model 6 demonstrates the downstream effects of the relevant receptors and signals regulated by the muscarinic acetylcholine receptors.



Model 5: Signals modulated by muscarinic acetylcholine receptors

2.1.7 Role of Vitamin A

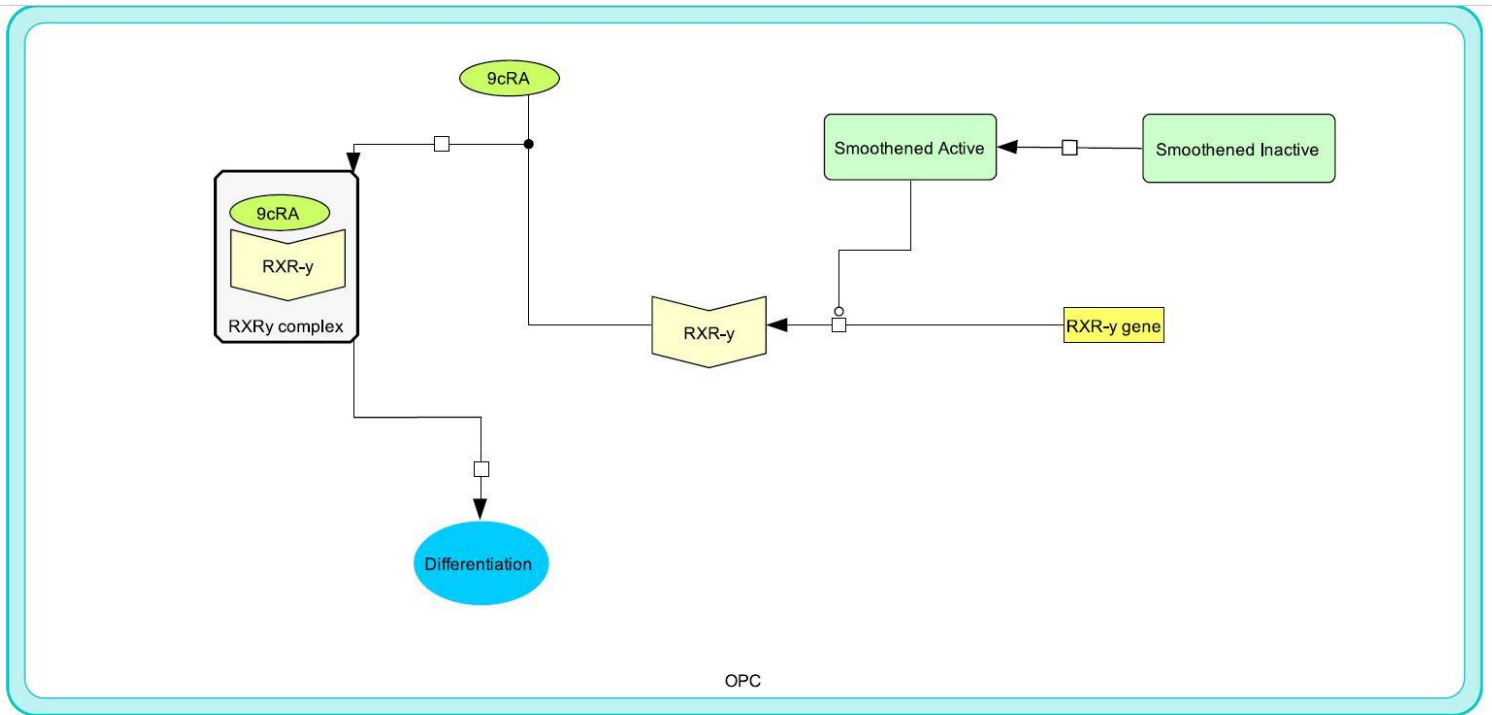
Evidence points to the role of several vitamins, primarily vitamin D, in the biochemistry of MS (Ascherio, Munger, & Simon, 2010). Another vitamin, vitamin A, plays a small role in remyelination. Vitamin A's derived metabolite, 9-cis-retinoic acid (9cRA), is an agonist of the retinoid X receptor gamma (RXR γ). Activation of RXR γ has been shown to lead to an increase in OPC differentiation (Huang et al., 2010). This pathway, outlined in Model 7, is of pharmaceutical interest, as the activation of the smoothened receptor (SMO) on the OPC leads to upregulation of RXR γ (Porcu et al., 2015).



Model 6: Downstream effects of signals regulated by muscarinic acetylcholine receptors

2.1.8 Major Cell Signaling Pathways and Transcription Factors Activated

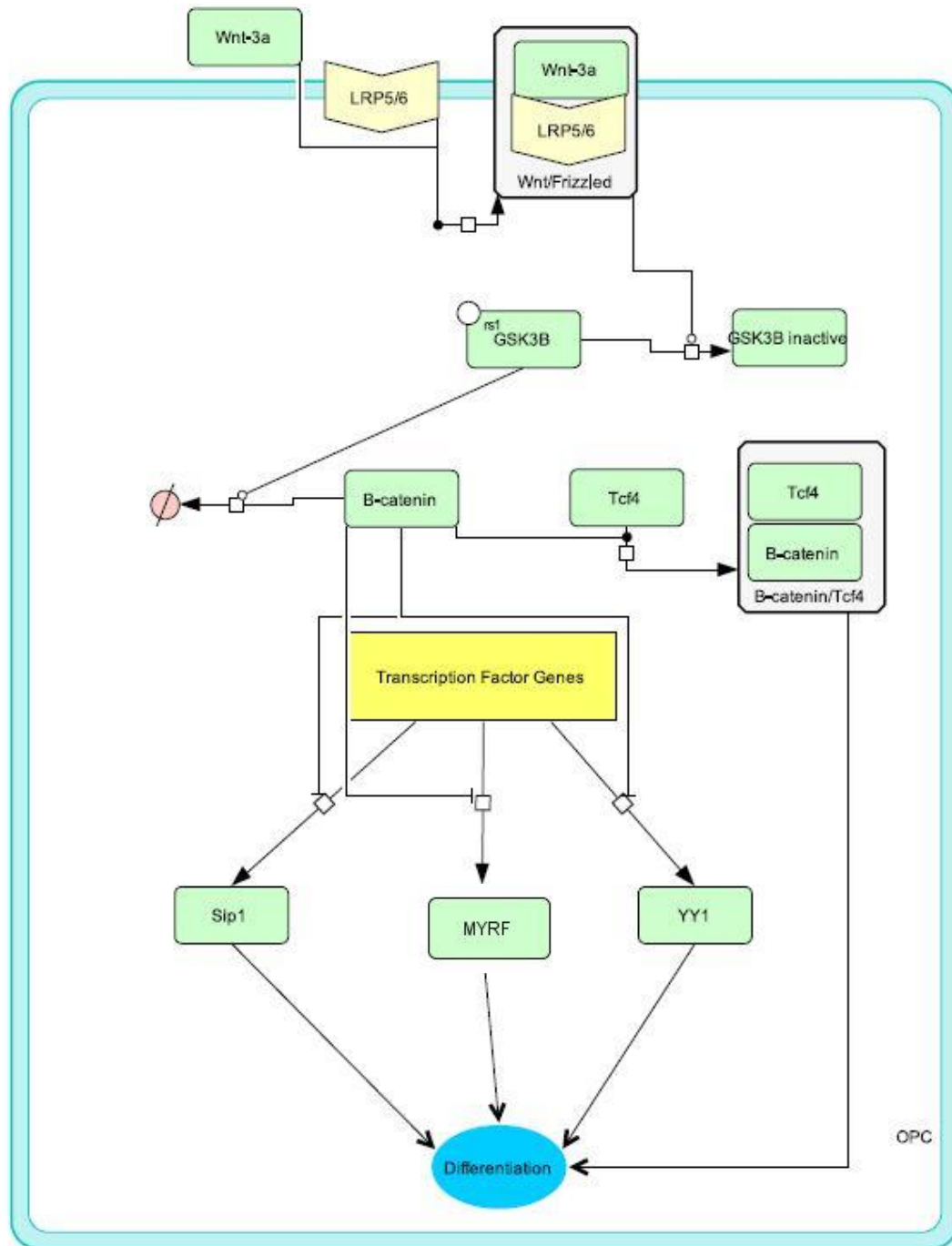
The next section outlines the common intracellular signaling pathways as they directly impact OPC differentiation. The end result of these pathways is the activation of major transcription factors directly involved in proteins responsible for the differentiation of OPCs. These pathways are activated or inhibited by multiple signals impacting the OPC as described in the above sections.



Model 7: Vitamin A metabolite in OPC Differentiation

2.1.8.1 Wnt Signaling Pathway

Protein Wnt-3a (Wnt-3a), found in MS lesions, begins an important intracellular signaling pathway in the OPC by binding to low-density lipoprotein related receptor proteins (LRP) 5 and 6, members of the Frizzled family of receptors, to inactivate glycogen synthase kinase 3 beta (GSK3 β) (Preisner et al, 2015; Xie et al., 2014) (Model 8). The active form of GSK3 β helps degrade β -catenin, a protein which inhibits the production of several important transcription factors, including zinc finger E-box-binding homeobox 2 (SIP1), myelin regulatory factor (MYRF), and yin-yang 1 (YY1), all of which are involved in OPC differentiation (Zhou et al., 2014). However, β -catenin also works with transcription factor 4 (Tcf4) through an unknown mechanism to encourage OPC differentiation (Xie et al., 2014).

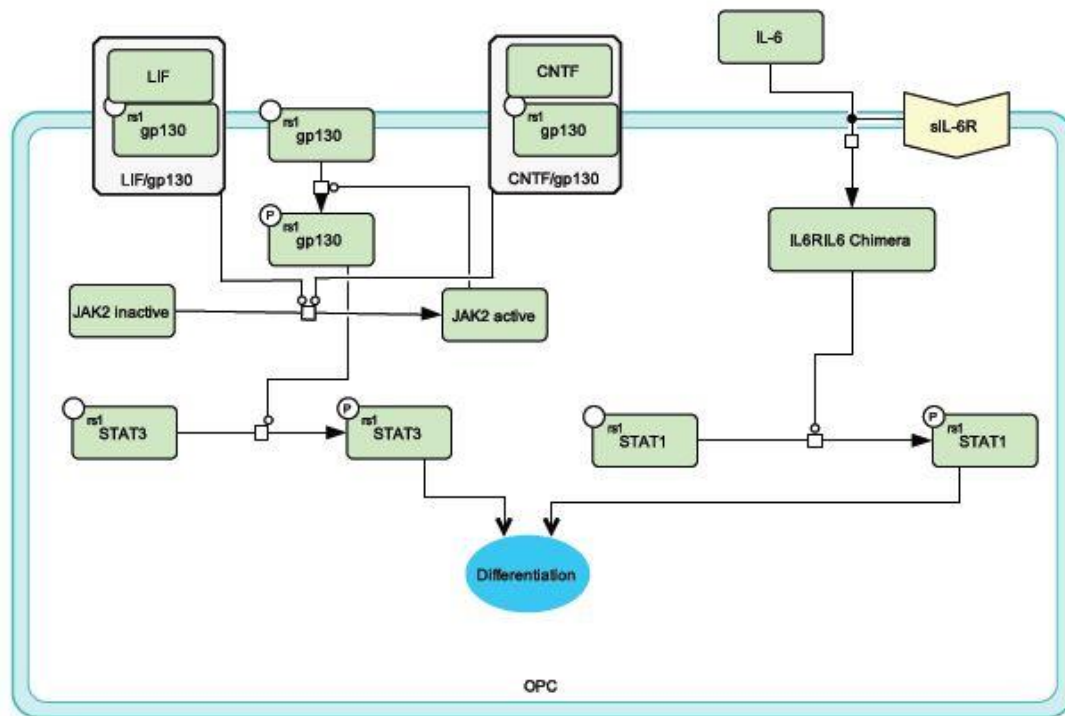


Model 8: Wnt signaling pathway in OPC

2.1.8.2 JAK/STAT Signaling

The specific actions of JAK/STAT pathways in a differentiating OPC are outlined in Model 9.

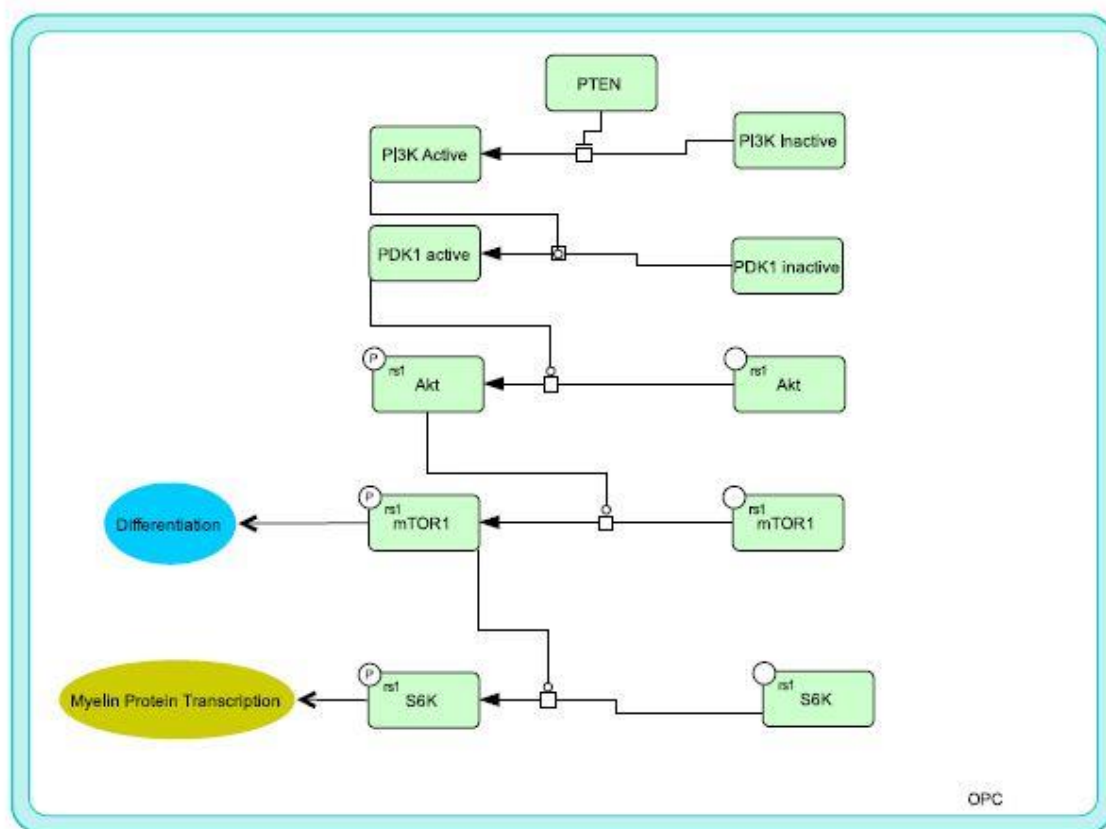
As outlined above, LIF and CNTF bind the gp130 receptor. This binding activates JAK2, which phosphorylates the gp130 receptor, leading to phosphorylation of STAT3, a key transcription factor involved in differentiation (Steelman et al., 2016). Another STAT pathway is activated by the presence of an interleukin found in MS lesions, IL-6. IL-6 binds to the soluble interleukin 6 receptor (sIL-6R) to form a chimeric protein which leads to phosphorylation and activation of STAT1, another transcription factor involved in OPC differentiation (Valerio et al., 2002).



Model 9: Activation of STAT transcription factors

2.1.8.3 Akt/mTOR Pathway

The molecular target of rapamycin (mTOR) is another vital transcription factor involved in the differentiation of OPCs and is activated through a phosphorylation cascade (Inoki et al., 2006) (Model 10). Activation of PI3K, inhibited by PTEN, leads to activation of 3-phosphoinositide dependent protein kinase-1 (PDK1) (McKinnon et al., 2005; Paintlia et al., 2010). PDK1 phosphorylates Akt, which subsequently phosphorylates mTOR to activate it (Lin et al., 2013; Luo et al., 2014). mTOR is also involved in activating the ribosomal protein s6 kinase beta-1 (S6K), which promotes the synthesis of myelin proteins (Michel et al., 2015).

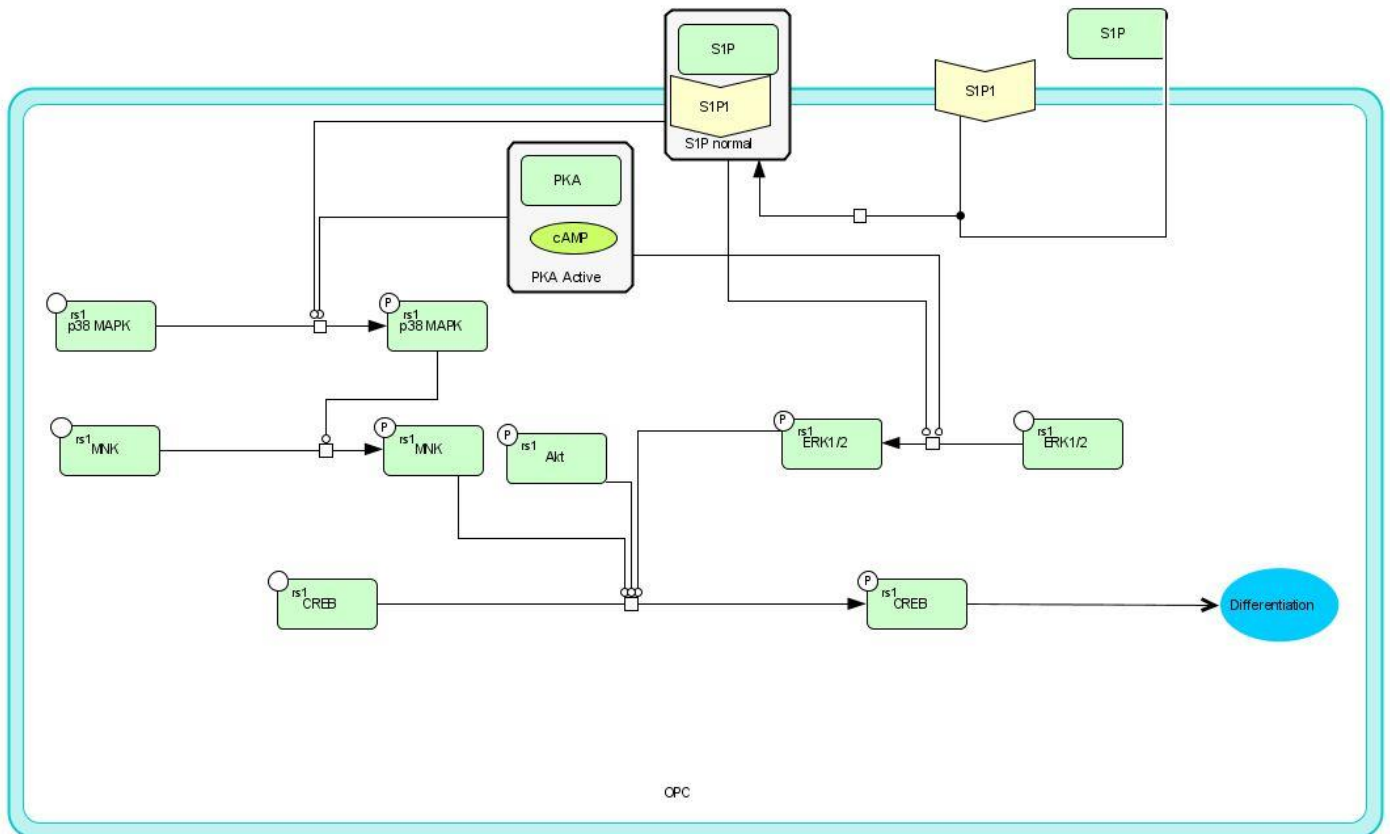


Model 10: Akt/mTOR signaling in the OPC

2.1.8.4 ERK, MAPK, and CREB

Phosphorylation of the cAMP response element-binding protein (CREB), an important transcription factor, is a key event in the differentiation of OPCs (Syed et al., 2013) (Model 11).

Three sources of phosphorylation are modeled for CREB in OPC differentiation. The first is the phosphorylation of p38 MAPK by signals mentioned above, including activated PKA, as well as sphingosine-1-phosphate (S1P) signaling (Cui, Fang, Kennedy, Almazan, & Antel, 2014). This phosphorylated p38 MAPK then phosphorylates MAP kinase-interacting serine/threonine-protein kinase (MNK), which phosphorylates CREB (Syed et al., 2013). The second signal is phosphorylation by activated Akt (Meffre et al., 2015). The third is activation by phosphorylated ERKs (Rodgers et al., 2015).



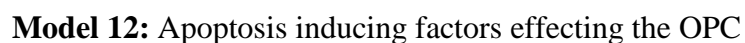
Model 11: Phosphorylation of CREB by multiple pathways

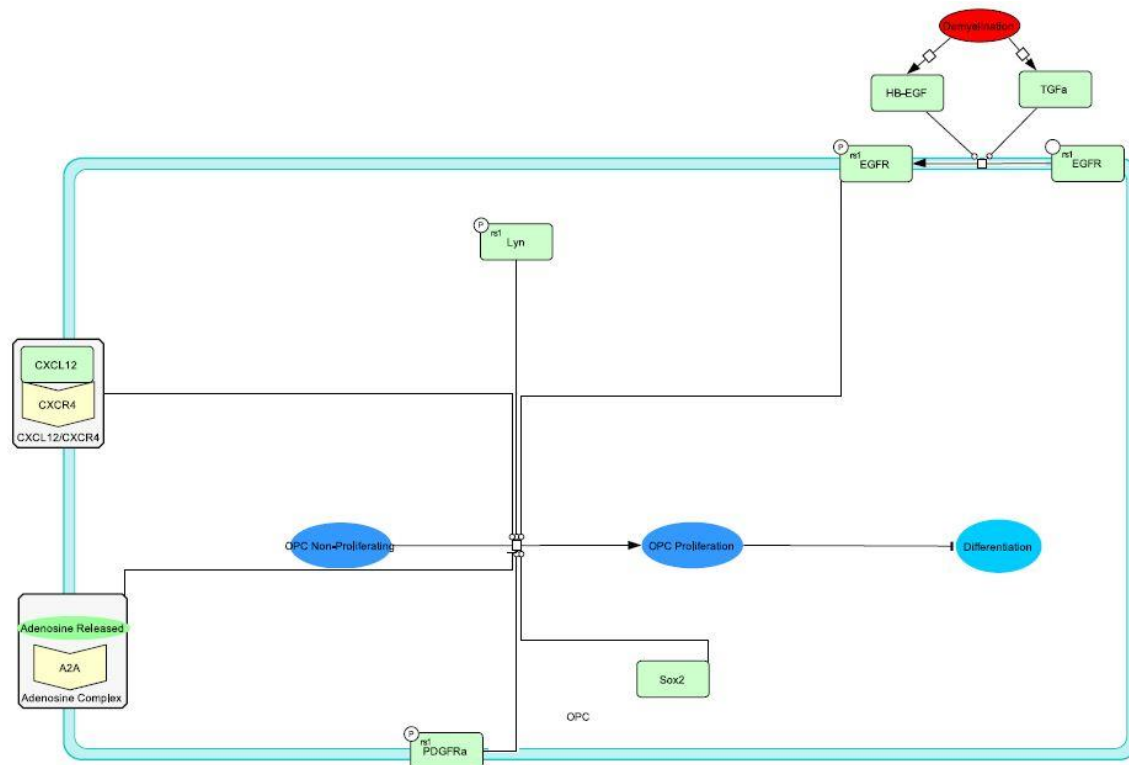
2.2 Apoptotic signals effecting OPCs

One reason remyelination in multiple sclerosis may fail is due to the death of OPCs. Model 12 outlines apoptotic signals received by the OPC. $\text{TNF}\alpha$, one of the main inflammatory signals found in MS, binds to death receptor 6 (DR6) on the OPC activating a caspase chain in which procaspase 8 is converted to caspase 8, which converts procaspase 3 to caspase 3 leading to apoptosis. This pathway is inhibited by the tyrosine-protein kinase Lyn (Mi et al., 2011). A second pathway, also inhibited by Lyn, but stimulated by apoptosis regulator Bax (Bax), is the release of cytochrome c (CytC) from the mitochondria into the cytoplasm. This release activates conversion of procaspase 9 to caspase 9, which may be phosphorylated and lead to apoptosis (Pang et al., 2007). Apoptosis is also directly stimulated by Bcl-2-associated death promoter (BAD). BAD is inhibited in this action by phosphorylation by Akt, or in binding to B-cell lymphoma 2 (Bcl-2) (Pang et al., 2007). Bcl-2 expression is increased by phosphorylated STAT3 (Steelman et al., 2016).

2.3 OPC Proliferation

An important part of remyelination not yet discussed is the proliferation of OPCs, or the expansion of the number of OPCs. In order for remyelination to be sustained, the pool of OPCs must remain active, especially if there is still potential for further attack by the immune system. However, OPC proliferation means continuation of the cell cycle by the OPC, preventing differentiation (Redwine et al., 1998; Murtie et al., 2004). For this reason, OPC proliferation may encourage remyelination over the long term, but inhibits remyelination in the short term. Because of the unclear extent to which OPC proliferation plays this dual role, it was considered primarily as an inhibitor of OPC differentiation. The signals involved in modulating OPC proliferation are shown in Model 13. Two signals, PDGF and CXCL12 have been described





Model 13: Factors encouraging OPC proliferation

2.4 OPC Migration

In addition to successful differentiation, OPCs must also be recruited to the site of the lesion for successful remyelination, in a process termed here as OPC migration. OPC migration is encouraged through multiple signals (Model 14). Binding of laminins will encourage the activation and complex formation of integrin-linked kinase (ILK) to members of the Parvin protein family, which play a role in binding actin (O' Meara et al., 2016). Fyn kinase may activate cyclin-dependent kinase 5 (Cdk5), leading to the phosphorylation of Wiskott-Alrich syndrome protein family member 2 (WAVE2), an important transcription factor for proteins binding actin (Miyamoto, Yamauchi, & Tanoue, 2008). Binding of glutamate, which may be present in the site of neurodegenerative lesions, to the *N*-methyl-D-aspartic acid (NMDA)

receptor leads to phosphorylation of T lymphoma invasion and metastasis 1 (Tiam1), a guanonucleotide exchange factor for Ras-related C3 botulinum toxin substrate 1 (Rac1), the activated form of which encourages OPC migration (Xiao et al., 2013). Finally, oligomers of hyaluronic acid (HA), binding to the CD44 antigen on OPCs has been shown to activate migration (Piao, Wang, & Duncan, 2013). HA has been shown to be prevalent in demyelinated lesions, especially in its high molecular weight (HMW) form and can act as an inhibitor of OPC differentiation (Back et al., 2005). HA interacts with myeloid differentiation primary response protein (MyD88) and Toll-like receptor 2 (TLR2) to inhibit OPC differentiation. The majority of HA acting in this signaling is produced when HMW-HA is broken down by the enzyme hyaluronidase to smaller HA subunits (Sloane et al., 2009).

2.5 Production of Myelin Components

The second focus of this model examines the production of proteins of the myelin sheath. There has not been substantial evidence that there is metabolic dysfunction in remyelination related to lipid catabolism (Wheeler et al., 2008; Podbielska et al., 2013). Of vital relevance is the need to transcribe and translate new proteins to support and maintain the new myelin sheath. The species representing OPC differentiation is modeled as catalyzing the production of these myelin proteins. There is evidence that remyelination follows similar pathways to that of developmental myelination (Miller & Mi, 2007; Fancy et al., 2011). For this reason, some evidence related to developmental myelination has been used to support the processes outlined here for remyelination.

2.5.1 MBP

MBP is the most studied of the myelin proteins, likely due to its role as the primary antigen in the immune response in MS (Tzakos et al., 2005). For this reason, MBP is the protein modeled in

expression of early growth response gene 2 (Egr2) which acts on the *MBP* gene (Cervellini et al., 2013). Transcription factors Olig1 and Sox10 work together to promote transcription of MBP (Li et al., 2007). Trans-acting transcription factor Sp5 (Sp5) acts to inhibit transcription of the gene (Xie, Li, & Zhang, 2014). Binding of bone morphogenic protein 4 (BMP4) released from neurons at its receptor (BMPR) has been shown to inhibit transcription of MBP and may inhibit OPC differentiation (Weng et al., 2012; Xie et al., 2014). Transcription factor Nkx2.2 has been shown to regulate the transcription of the *MBP* gene by recruiting a complex of histone deacetylase 1 (HDAC1) and paired amphipathic helix protein Sin3a (mSin3a), but is inhibited in this action by transcriptional activator protein Pur-alpha (Pur- α) (Wei, Miskimins, & Miskimins, 2005).

2.5.1.2 MBP mRNA Translocation

MBP mRNA packs into granules with all the necessary components for translation and translocates to the site of myelination before translation occurs (Müller et al., 2013). The factors assisting in this process are shown in Model 16. PDGF encourages this translocation through a still unknown mechanism (Amur-Umarjee, Schonmann, & Campagnoni, 1997). The granules travel along the microtubule network, and the microtubule associated protein tau (MAPt) is vital to the assembly of this network (Seiberlich et al., 2015). The movement along the microtubules is facilitated by kinesin motor protein Kif1b (Lyons et al., 2009). Finally, heterogeneous nuclear ribonucleoprotein A2 (hnRNP A2) is an essential trafficking factor that assists in the formation of the transport granules, and binds the mRNA to prevent translation until transport is complete (Francone et al., 2007; Müller et al., 2013). Small non-coding RNA 715 (sncRNA 715) has also been shown to inhibit translation of MBP mRNA until proper translocation is complete (Bauer et al., 2012).

2.5.1.3 MBP mRNA Translation

Translation of MBP is a highly regulated process (Model 17). Once localized to the site of myelination, translation is initiated by eukaryotic initiation factor 4e (eIF4e). eIF4e is inhibited by 4e binding protein 1 (4EBP1). The binding of neurotrophin-3 (NT-3) at the TrkC receptor activates p38 MAPK and Akt signaling, which leads to phosphorylation of both eIF4e and 4EBP1, allowing the former to initiate translation (Coelho et al., 2009). Ribosomal protein s6 (S6RP), a major protein of the ribosomal complex, is phosphorylated by S6 kinase (S6K) in response to ERK signaling, allowing for proper translation (Michel et al., 2015). As described previously, hnRNP A2 acts to repress translation until proper translocation of the mRNA, but this action is relieved when Fyn kinase phosphorylates hnRNP A2 (White et al., 2008). There is evidence that tumor overexpressed gene protein (TOG) assists in the alleviation of hnRNP A2 repression of translation (Francone et al., 2007).

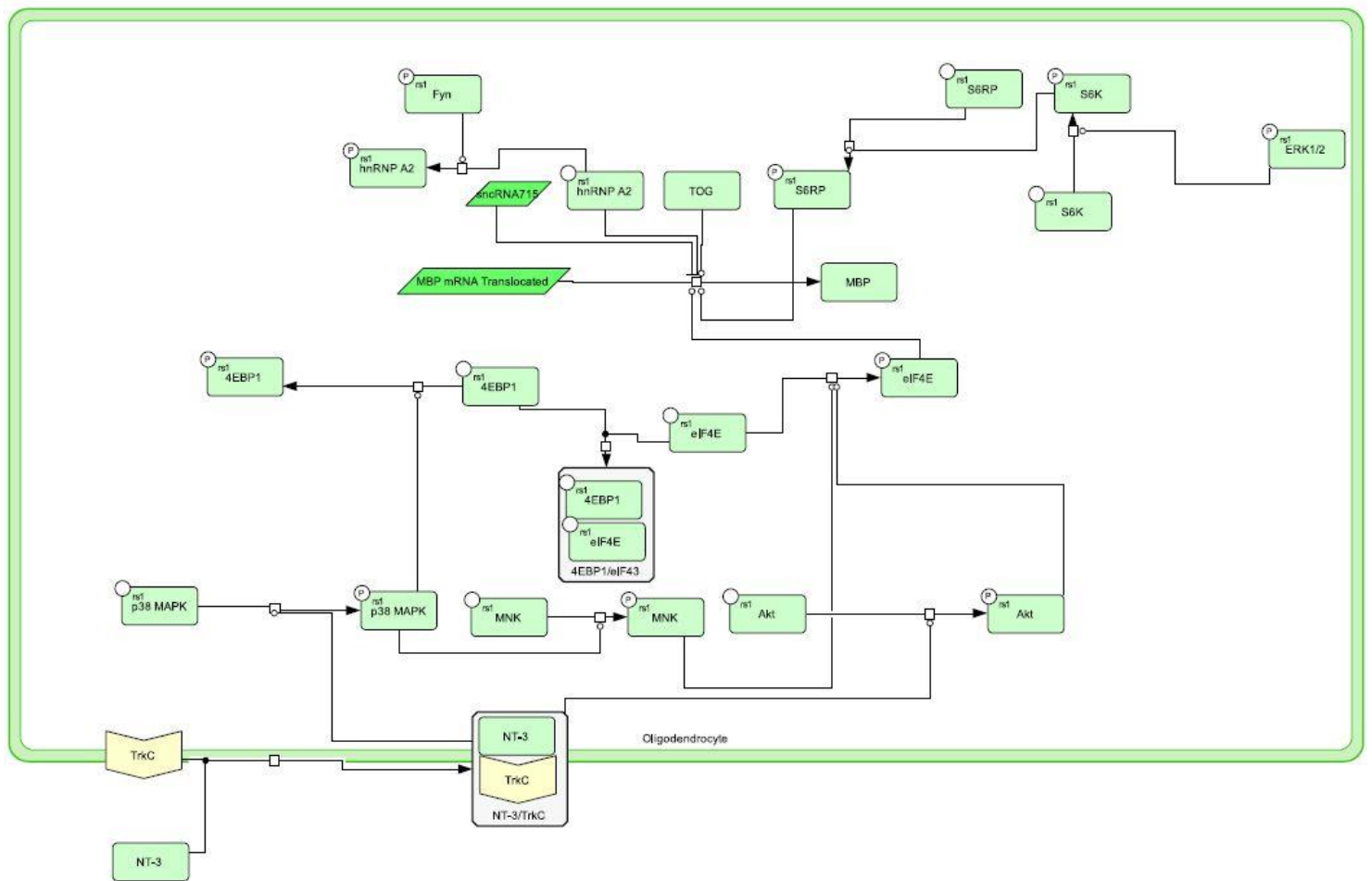
2.5.2 PLP

Proteolipid protein (PLP) is the most abundant protein in CNS myelin (Tzakos et al., 2005). The transcription and translation of PLP are shown in Model 18. Activators of PLP transcription include the following transcription factors: Nkx2.2, Gtx, Olig2, YY1, and MYRF (Fu et al., 2002; Sim, Hinks, & Franklin, 2000; Berndt et al., 2001; Emery et al., 2009). In addition, HDAC11 relieves the inhibition of histone 3 (H3) in the area of the PLP gene (Liu et al., 2009). Finally, the nuclear lamin B proteins have been shown to increase transcription of PLP through an unknown mechanism (Lin et al., 2013).

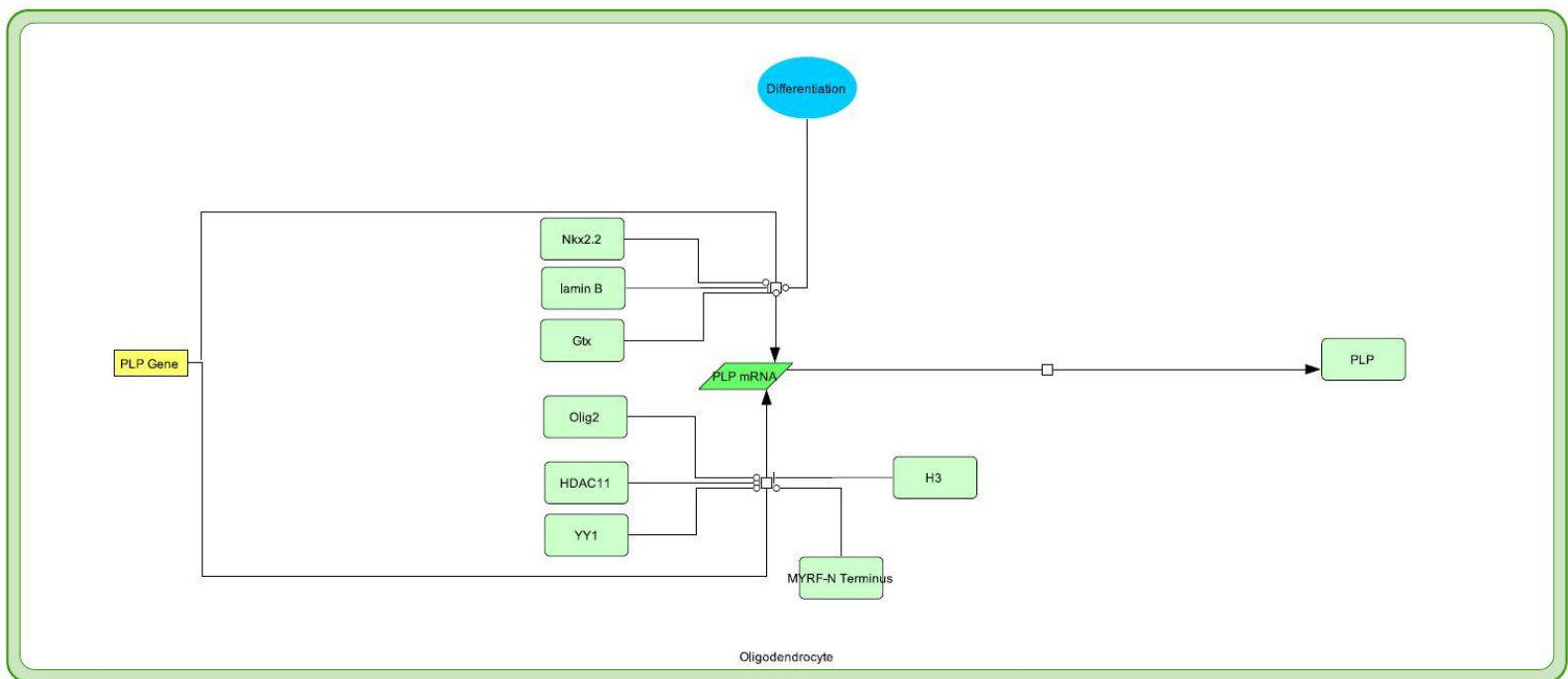
The diagram illustrates the mechanism of MBP mRNA translocation in an oligodendrocyte. It shows three proteins (Kif1b, MAPt, and phosphorylated PDGFRα) interacting with a central translocation pore. MBP mRNA is shown entering the pore from the left and emerging as translocated mRNA on the right.

Oligodendrocyte

Model 16: Translocation of MBP mRNA



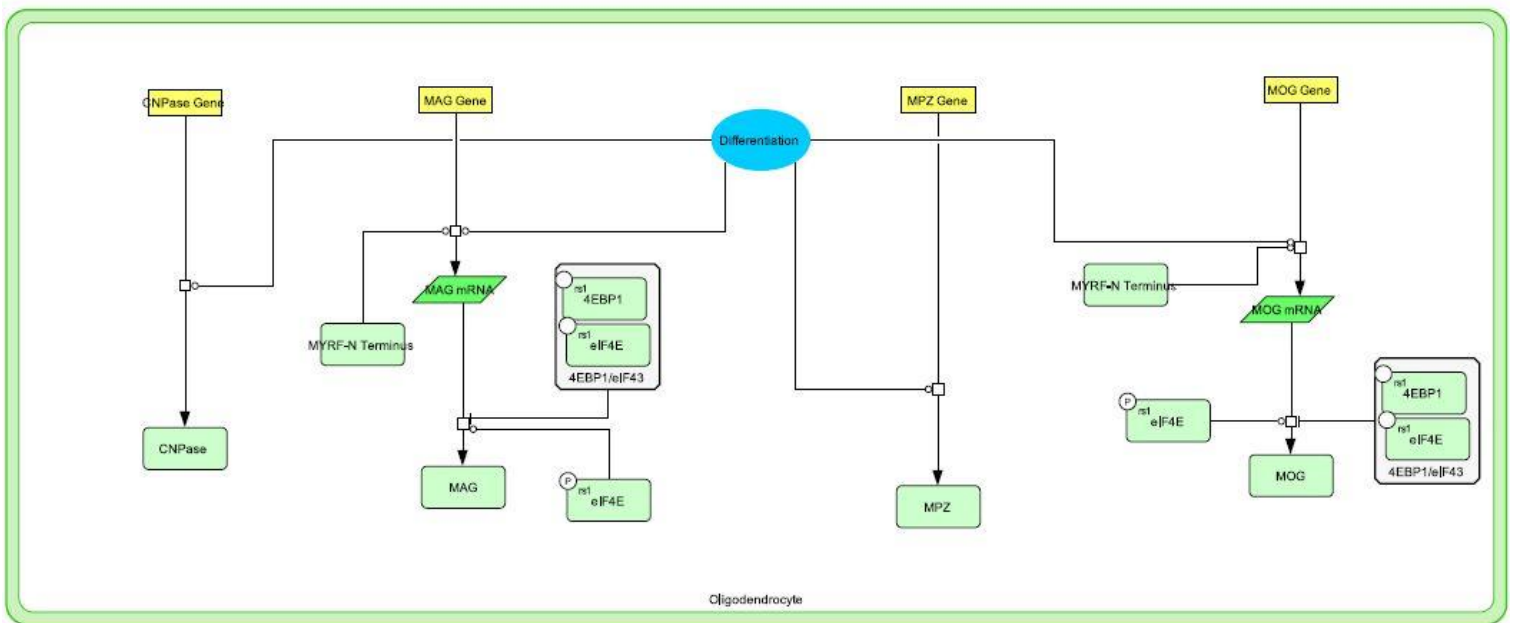
Model 17: Translation of MBP



Model 18: Transcription and translation of proteolipid protein

2.5.4 Minor Myelin Components

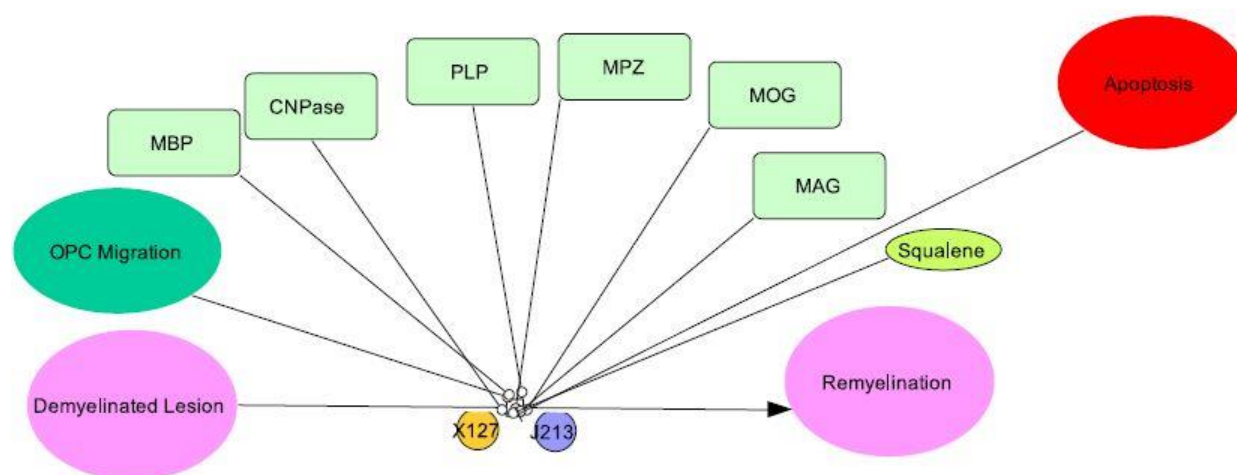
Though important to the integral structure of myelin, several myelin proteins are considered minor contributors in this model (Model 19). This consideration is primarily due to a lack of literature related to the production of these proteins in a remyelination context. These proteins included in this model include: 2', 3'-Cyclic-nucleotide 3'phosphodiesterase (CNPase), myelin-associated glycoprotein (MAG), myelin protein zero (MPZ), and myelin oligodendrocyte glycoprotein (MOG). All proteins were modeled to have their production stimulated by OPC differentiation. MYRF stimulates the transcription of both the *MAG* and *MOG* genes (Emery et al., 2009; Bujalka et al., 2013). Phosphorylated eIF4e is known to stimulate translation of the *MAG* and *MOG* mRNAs, while the eIF4e/4EBP1 complex inhibits translation (Coelho et al., 2009).



Model 19: Production of minor myelin contributors

2.6 Overall Factors Contributing to Remyelination

Remyelination was itself considered as a reaction progressing demyelinated lesions to remyelination (Model 21). Differentiation was considered only for its role in the production of the various myelin components, and therefore is not represented in the modulation of this reaction. The reaction is shown to be upregulated by the following myelin components: MBP, CNPase, PLP, MPZ, MOG, MAG, and squalene. Remyelination was also catalyzed by OPC migration. Inhibiting remyelination is apoptosis, as the death of myelin producing cells would prevent remyelination.



Model 21: Factors directly considered in remyelination as a species

2.7 Computer Modeling

The visualized CellDesigner model was converted into a mathematical form using BST. MATLAB coding software was used to model species concentrations and reaction rates over time. For examples of applications of BST to neurodegenerative disease see this lab's previous work (Broome & Coleman, 2011; Braatz & Coleman, 2015). For a full copy of the MATLAB code used in this model, see the Appendix.

2.7.1 Differential Equations

The model constructed here is a system of nonlinear, first order, autonomous ordinary differential equations. The equations fall into two categories: system equations and rate equations.

2.7.1.1 System Equations

System equations are assigned to each dependent variable to describe the change in concentration of that species over time. The concentration of a reactant leading to a particular species is multiplied by a rate constant or rate equation, and these values are then summed together to form a species' system equation. Likewise, if a dependent variable species leads to another species, then the appropriate rate constant or rate equation multiplied by that species concentration is subtracted in the first species' rate equation. For example,

$$dX(287) = X(102) * Xind(99) - X(118) * X(287)$$

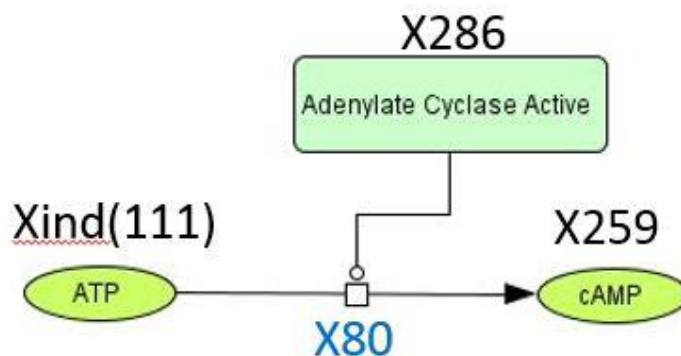
where $dX(287)$ represents the change in concentration of $X(287)$, MBP mRNA, $Xind(99)$ represents the MBP gene, and $X(102)$ and $X(118)$ represent the related rate equations. The first part of the statement represents the transcription of the gene, and the second, the mRNA being translated.

2.7.1.2 Rate Equations

Rate equations are a way of representing modifiers to the rate of a specific reaction. If a reaction has no catalyzers or inhibitors, it was given a rate constant value, represented as “k”. For example, the production of O1 was given an equation of:

$$dX(252) = k(71) * Xind(103)$$

where X(252) is O1 and Xind(103) is the O1 gene. For reactions with modifiers, rate equations were written. These equations consist of a constant multiplied by a sum of all species promoting or inhibiting the reaction, with inhibitors being viewed as negative. Model 22 is used to show an example of a rate equation.



Model 22 – Production of cAMP

Model 22 would be given the following associated equations:

$$dX(80) = 0.01 * X(286)$$

$$dX(259) = X(80) * Xind(111)$$

The first equation is a rate equation corresponding to how quickly or slowly X(286), adenylate cyclase, increases the rate of the reaction, X(80). The second equation is a system equation demonstrating the rate of change in the concentration of X(259), cAMP, as it relates to the rate, X(80), and the concentration of reactant, Xind(111), ATP.

2.7.2 Initial Values

Each variable in the model was assigned an initial value. Variables were given one of two designations: independent or dependent. Independent variables are those which are not a product of any reaction in the model. The values were obtained in parts per million through the use of the proteomics database PaxDB and converted using mean values on brain size and mass. In addition, values were modified on a relative basis allowing for estimation of values when no data is available.

2.7.3 Baseline, Disease, and Treatment Conditions

Data was analyzed through a baseline control state, a disease state, and various treatment conditions. The analysis is represented as a difference between the disease and the baseline state. Therefore, any species with a positive value indicates that the model predicts an increase in that species during MS. Likewise, any negative value implies a decreased concentration of that species in MS. Treatment states are compared to the baseline state in the same fashion as a disease state. Two types of treatment condition were examined. The first was a condition in which the treatment species concentration was active from the beginning of the run ($t = 0$). The second was a condition in which the treatment species concentration began at zero, but was initiated part way through the run ($t = 75$). This second method represents treatment of a disease after a period of time during which symptoms would appear and a diagnosis was made.

3. Results

Results examine various treatments for MS and their impact on remyelination. The results presented are a qualitative analysis of relative differences between various states. The representation is presented as five different scenarios: a baseline disease state, treatment from $t=0$ at low dose, treatment at $t=75$ at low dose, treatment at $t=0$ at high dose, and treatment at $t=75$ at high dose. The doses examined, when compared against the values obtained for protein concentration data, represent concentrations of 0.01 nM for low dose and 0.1 nM for high dose. Each treatment is considered and results are presented with relevance to the molecular signaling pathways effected.

3.1 Disease/Baseline State Overall

The state referred to as the “disease state” or “baseline state” is a representation of the difference between the model run in MATLAB with MS-related initial concentrations and a healthy state

with no MS-related initial concentrations. The primary difference between these two runs is the presence of the species labeled “demyelination”. Figure 1 shows the qualitative result of the baseline state with regard to the species “remyelination”, which is an overall indicator of disease progression in the model. The model predicts three distinct phases. The first is a segment of little difference between a healthy and disease individual with regard to myelination. The second segment shows a marked increase in myelination compared to a healthy individual with no demyelination. The third and final period is a steady decline in overall myelination over time. Of note is the continuing occasional spiking seen during this myelination decline, implying occasional successful myelination. These results are the baseline for which all treatments were examined for their overall efficacy.

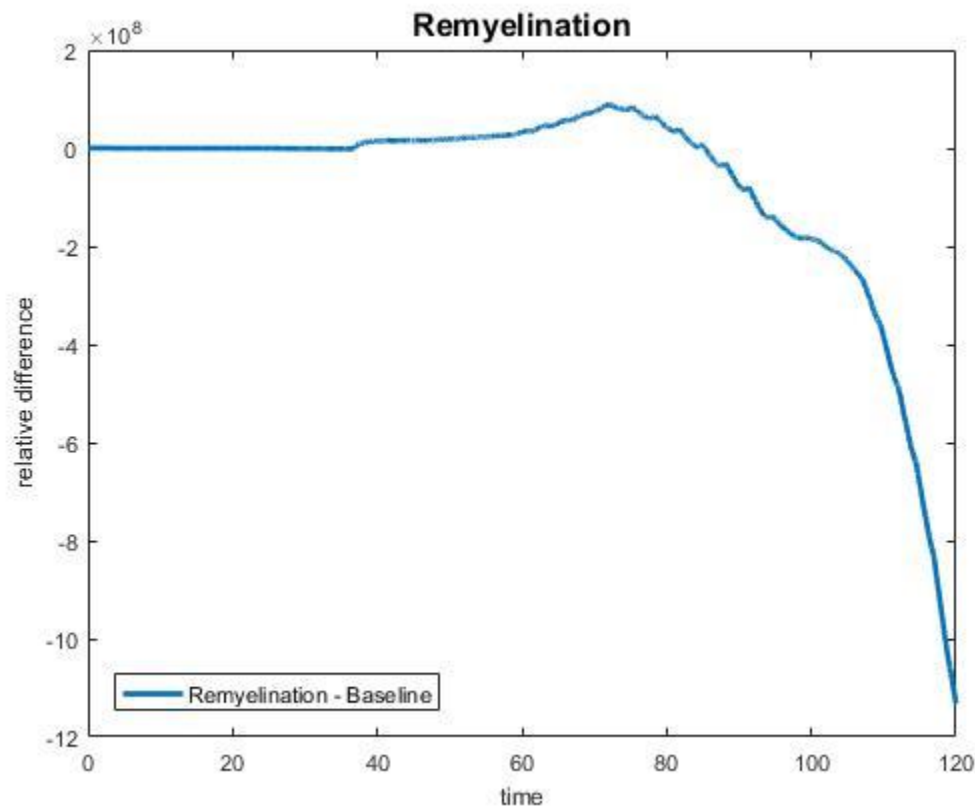


Figure 1 - Baseline remyelination predicted by MATLAB model

3.2 Treatments for MS

The results that follow examine pharmaceutical treatments that are already in use or are in consideration for use in the treatment of MS. The treatments are separated by their respective mechanisms of action.

3.2.1 Immunomodulation

The first drug considered is Glatiramer Acetate (GA). GA is used currently in the treatment of relapsing-remitting MS and targets immune cells, including the activation of Th2 helper cells. The role of these cells was described in section 2.1.4. Evidence has shown that GA will promote the expression of important neurotrophic factors by the Th2 Helper cell, including PDGF, BDNF, and IGF-1 (Skihar et al., 2009). While GA is already a viable treatment option for targeting immune response in MS, this model examines its efficacy in promoting remyelination, exploring its potential dual role in treatment. The effect of GA on overall remyelination is demonstrated in Figure 2. Use of a high dose from the beginning of pathology results in a delayed, but overall more significant remyelination compared to all other states. All other states follow a relatively similar pathway of disease progression, but over time it is clear that a higher dose, even given part way through disease progression, results in increased remyelination compared to the baseline state. The low dose curves show some improvement over baseline, but not at the level of the higher dose. Among the factors modeled as effecting remyelination success, the model predicts treatment with GA significantly lowers levels of apoptosis (Figure 3).

3.2.2 Anticholinergics

Other considerations for treatment have looked at the effect of neurotransmitters on oligodendrocyte differentiation and subsequent remyelination. Two such drugs to be recently

examined are Benztropine and Clemastine (Deshmukh et al., 2013; Mei et al., 2014). Both drugs are anticholinergic drugs, with Benztropine known to exert its action on specifically the M1 and M3 receptor subtypes, while Clemastine is primarily an antihistamine with anticholinergic properties (Deshmukh et al., 2013; Mei et al., 2014). As of May 2016, both drugs were being considered for clinical trial, and of particular interest as both are already approved by the Food & Drug Administration (Juarez, He, & Lu, 2016). The model successfully reduces the number of complexes between ACh and muscarinic receptors (Figure 4). The model predicts full, early

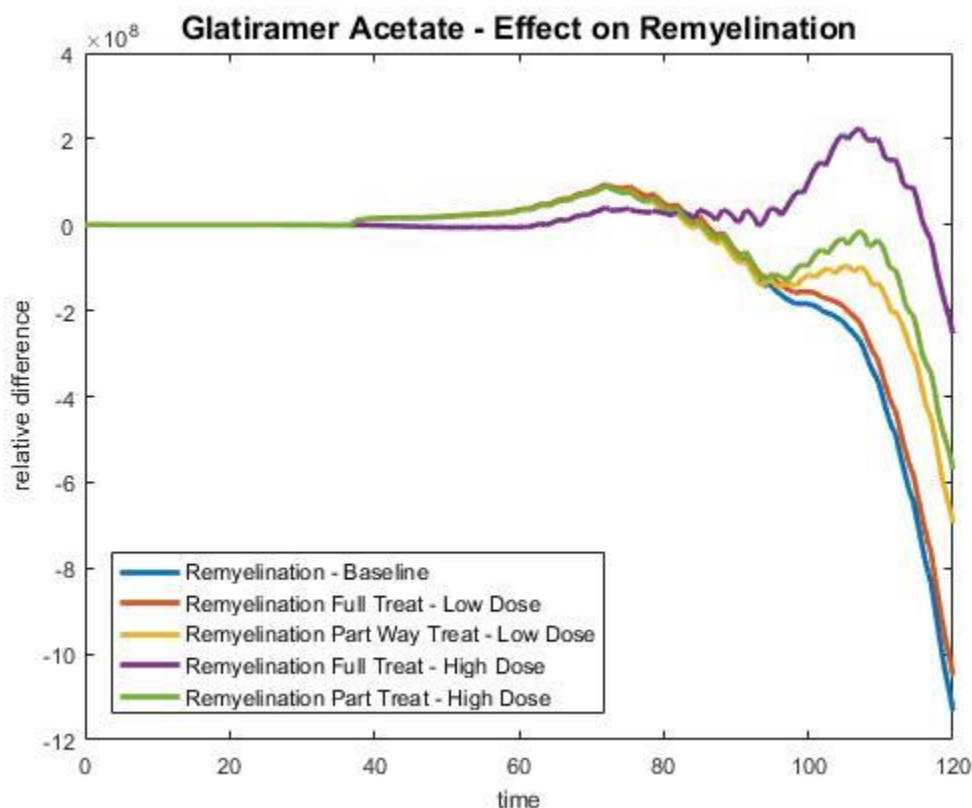


Figure 2 – Effect of Glatiramer Acetate on remyelination

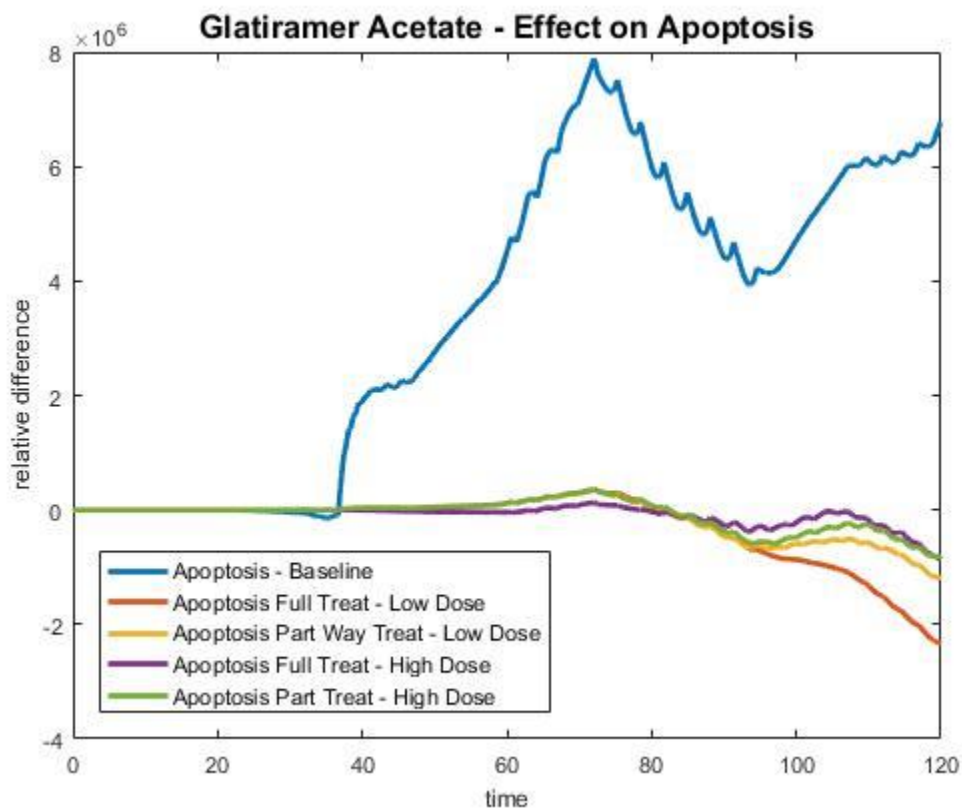


Figure 3 – Effect of Glatiramer Acetate on apoptosis

treatment with both high and low doses of anticholinergic medications results in increased remyelination, with a higher dose being most effective (Figure 5). However, the model also predicts that only low doses are successful in improving remyelination when administered part way through disease progression (Figure 5). The model shows that anticholinergics in particular have a strong impact on OPC Migration to the site of a lesion (Figure 6).

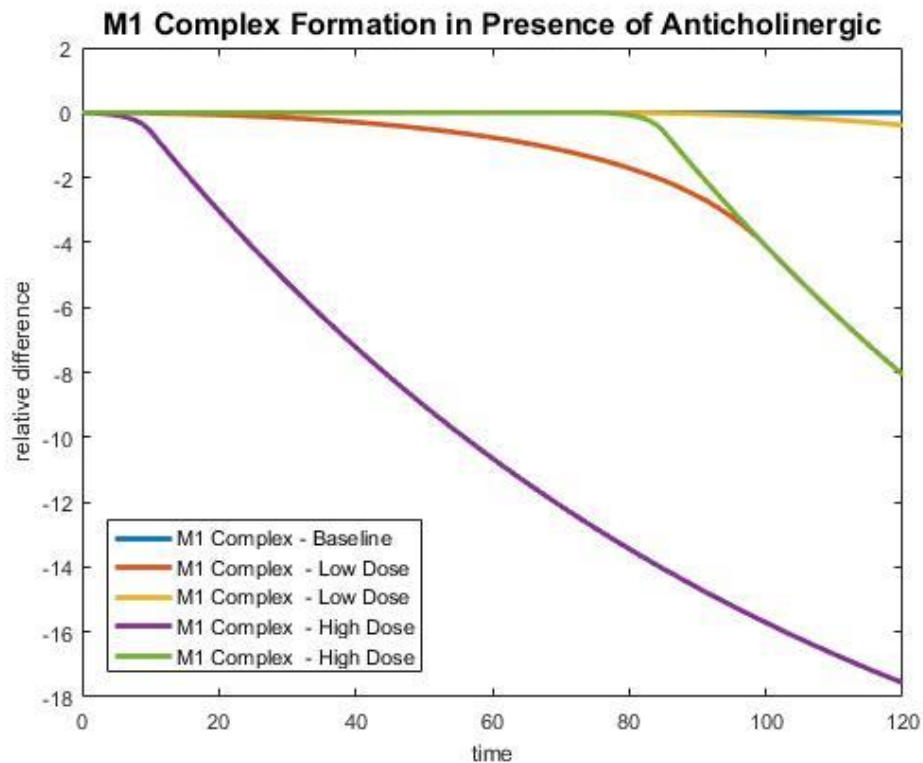


Figure 4 – Inhibited M1 receptor complex formation

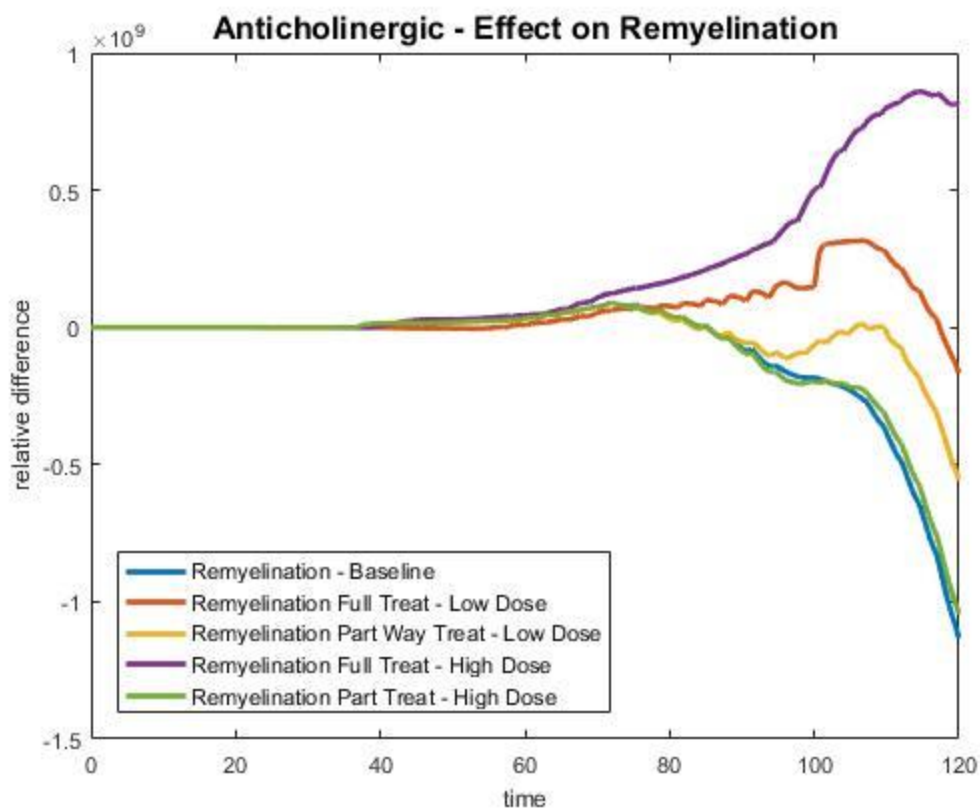


Figure 5 – Anticholinergic effects on remyelination

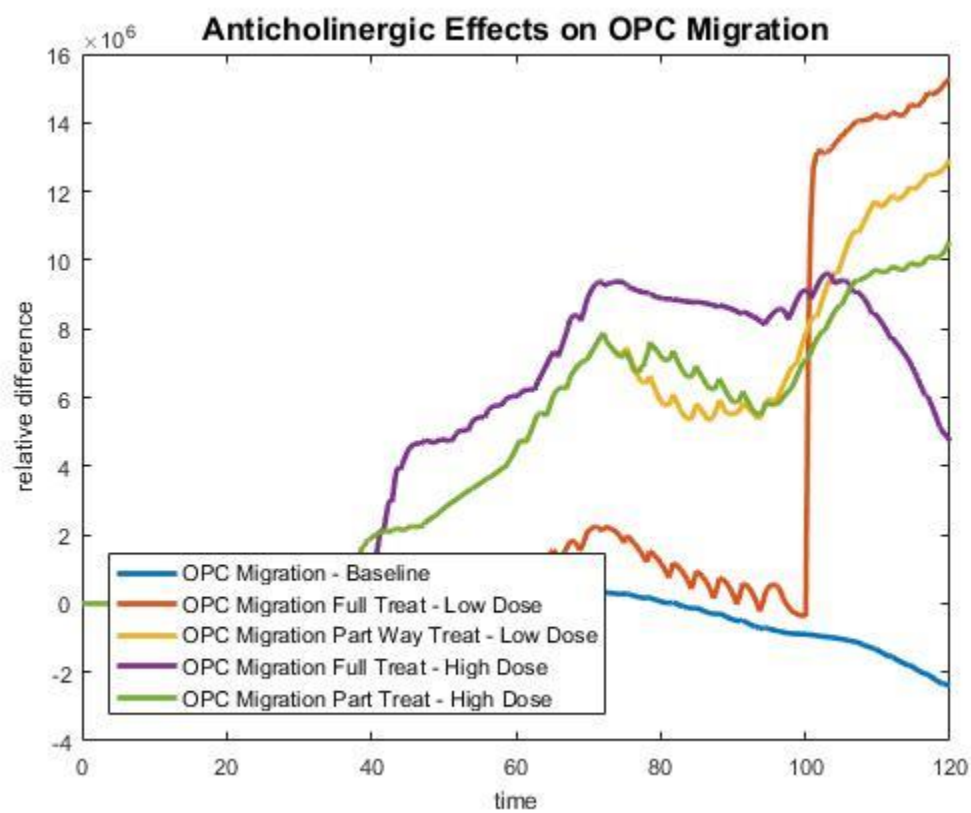


Figure 6 –Anticholinergic effects on OPC Migration

3.2.3 Cholesterol Synthesis

The next treatment examined is the use of HMG-CoA Reductase inhibitors, otherwise known as statins. There is evidence that the use of statin drugs leads to lower levels of geranylgeranyl pyrophosphate, important in the geranylation of proteins, which may be involved in activation of phosphatases targeting the p38 MAPK pathway (Paintlia et al., 2010) (Model 4). As of January 2016, Simvastatin had completed phase II trials in which it was shown to reduce brain atrophy in patients with progressive MS (Shirani, Okuda, & Stüve, 2016). Figure 7 confirms the successful reduction of geranylgeranyl pyrophosphate upon administration of different dosages of a statin. Use of a statin for any dose examined in this model predicts no significant improvement of remyelination, with high doses impairing remyelination (Figure 8).

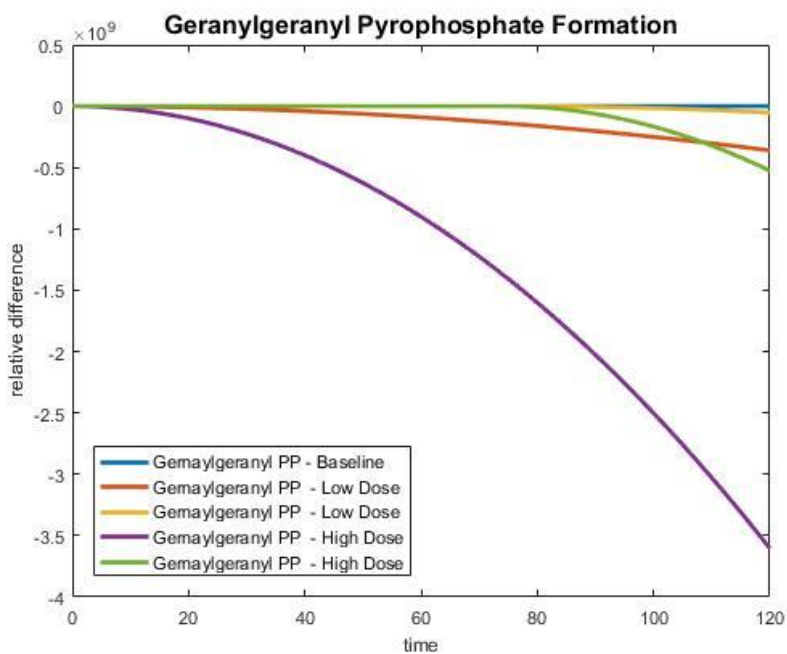


Figure 7 – Reduction of geranylgeranyl pyrophosphate formation with statins

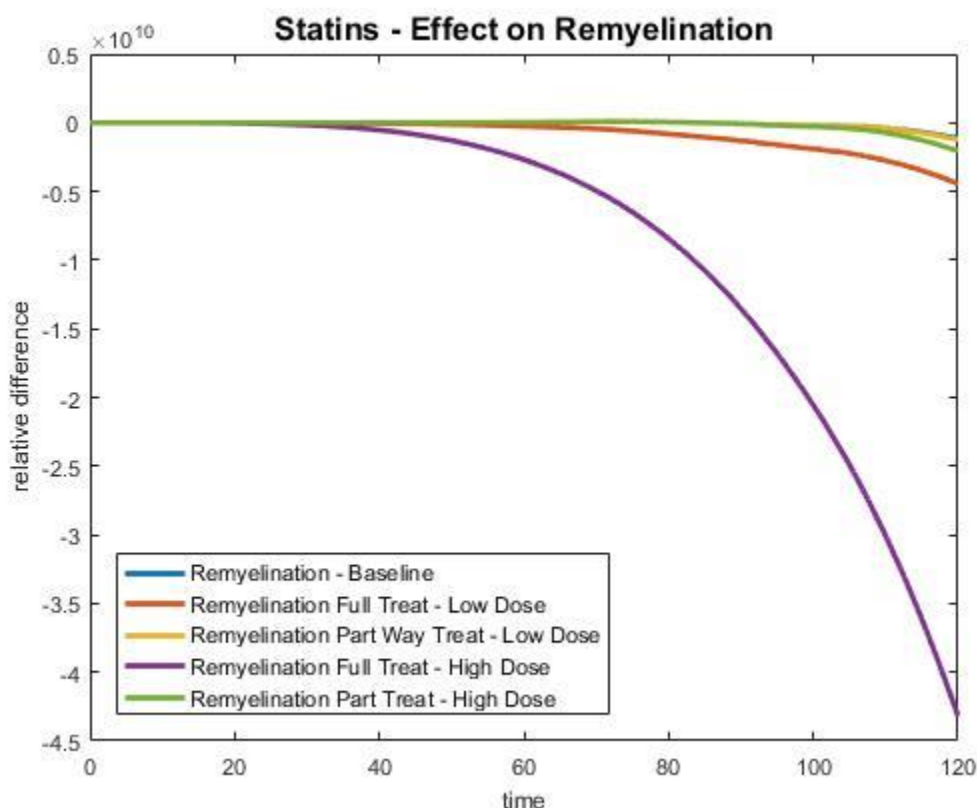


Figure 8 – Effect of statins on remyelination

3.2.4 Smoothened Receptor Agonists

It has been noted that activation of $\text{RXR}\gamma$ by binding with 9cRA encourages OPC Differentiation (Huang et al., 2010) (Model 7). Furthermore, activation of the smoothened receptor protein results in increased expression of $\text{RXR}\gamma$. For this reason, SMO agonists have been suggested as a potential target for MS treatment (Porcu et al., 2015). So far, no trial has been undertaken to examine the clinical effectiveness of SMO agonists in multiple sclerosis. Two SMO agonists under consideration are clobetasol and halcinonide. Both drugs are corticosteroids currently used primarily as topically treatments for certain skin disorders. Addition of a SMO agonist to the mathematical model results in an increase in the number of complexes formed between $\text{RXR}\gamma$ and 9cRA (Figure 9). The model predicts successful remyelination upon application of a SMO agonist (Figure 10). Use of a lower dose of the SMO agonist resulted in more successful

remyelination than compared to a higher dose. In addition, administration of the agonist part way through the model predicts improved, but less substantial, remyelination compared to full treatment.

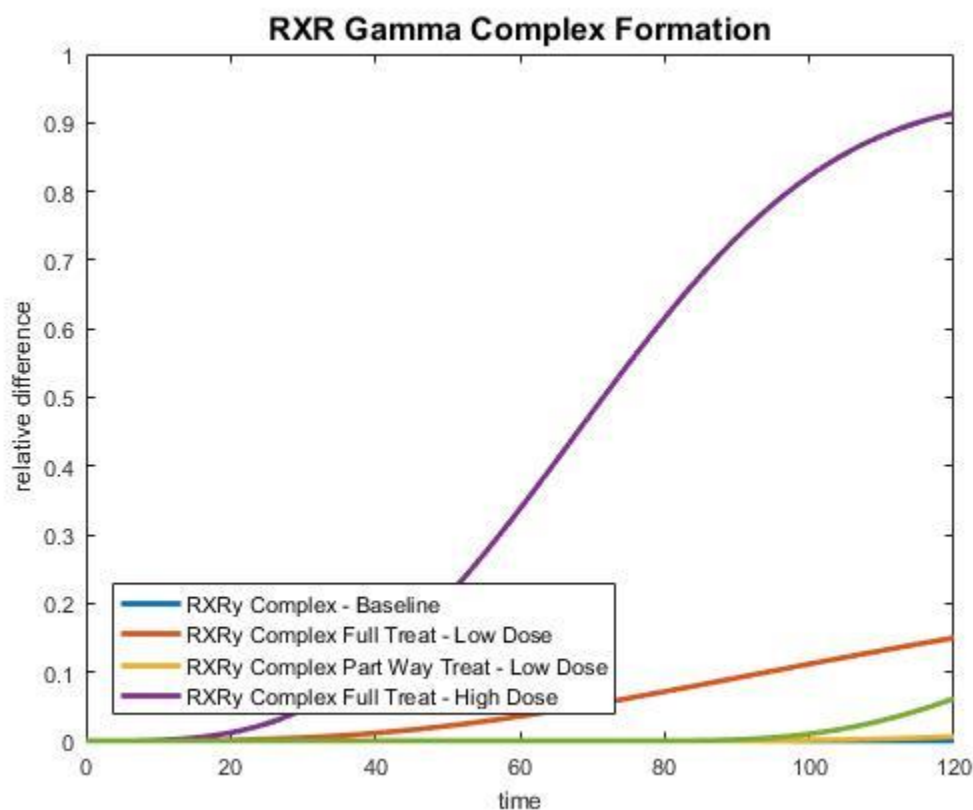


Figure 8 – RXR γ /9cRA complex formation in presence of smoothened agonists

3.2.5 Integrin Signaling

Evidence has shown the value of immunoglobulin antibodies to target specific proteins to promote remyelination. One example is the activation of the $\beta 3$ integrin protein by rHlgM22. This antibody promotes activation of Lyn kinase through integrin signaling (Watzlawik et al., 2010). As of 2015, rHlgM22 had cleared safety assessment and was awaiting clinical trials (Kremer et al., 2015). Implementation of this antibody in the model successfully increases Lyn kinase activation, with a larger dose leading to further activation (Figure 10). In addition, the

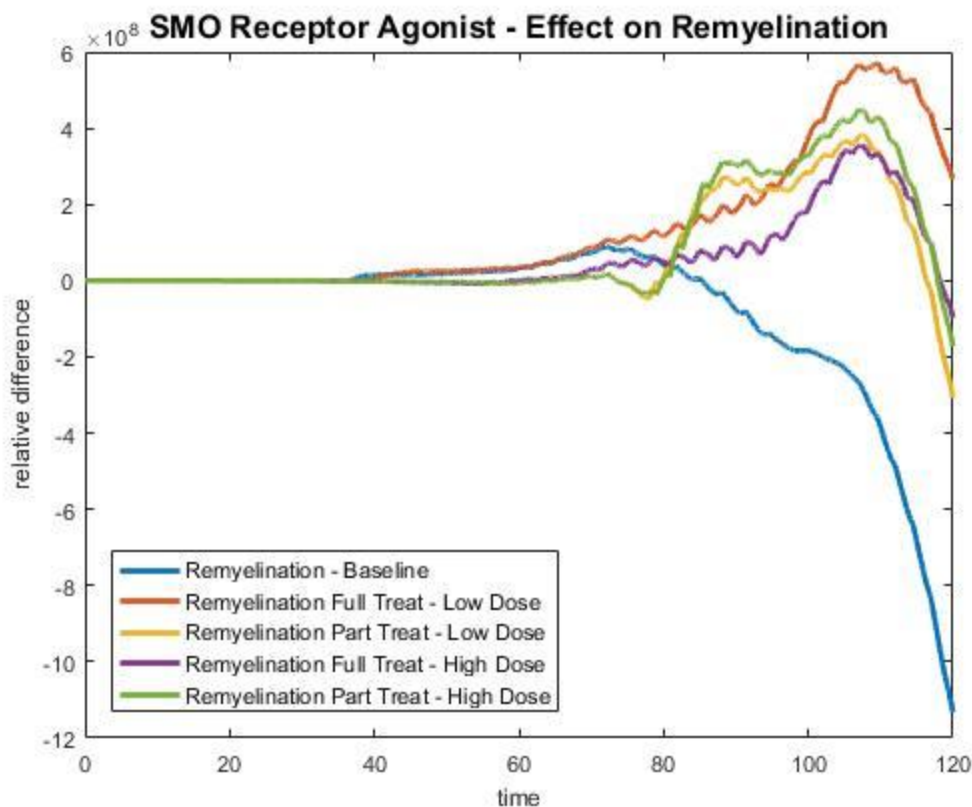


Figure 9 – Effect of smoothened agonists on remyelination

integrin antibody lowered levels of apoptosis (Figure 11). Partial treatment led to the lowest levels of apoptosis, with the higher dose reducing levels furthest. Overall, the integrin antibody showed improved remyelination, with full treatments showing significant increases in remyelination and partial treatments showing a lower, but substantial positive increase in remyelination (Figure 12).

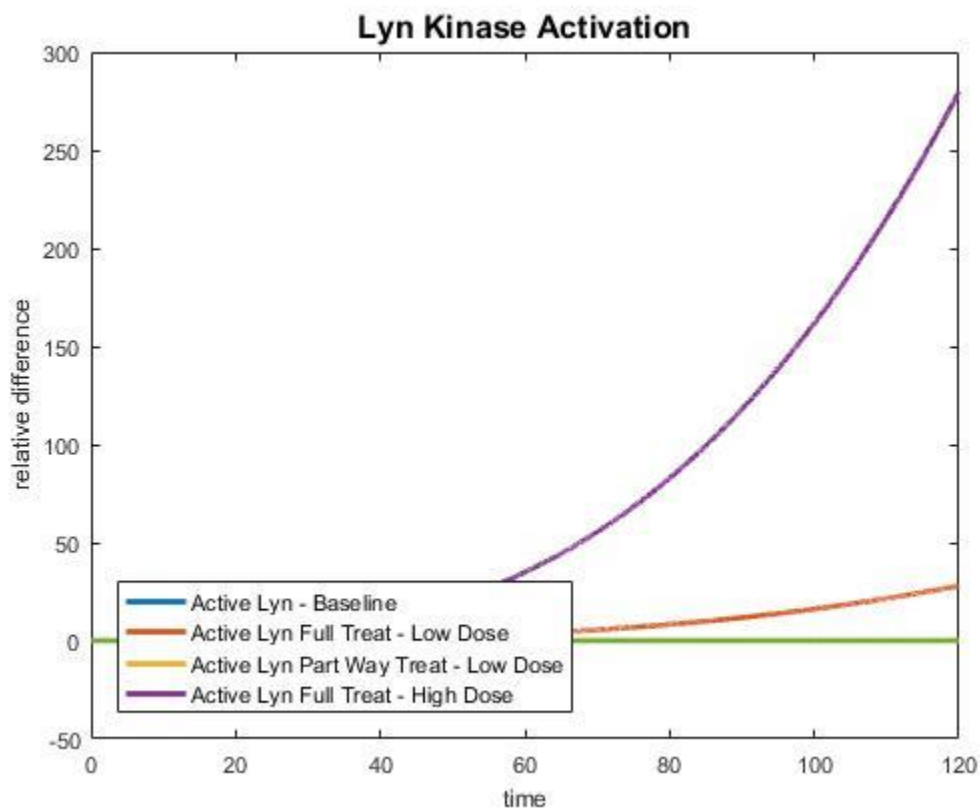


Figure 9 – Activation of Lyn Kinase in presence of rHIgM22

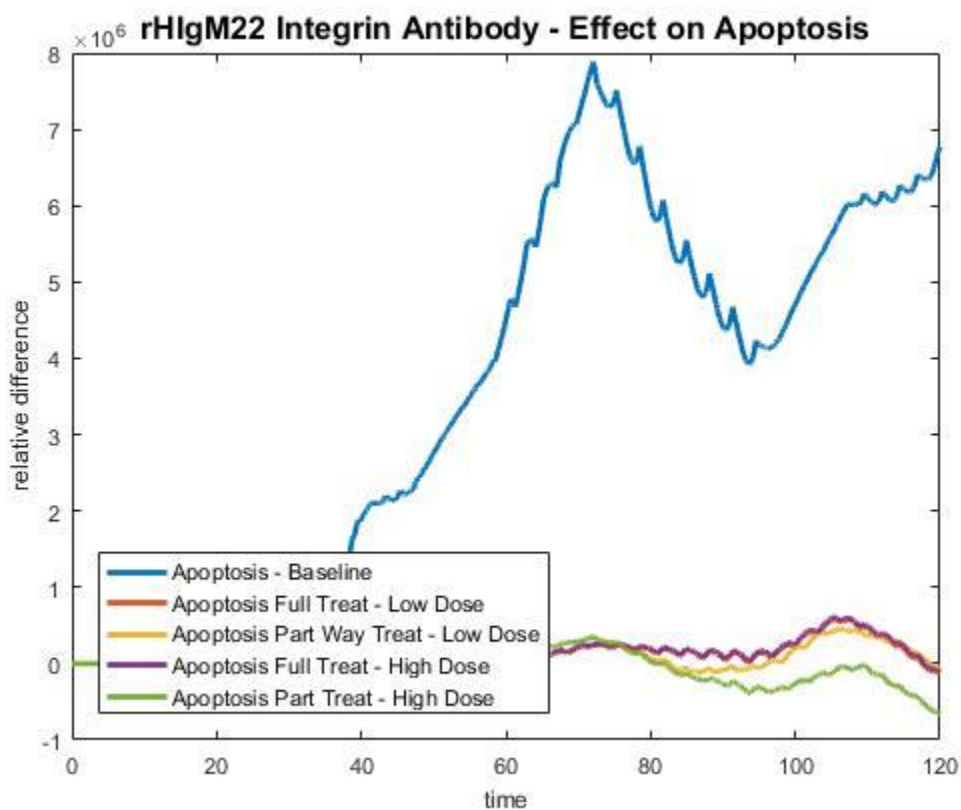


Figure 10 – Effect of rHIgM22 on apoptosis

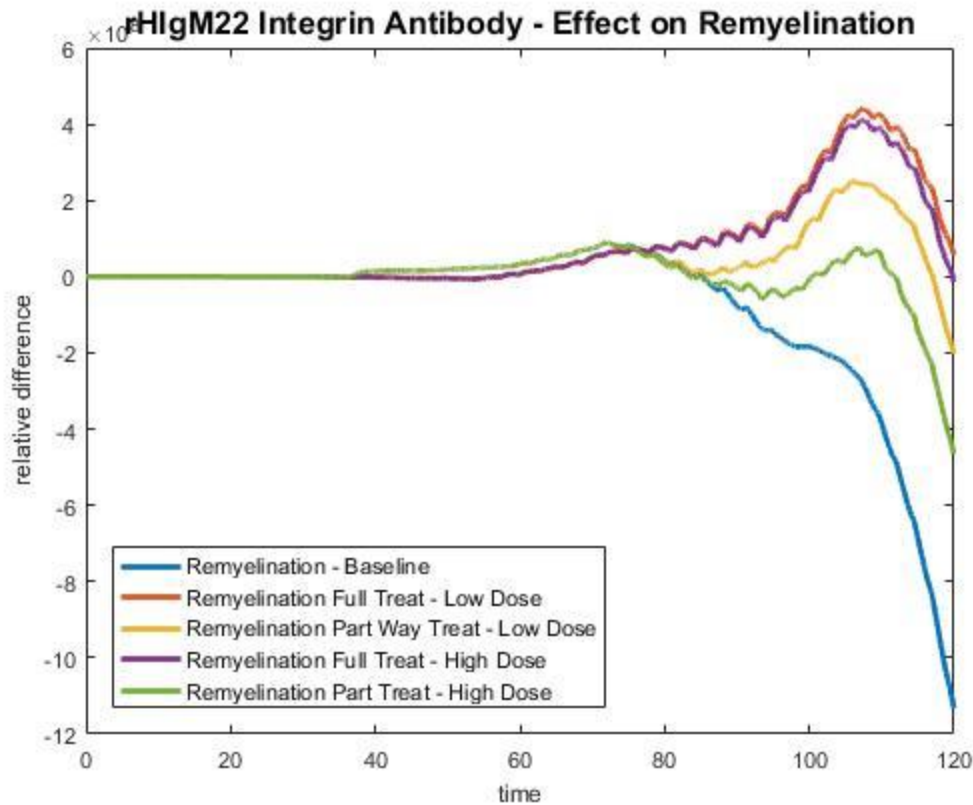


Figure 11 – Effect of rHlgM22 on remyelination

3.2.6 Sphingosine Receptor

Activation of the major kinase pathways, including the p38 MAPK and ERK signals, is vital to successful OPC differentiation and remyelination. One activator of these pathways in OPCs is the sphingosine 1-phosphate receptor (Cui et al., 2014) (Model 11). For this reason, the S1PR receptor has become a target of interest in upregulating remyelination. One activator of this receptor is the drug fingolimod. Like glatiramer acetate, fingolimod, also known as FTY720, is a drug currently in use for the treatment of multiple sclerosis. Fingolimod activates the S1PR receptor to encourage the differentiation of OPCs and increase remyelination in *in vitro* experiments (Cui et al., 2014). For these reasons, fingolimod was examined using this mathematical model. Figure 12 shows the successful inclusion of fingolimod complexes into the

model. Inclusion of fingolimod led to increases in remyelination compared to baseline, with full treatment at a higher dose proving the most successful. Furthermore, partial treatment showed lower success compared to full treatments, with a higher delayed dose proved more successful at remyelination compared to the lower dose (Figure 13).

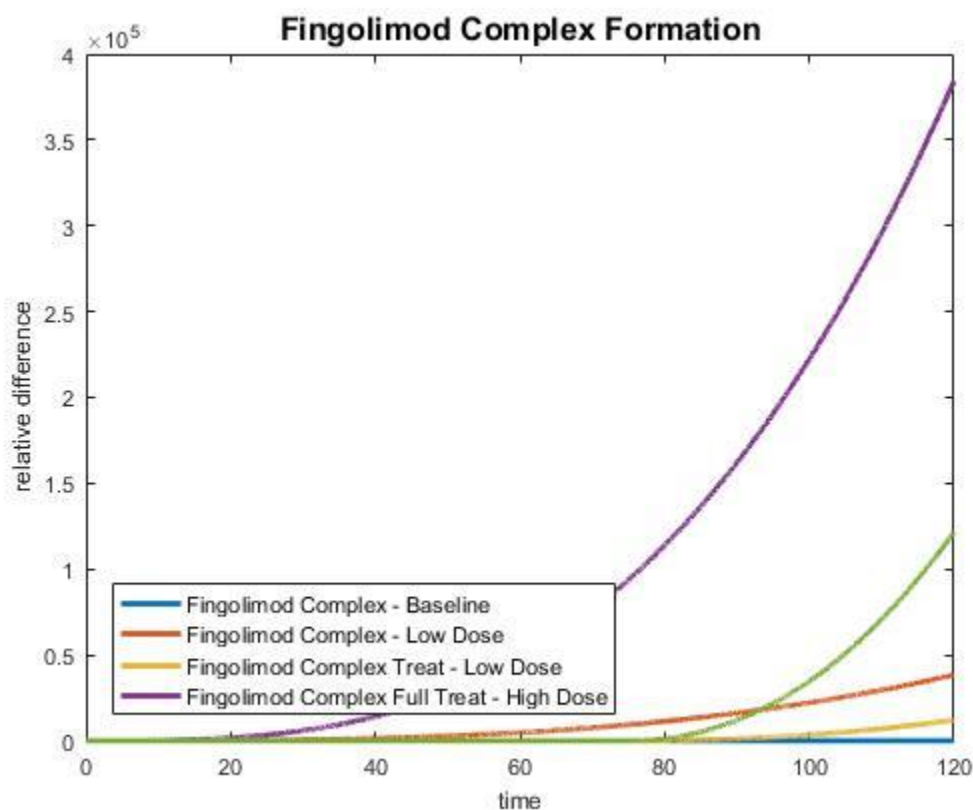


Figure 12 – Fingolimod complex formation with S1PR

3.2.7 *Wnt/β-catenin* Signaling

The *Wnt/β-catenin* signaling pathway plays a complex role in remyelination in which certain species may stimulate OPC differentiation, while others inhibit it (Xie, Li, Zhang, & Guan, 2014) (Model 8). Therefore, modulation of the pathway is a potential target for pharmaceutical treatments for remyelination. Indomethacin, a non-steroidal anti-inflammatory drug, is known to inhibit the *Wnt/β-catenin* pathway. Furthermore, experimental evidence suggests that this

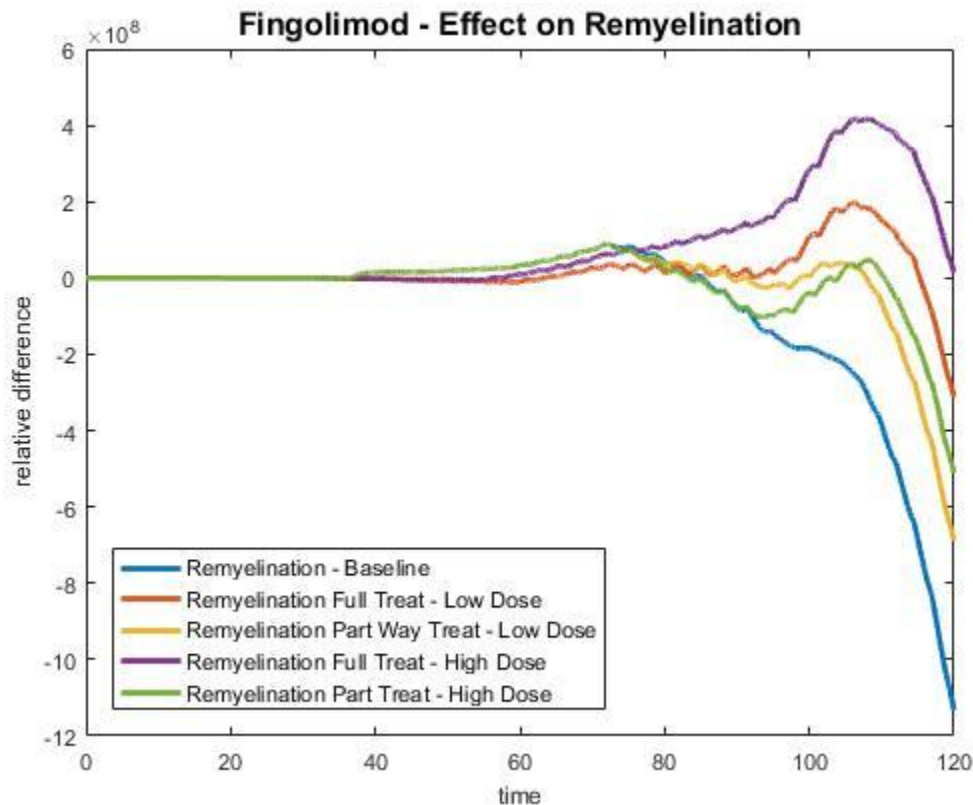


Figure 13 – Effect of fingolimod on remyelination

inhibition leads to improved remyelination (Preisner et al., 2015). As of April 2016 there are no planned clinical trials for indomethacin with regard to treatment of MS (Kremer et al., 2016).

Addition of indomethacin increased degradation of β -catenin as modeled (Figure 14).

Indomethacin also increased overall remyelination in both full treatment states, with a higher dose leading to more remyelination. However, the model predicts no change in remyelination with addition of a delayed treatment compared to the baseline state (Figure 15).

Another modulator of Wnt signaling is lithium chloride (LiCl). LiCl is a known stimulator of the Wnt signaling pathway, but has other mechanisms of action. LiCl is also known to activate Akt/CREB pathways, and has been shown to activate OL expression of MBP and PLP (Meffre, Massaad, & Grenier, 2015). Although it is currently used in the treatment of a variety

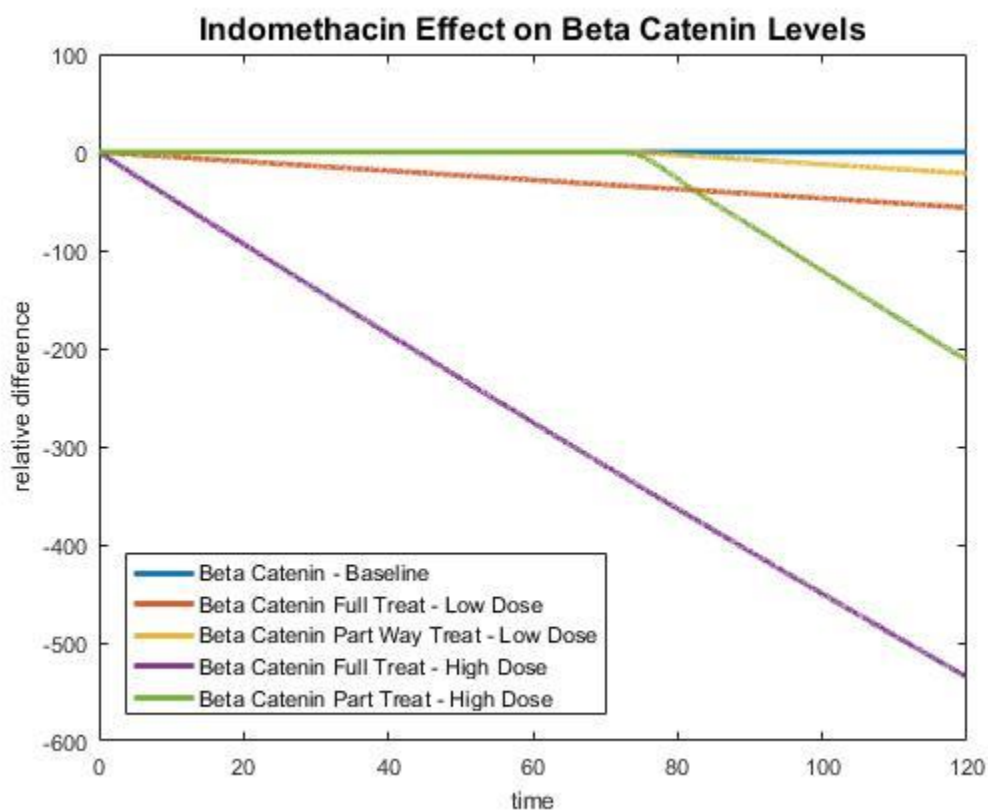


Figure 14 – Indomethacin effect on β -catenin levels

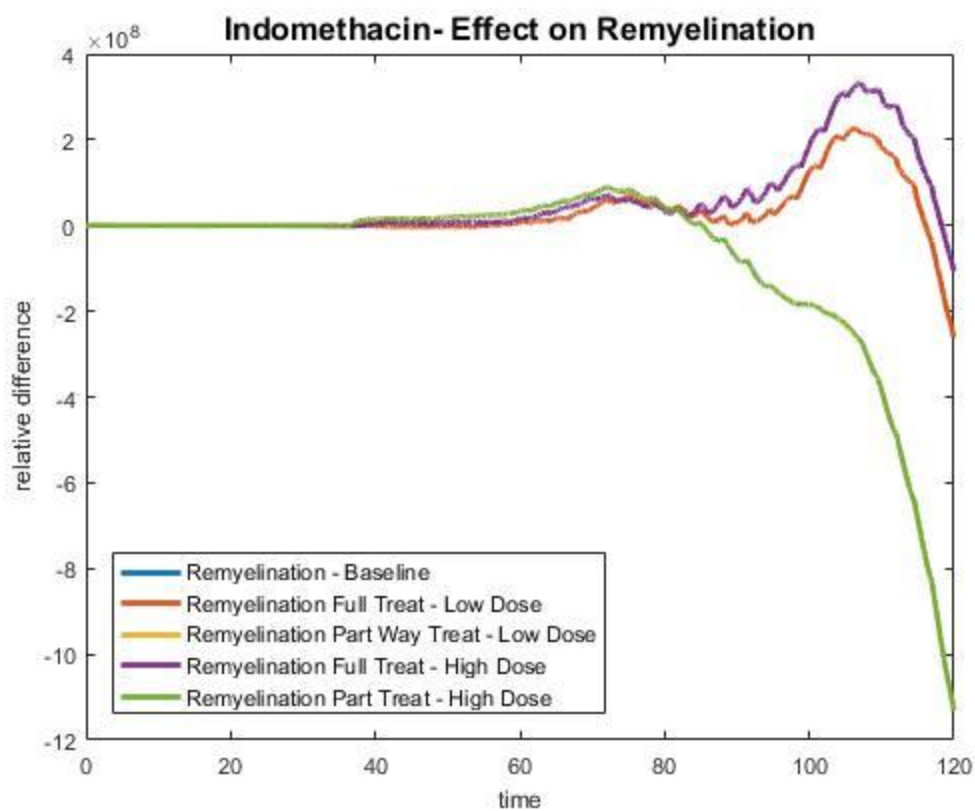


Figure 15 – Effect of indomethacin on remyelination

of neurological disorders, there are no planned clinical trials for LiCl effectiveness in MS. LiCl was examined in this model for its overall efficacy towards MS. Both the Akt/CREB (Figure 16) and Wnt (Figure 17) signaling pathways were increased by the addition of LiCl. In addition, remyelination was only impacted by full treatment states, with both doses improving remyelination (Figure 18). Shifting of partial treatments to earlier time of treatment had no effect. For full treatments, the higher dose treatment resulted in lower remyelination than the lower dose. For this reason, a third state was added, a larger dose equivalent to 1 nM concentration, to determine if there is a point at which the treatment becomes harmful. Figure 19 demonstrates that there is such a point at which the model predicts administration of LiCl reduces remyelination.

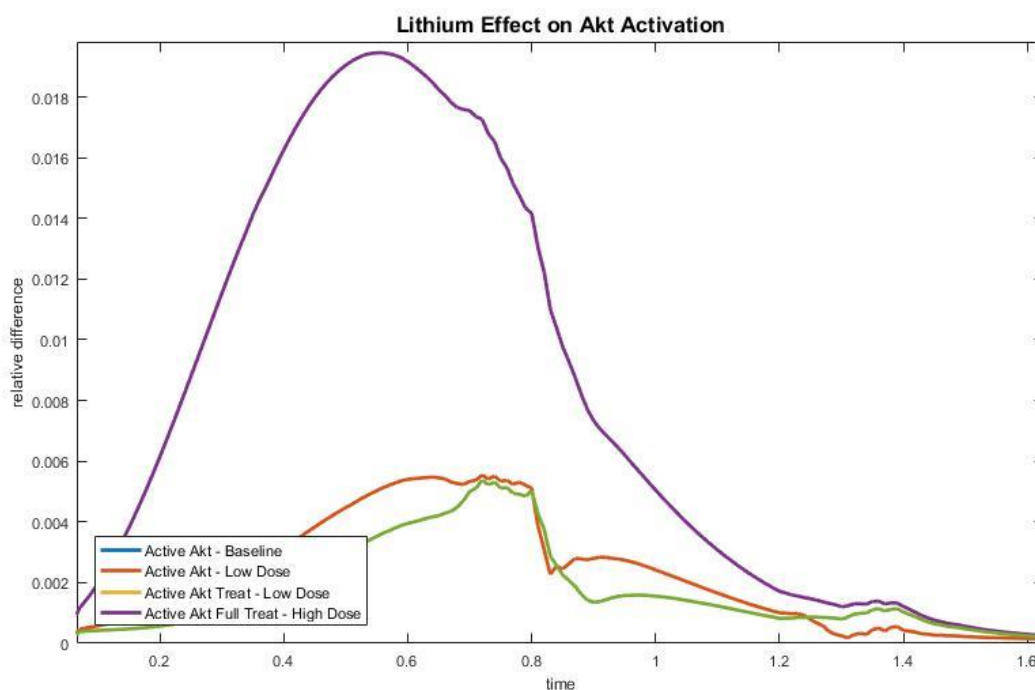


Figure 16 – Activation of Akt signaling in presence of LiCl

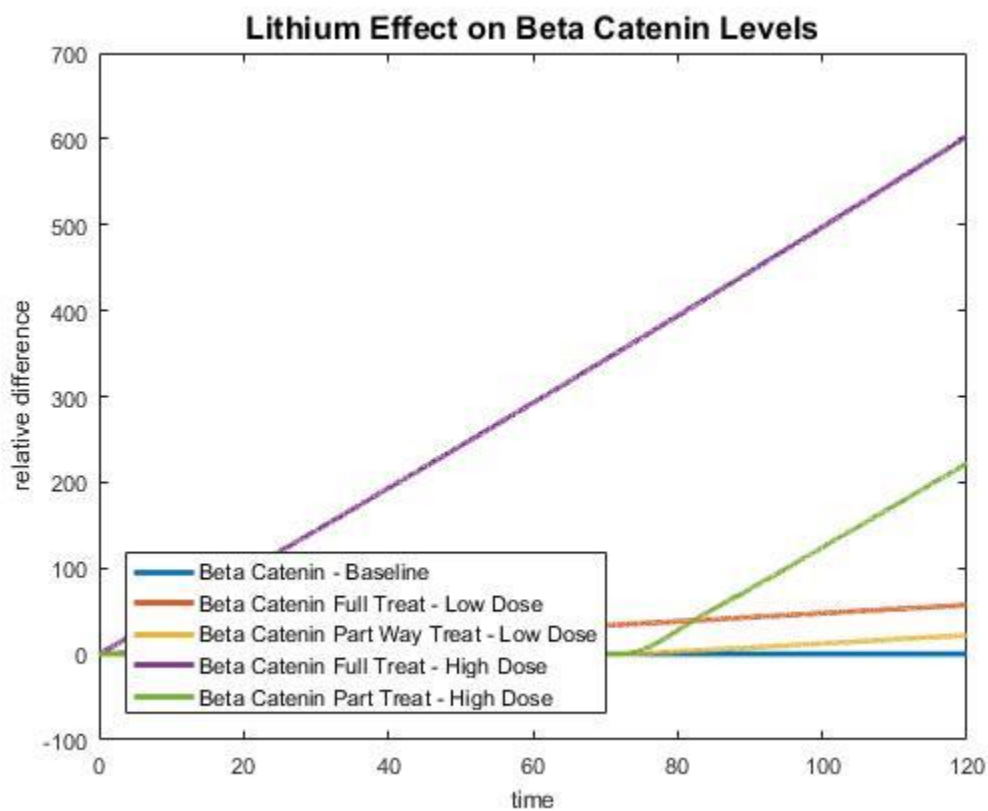


Figure 17 – Impact of LiCl on levels of β -catenin

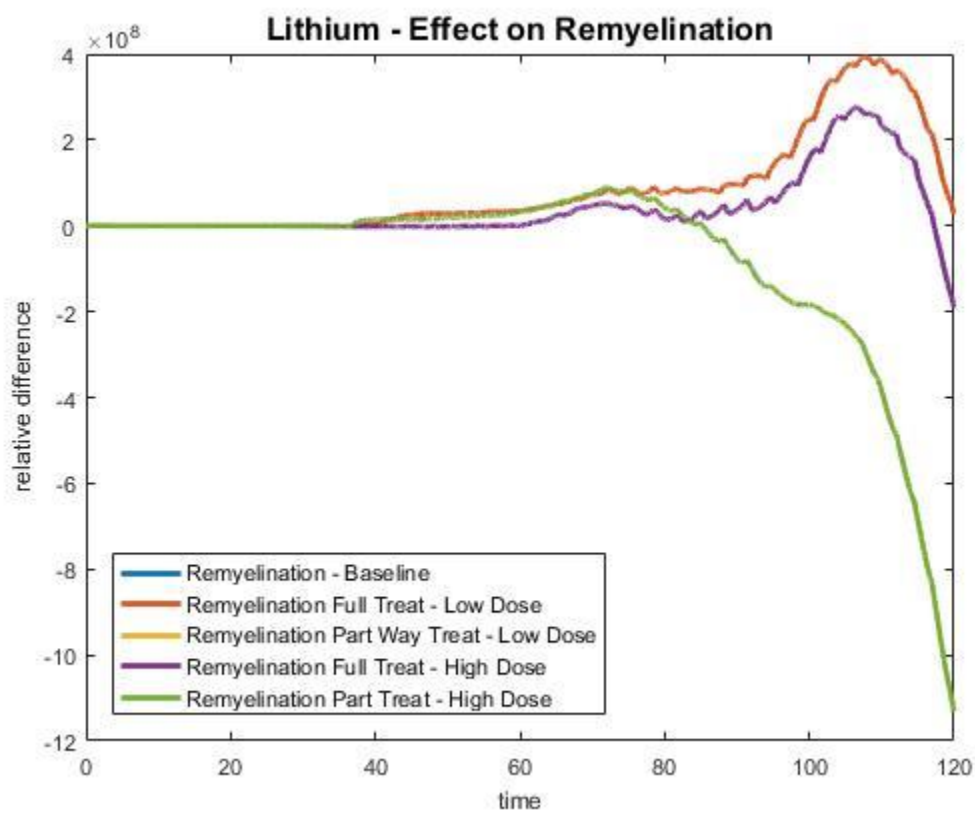


Figure 18 – Effect of LiCl on remyelination

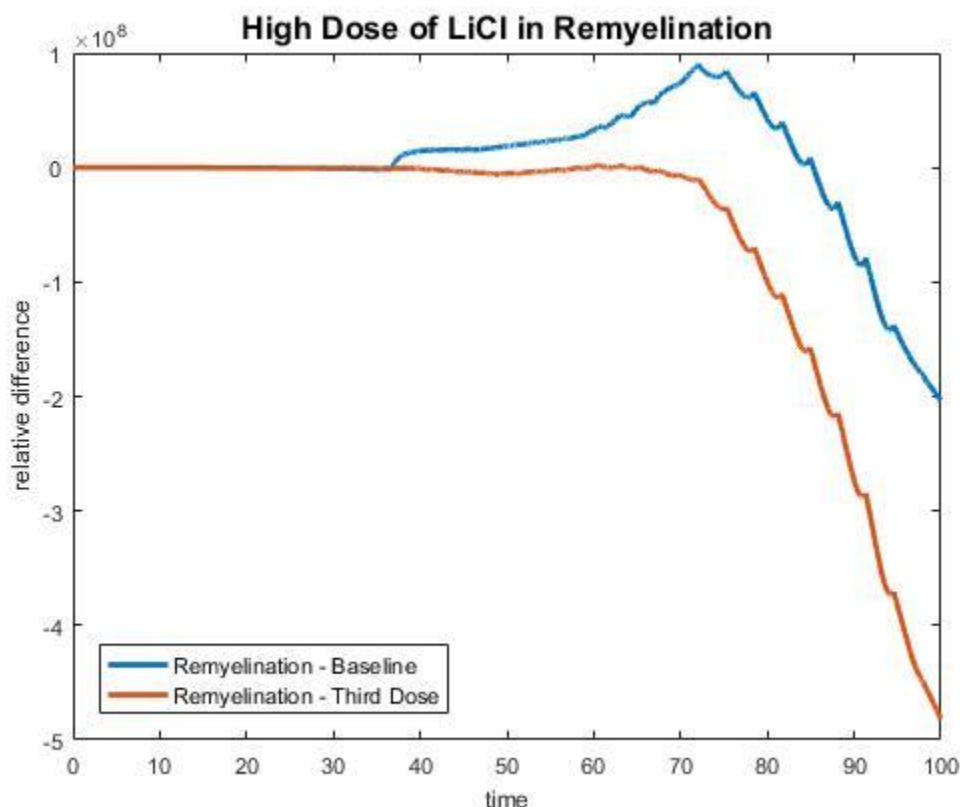


Figure 19 – Effect of highest dose of LiCl on remyelination

3.2.8 *LINGO-1*

A wide body of MS literature implicates LINGO-1 as a major player preventing proper remyelination (Mi et al., 2009; Jepson, et al., 2012; Tran, et al., 2014). As described previously, LINGO-1 plays a role in modulating BDNF and p38 MAPK signaling pathways (Mi, Pepinsky, & Cadavid, 2013) (Model 4). Therefore, LINGO-1 has become the leading target for use of protein antibodies in the treatment of MS. Currently in development, the protein antibody BIIB003 finished phase II clinical trials in March 2016 and inhibits LINGO-1 complex formation (Kremer et al., 2016). The use of this antibody is thought to be of significant use as a supplement to other MS therapies acting on inflammation and the immune system (Kremer et al., 2016). Addition of BIIB003 to the model predicts significantly greater remyelination for full

treatment states, with no significant change for partial treatment states (Figure 20). In addition, the antibody impacts remyelination in part by lowering levels of apoptosis (Figure 21).

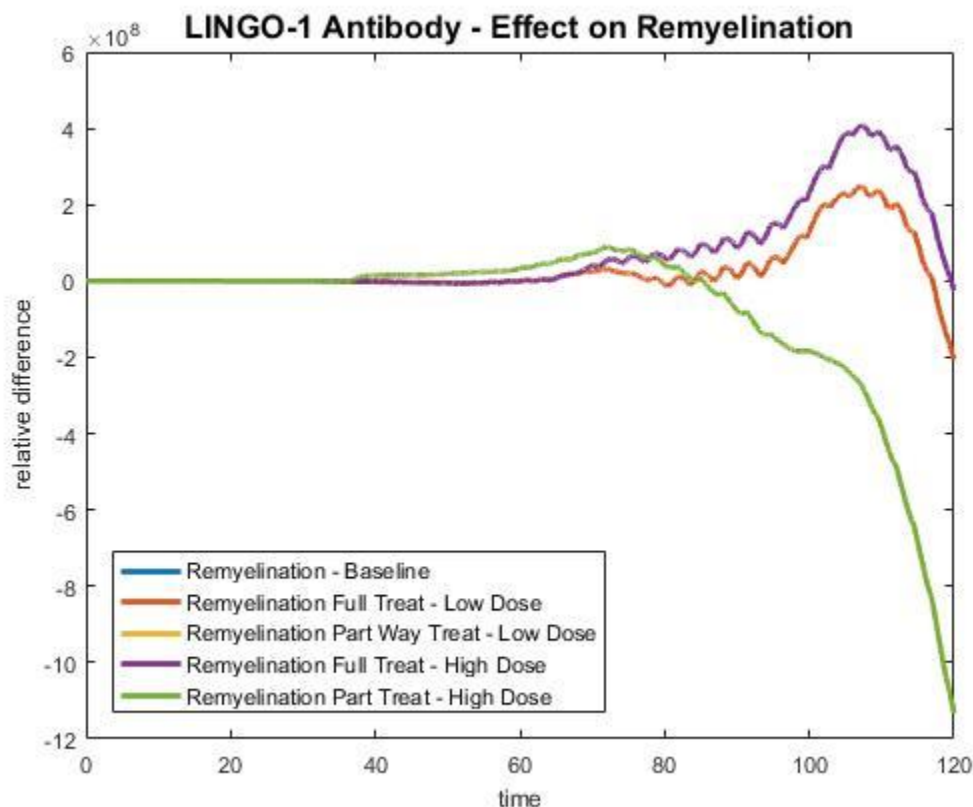


Figure 20 – BIIB003 effect on remyelination

3.3 Mixed Treatments

To further examine potential pharmaceutical treatments aimed at improving remyelination, several combined treatment states were explored. These combined treatment states utilize the most effective dose of each drug as described in the results above. The combinations used examined drugs unlikely to interact due to operation through separate mechanisms of action.

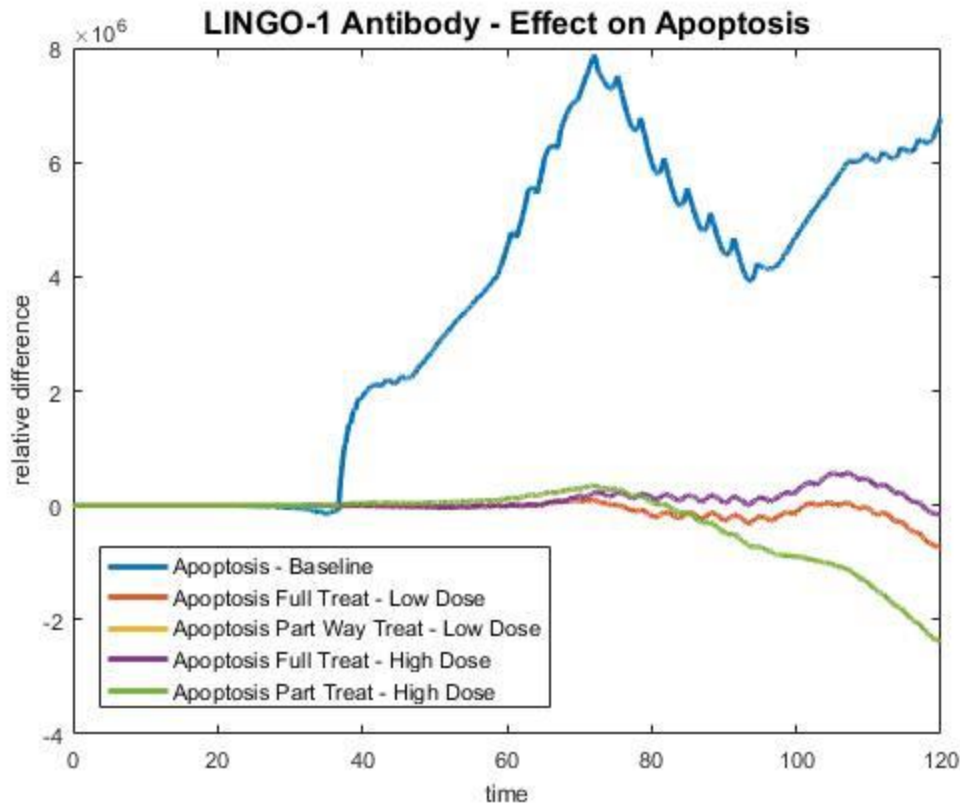


Figure 21 – BIIB003 effect on apoptosis

3.3.1 Glatiramer Acetate + Anticholinergic

The first combined treatment examined utilized a higher dose of GA and a lower dose of an anticholinergic. Results were compared directly with those of the anticholinergic alone. Use of both drugs led to significantly reduced levels of apoptosis (Figure 22). The model predicts combined use of these drugs in a full treatment state is effective in recovering remyelination compared to baseline, but not as effective as only benztropine at its higher dose (Figure 23). However, the combined treatment was as effective as low dose benztropine at recovery in a partial treatment (Figure 24).

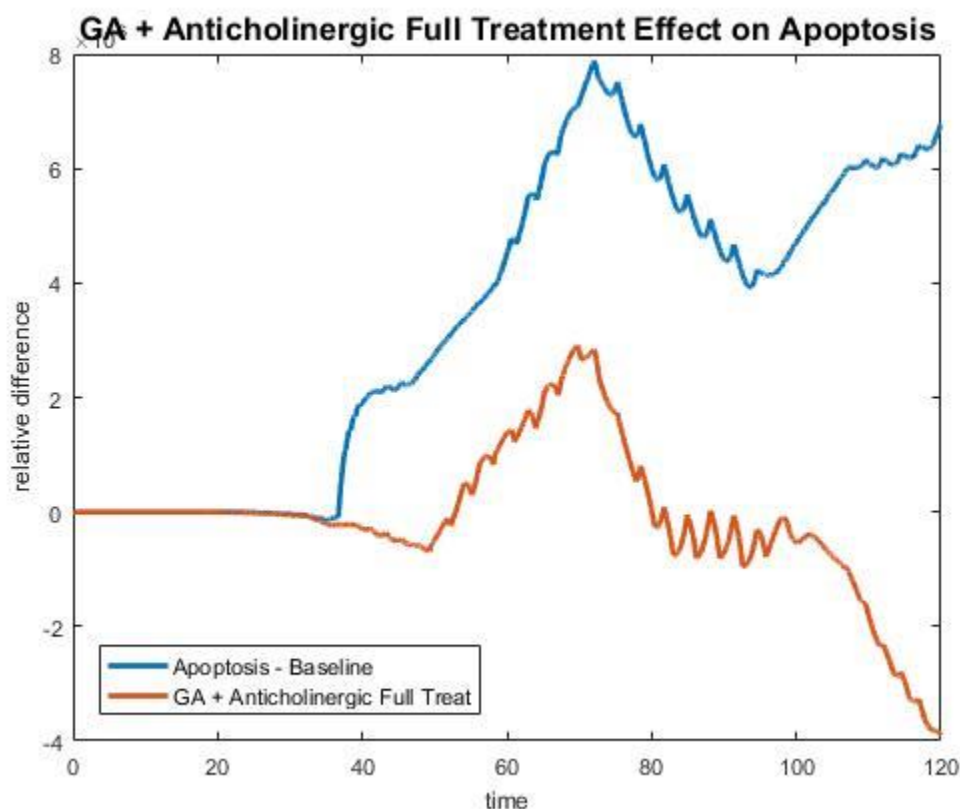


Figure 22 – GA and benztropine combined effects on apoptosis

3.3.2 Smoothened Agonist + Fingolimod

The next combined treatment examined is the use of a SMO agonist (clobetasol or halcinonide) with fingolimod. Results were compared directly with those of a SMO agonist. The model predicts combined treatment with these two drugs significantly increases rates of OPC migration (Figure 25). In addition, this also leads to a predicted decrease in levels of apoptosis (Figure 26). Overall, this combination is effective at increasing remyelination in a full treatment state (Figure 27), but not as successful in a partial treatment state when compared to fingolimod alone (Figure 28).

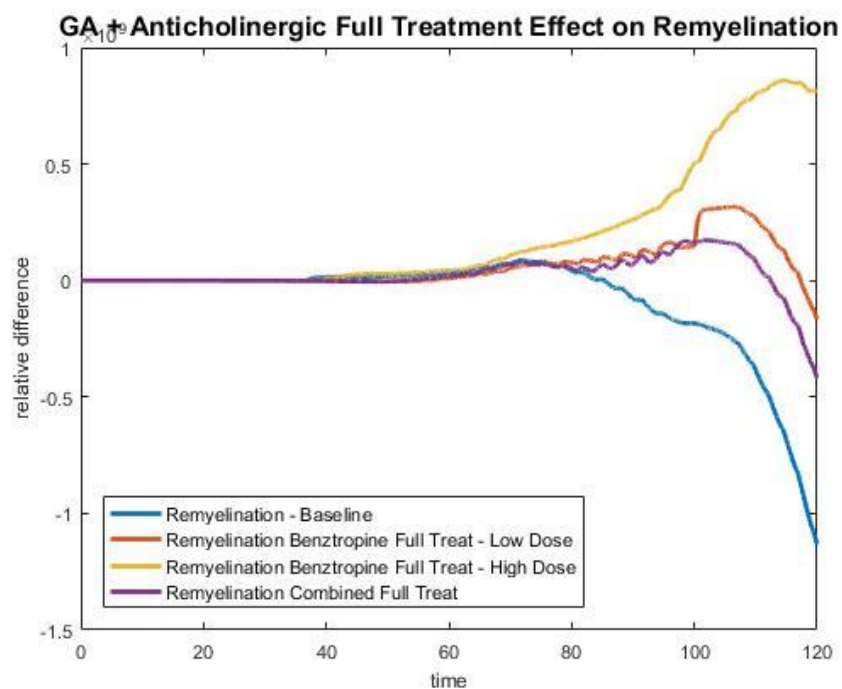


Figure 23 – GA and benztropine combined effect on remyelination in full treatment state

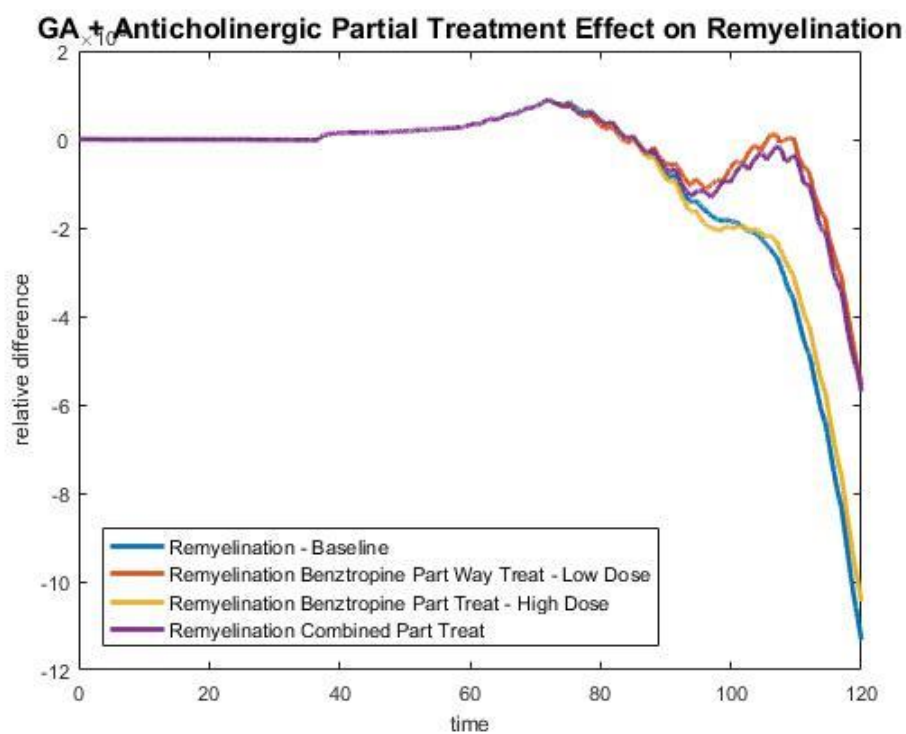


Figure 24 – GA and benztropine combined effect on remyelination in partial treatment state

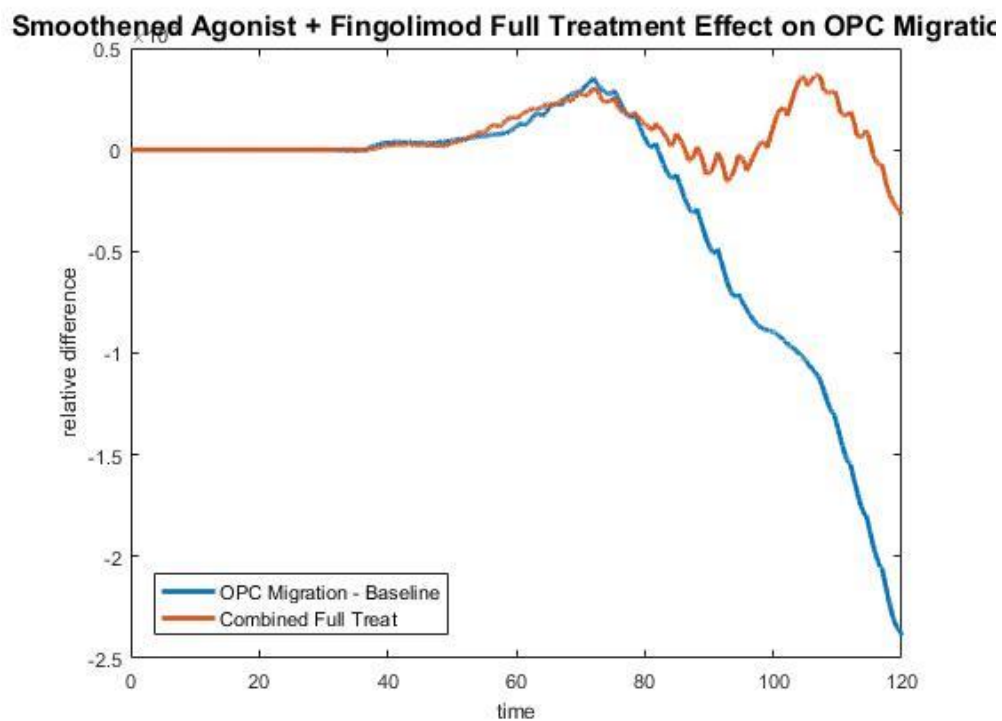


Figure 25 – Smoothed agonist and fingolimod effect on OPC Migration

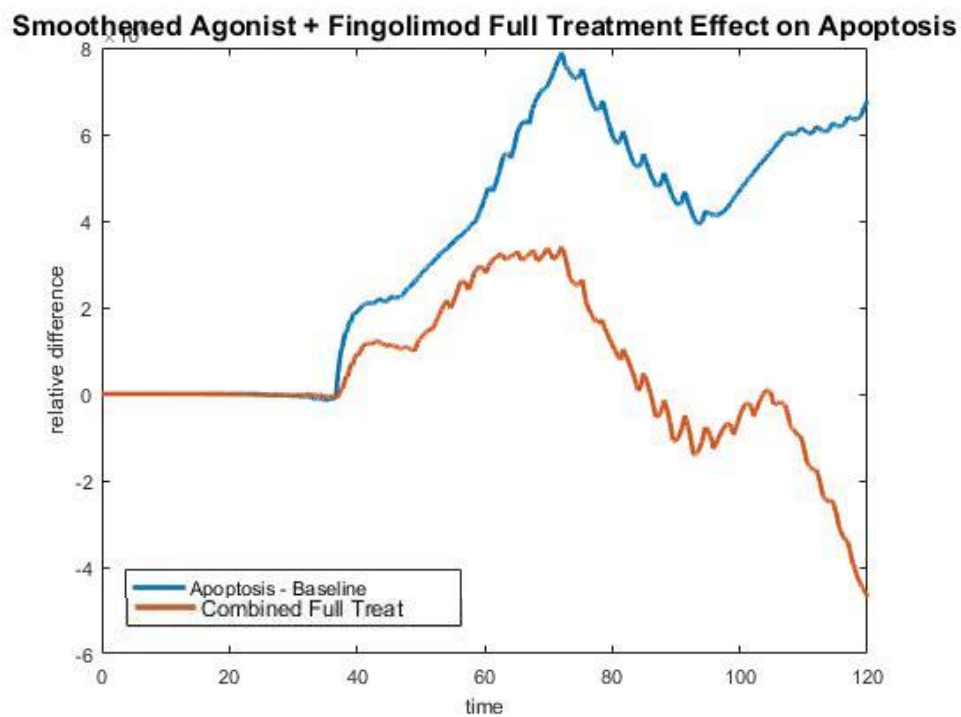


Figure 26 – Smoothed agonist and fingolimod effect on apoptosis

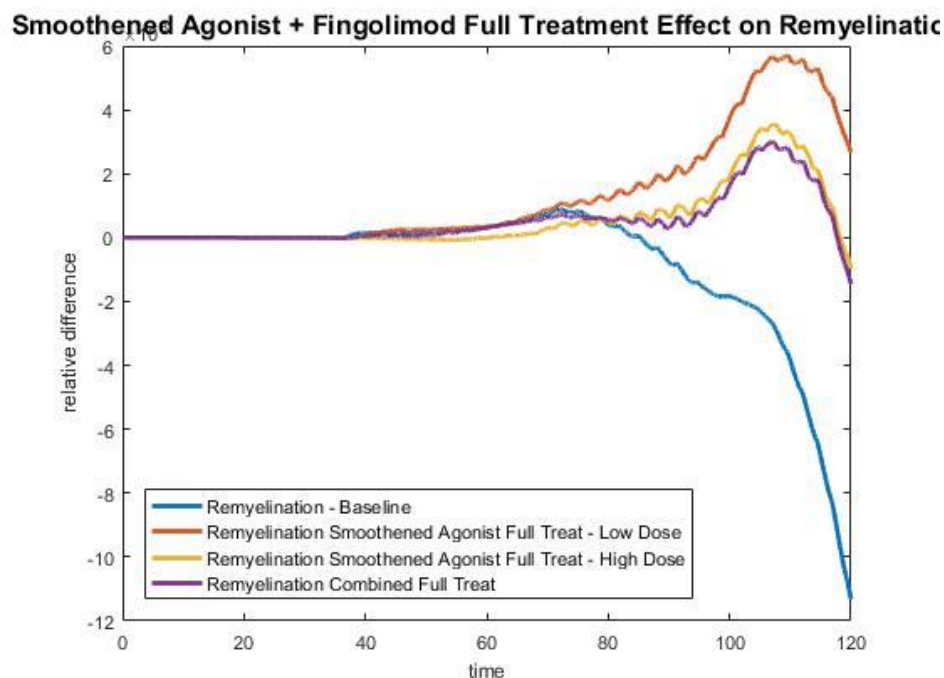


Figure 27 – Smoothened agonist and fingolimod effect on remyelination in full treatment state

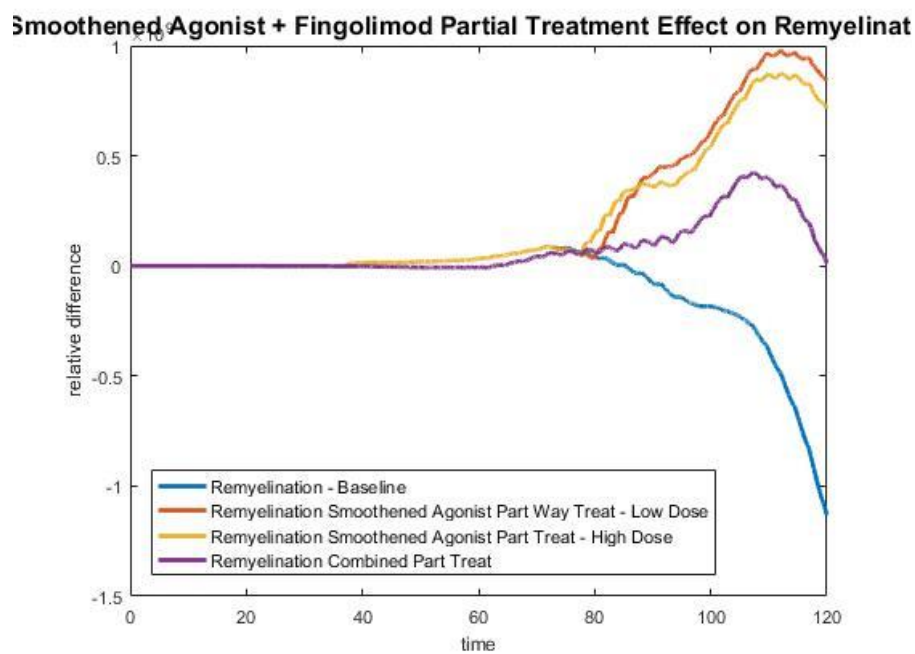


Figure 28 – Smoothened agonist and fingolimod effect on remyelination in partial treatment state

3.3.3 GA + rHIgM22

The final combined treatment examined is the use of GA with the integrin antibody rHIgM22.

The lower dose of integrin antibody was selected as it was more successful than the higher dose at stimulating remyelination. The combined treatment was able to significantly lower predicted levels of apoptosis (Figure 29). However, full treatment with a combination of these drugs does not promote remyelination (Figure 30). Furthermore, partial treatment is not as effective as stimulating remyelination as the integrin antibody alone, but is still improved from baseline (Figure 31).

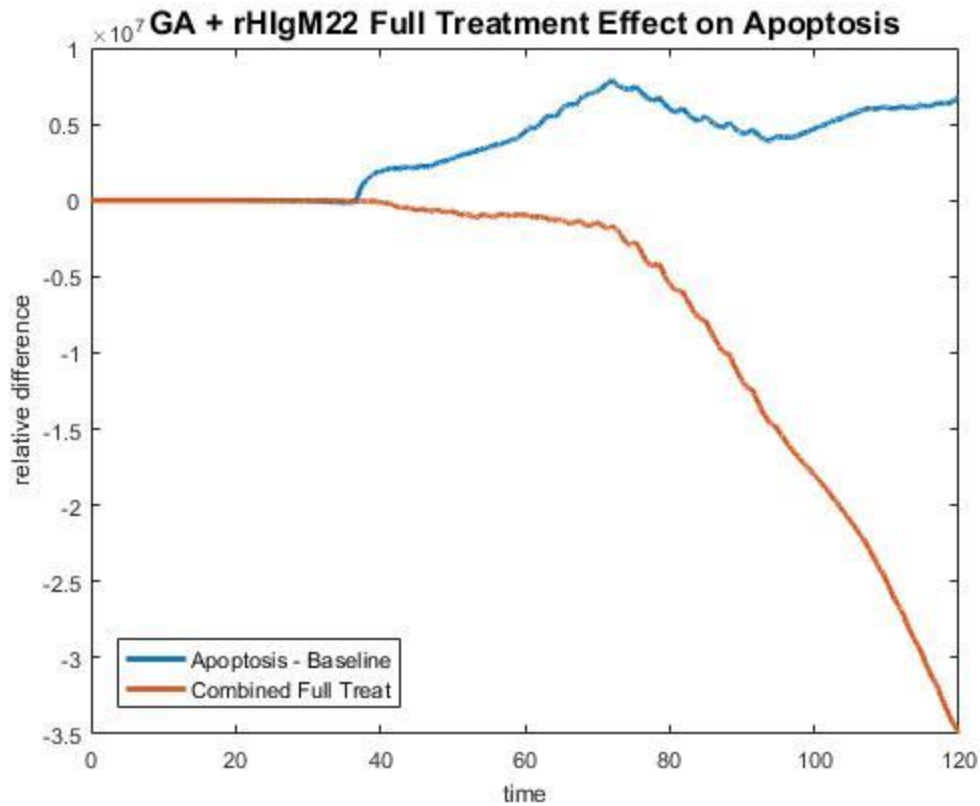


Figure 29 - Combined effect of GA and rHIgM22 on apoptosis

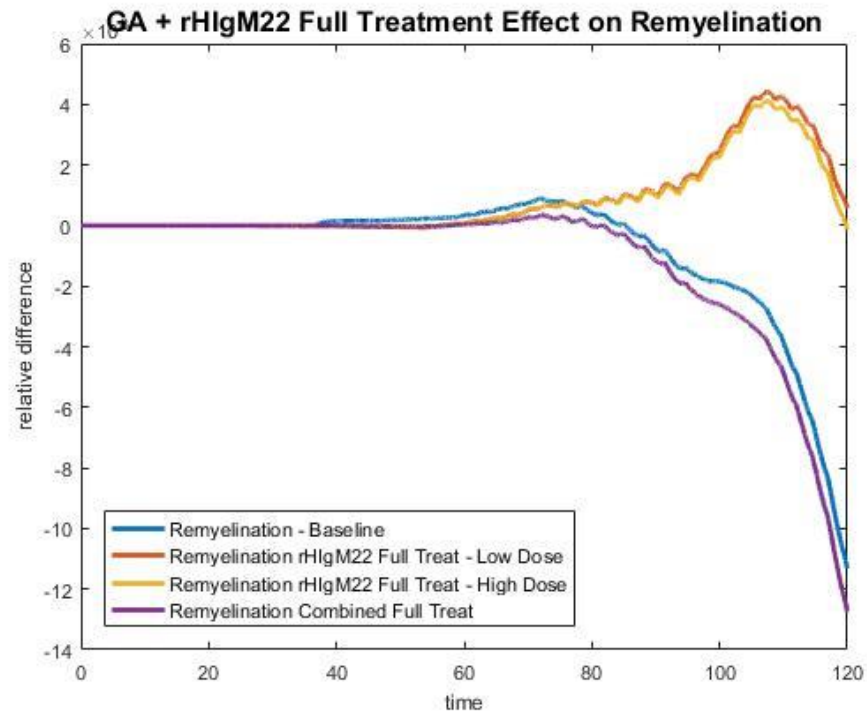


Figure 30 – Combined effect of GA and rHlgM22 on remyelination in full treatment state

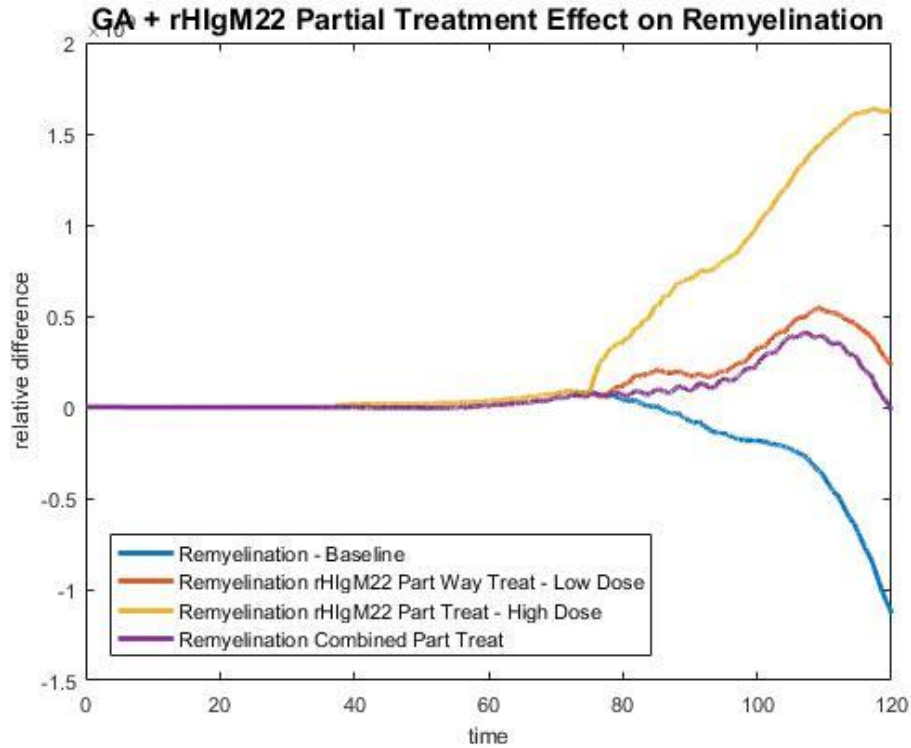


Figure 31 – Combined effect of GA and rHlgM22 on remyelination in partial treatment state

3.4 New Targets

Research into remyelination in multiple sclerosis is still a developing field. Most MS treatments target the immune response, and do not focus on activation of remyelination. The treatments examined above are not in mainstream use for the treatment of MS, and there remains a need for new information about pharmaceutical targets which may improve remyelination. Therefore, an exploration was undertaken aimed at finding potential pharmaceutical targets by utilizing hypothetical drugs in the mathematical model. This hypothetical drug would act to modulate a particular reaction through its rate equation.

3.4.1 Hyaluronic Acid Signaling

Hyaluronic acid has been described as a blocker of OPC differentiation (Back et al., 2005; Sloane et al., 2009). In addition, HA has been shown to improve OPC migration (Piao, Wang, & Duncan, 2013). Its presence in myelin lesions has led it to be a suggested target of interest in modulating remyelination. Two methods of modulation of HA signaling were examined. The first is the inhibition of hyaluronidase, the enzyme cleaving HMW-HA into HA oligomers. Use of this inhibitor reduced apoptosis in all cases except for full treatment at high dose in which it increased apoptosis (Figure 32). Furthermore, addition of a hyaluronidase inhibitor to the model led to increased remyelination in all cases, with higher doses leading to greater remyelination (Figure 33).

A second target considered is the Toll-like receptor 2. TLR2 has been shown to be the receptor through which HA operates to inhibit OPC differentiation (Sloane et al., 2009). TLR antagonists have been examined for their role in limiting inflammation in diseases such as rheumatoid arthritis. Therefore, a TLR2 antagonist was added to the mathematical model to examine its efficacy in improving remyelination. Addition of this antagonist greatly lowered levels of

apoptosis in all doses (Figure 34). The TLR2 antagonist also improved remyelination in all treatment states, and higher doses improved remyelination more than lower doses in both full and partial treatment states. (Figure 35).

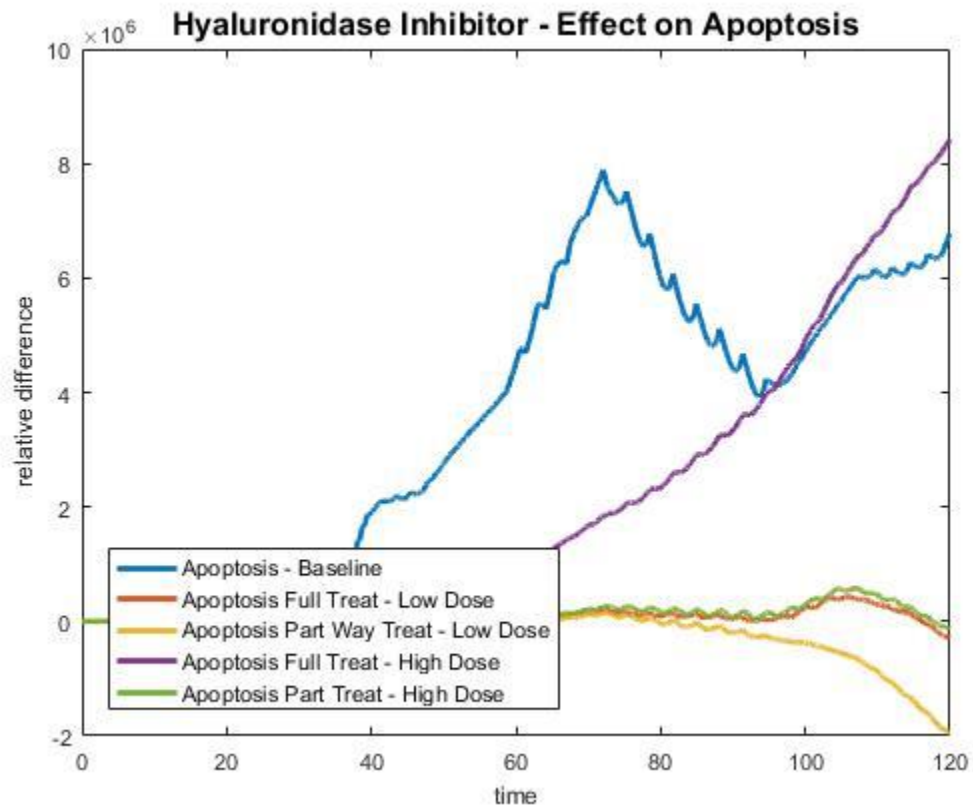


Figure 32 – Predicted effect of hyaluronidase inhibition on apoptosis of OPCs

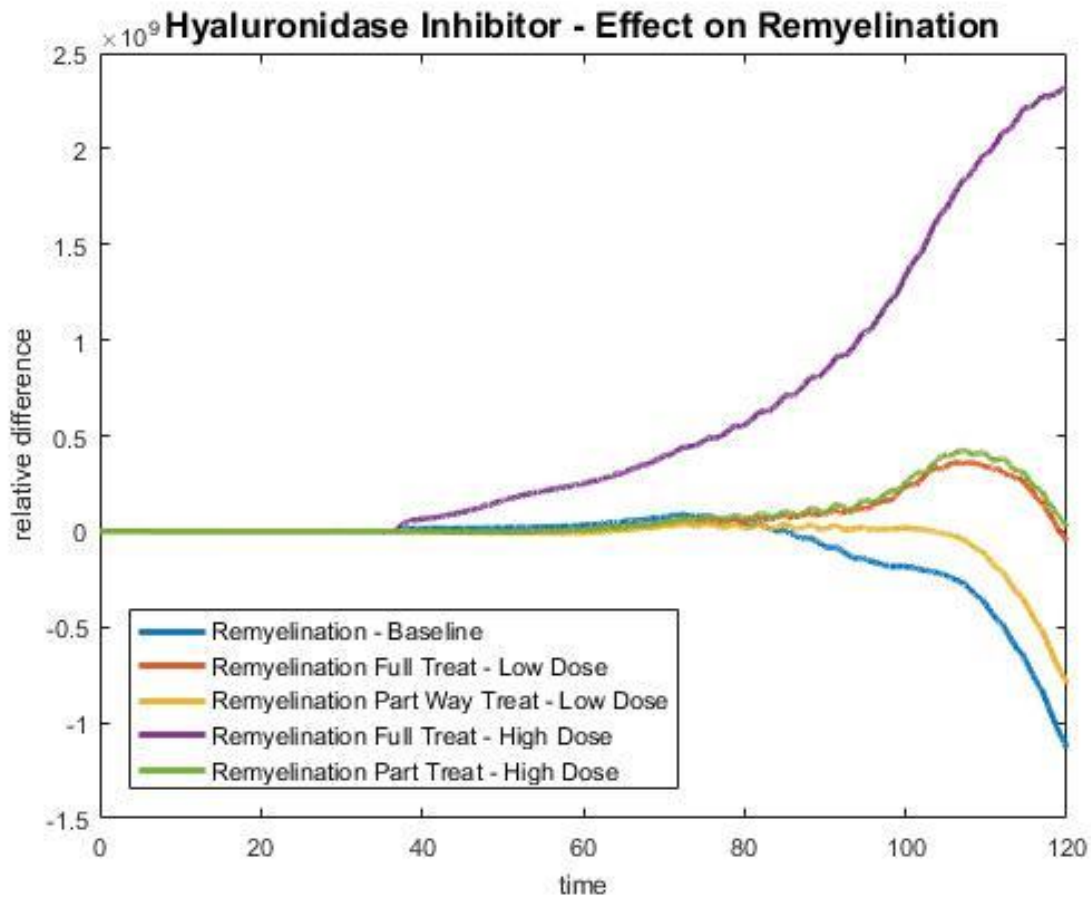


Figure 33 – Predicted effect of hyaluronidase inhibition on remyelination

3.4.2 Bone Morphogenic Protein Receptor

The second target suggested by the model is the BMPR. BMPR activation has been shown to inhibit the transcription of myelin basic protein as well as inhibit OPC differentiation (Weng et al., 2012; Xie et al., 2014). Currently there is no BMPR antagonist in clinical use. Use of the BMPR antagonist predicts increased expression of MBP compared to baseline in full treatment states, but not partial treatment states (Figure 36). In addition, there is a significant increase in remyelination in full treatment states, but not partial treatment states (Figure 37).

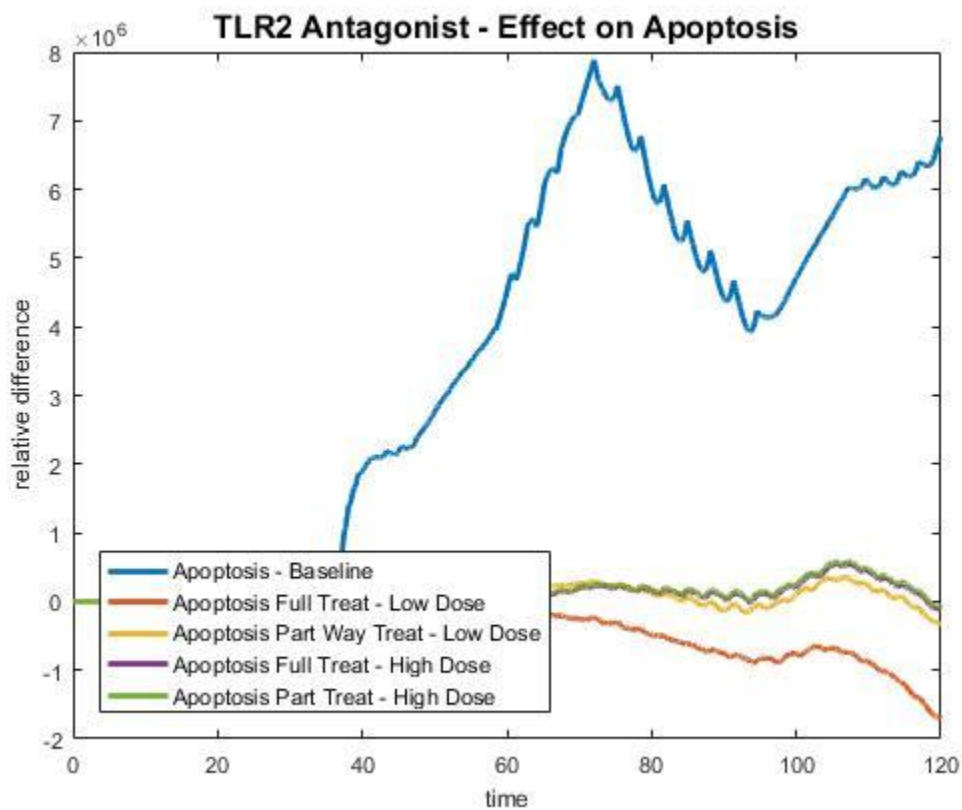


Figure 34 – Predicted effect of TLR2 antagonist on apoptosis of OPCs

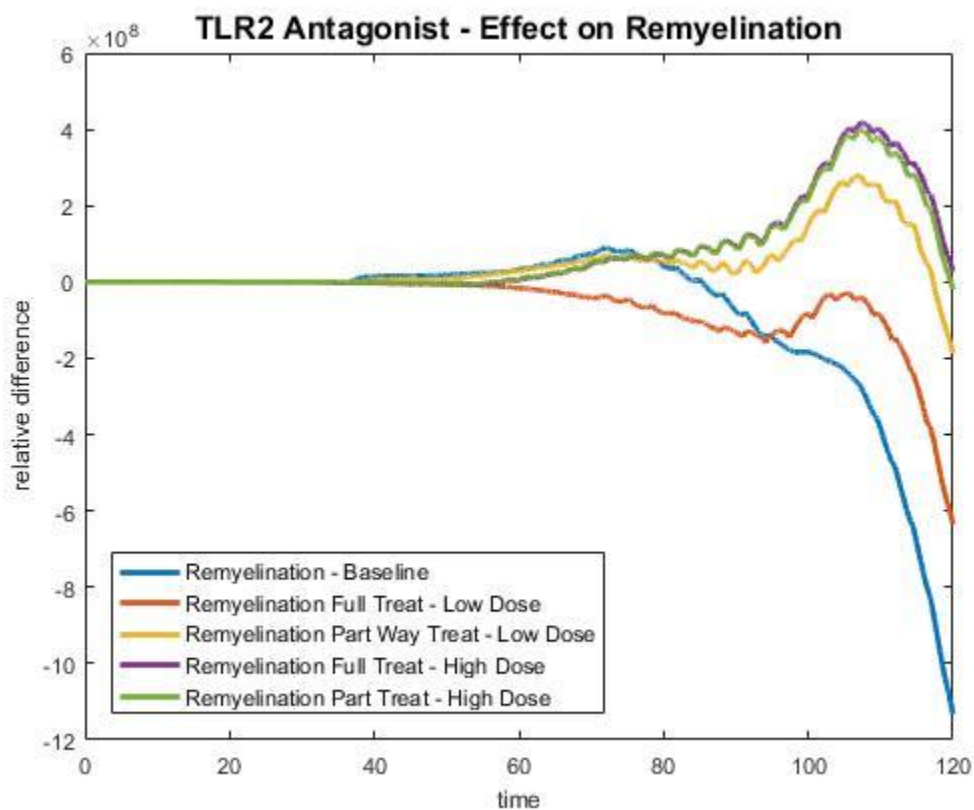


Figure 35 – Predicted effect of TLR2 antagonist on remyelination

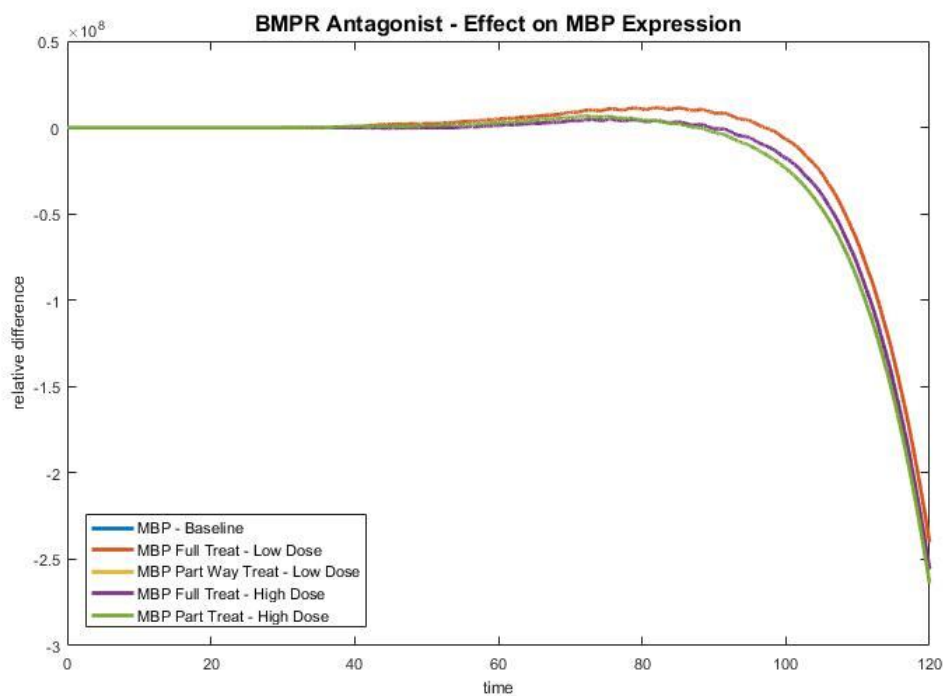


Figure 36 – Predicted effect of BMPR antagonist on MBP expression

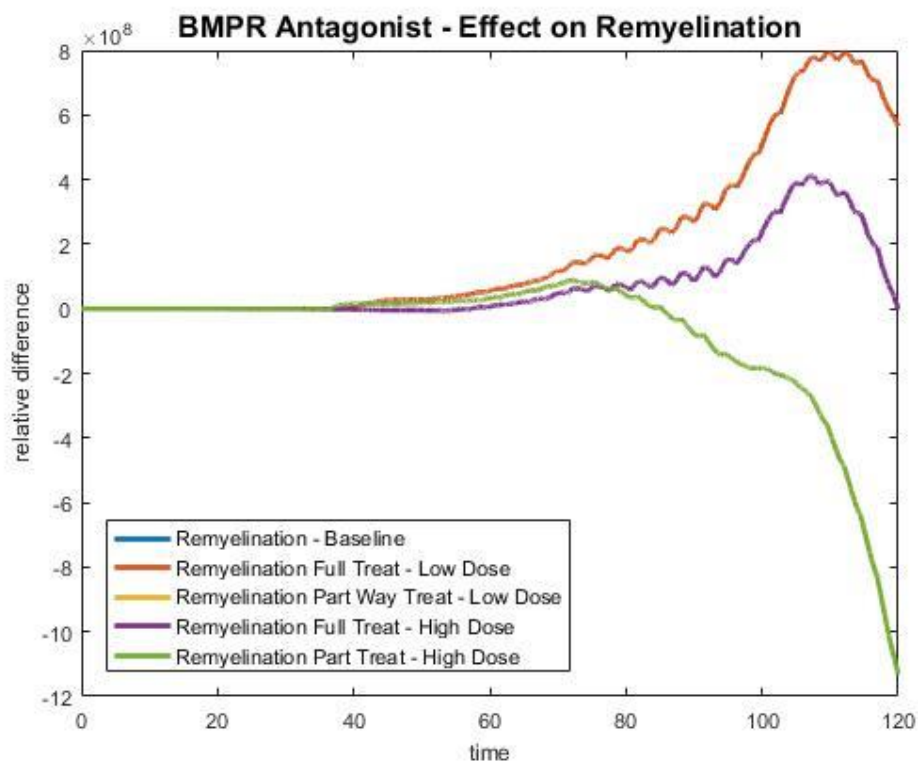


Figure 37 – Predicted effect of BMPR antagonist on remyelination

Treatment	Target	Full Treatment Efficacy	Partial Treatment Efficacy	Significant Effects
Glutiramer Acetate	Th2 Helper Cell – neurotrophic factors	High	Low	Increase in neurotrophic signals (i.e. BDNF)
Anticholinergic (Benztropine, Clemastine)	M1 + M3 muscarinic ACh receptors	High	Low	Improved OPC migration
Statins	HMG-CoA Reductase	Very low	None	Reduction in germylation of proteins
Smoothened Agonist (Halcinonide, Clobetasol)	Smoothened Receptor	High	High	Increase in RXR γ
rHlgM22	B3 integrin subunit	High	Low	Decrease in apoptosis, activation of Lyn kinase
Fingolimod	Sphingosine-1 phosphate receptor	High	Low	Stimulation of major kinase pathways
Indomethacin	Inactivation of GSK3 β	High	None	Mixed improvement of transcription factor expression
Lithium	Inhibition of β -catenin degradation	High (only at low doses)	None	Increase in active protein kinase B (Akt)
BIIB003	LINGO-1 inhibition	High	None	Reduced levels of apoptosis

Table 1 – Summary of treatments aimed at improving remyelination

Treatment	Full Treatment Efficacy	Partial Treatment Efficacy	Significant Effects
Glatiramer Acetate and Anticholinergic	Medium	Medium	Lower levels of apoptosis
Smoothened agonist and Fingolimod	High	Medium	Slight increase in levels of apoptosis
Glatiramer Acetate and rHlgM22	None	Low	Lower levels of apoptosis

Table 2 – Summary of drug cocktails examined and their efficacy

Target	Predicted Full Treatment Efficacy	Predicted Partial Treatment Efficacy	Predicted Significant Effects
Inhibition of Hyaluronidase	Medium	Low	Lower levels of apoptosis at low doses
TLR2 Antagonism	High	High	Lower levels of apoptosis, higher doses less effective
BMPR Antagonism	High	None	MBP expression increase

Table 3 – Summary of theoretical drug treatments for improving remyelination in MS

4. Discussion

4.1 Baseline/Disease State

The baseline state model properly mimics the current view of remyelination in MS, with particular regard for relapsing-remitting MS. For all positive, major contributing factors to remyelination there is a period of little change followed by short term successful increase in the form of brief spikes, followed by a predicted decline over the long term, while maintaining the spiking pattern. These results correlate strongly to the pathology of relapsing-remitting MS. MS pathology would show a period of demyelination in which the body would be slow to respond, followed by some successful remyelination which then fails over the long term. All major myelin proteins (MBP, PLP, and CNPase) follow this pattern, as does OPC migration, OPC differentiation, and overall remyelination. Counter to this, levels of apoptosis rise in the baseline state, which could be a driving force in the overall failure of remyelination.

4.2 Treatment State

Use of this mathematical model presents several treatment options which predict improvement of remyelination for multiple sclerosis. Glatiramer acetate, anticholinergics, statins, rHIgM22, fingolimod, indomethacin, lithium, and BIIB003 all show some form of efficacy in improving remyelination in MS (Table 1). Glatiramer acetate, already used in MS treatment, upregulates immune expression of certain neurotrophic factors for differentiating OPCs. The success of a higher dose offers encouragement that early use of glatiramer acetate could significantly improve remyelination. However, the more realistic delayed treatment scenarios improve remyelination only slightly, and also slightly increase rates of apoptosis. This increase in apoptosis may be in part related to the release of PDGF by Th2 cells, which has been shown to prevent slow differentiation and encourage cell division, leaving OPCs vulnerable to further inflammation

before eventually differentiating. Therefore, this implies glatiramer acetate may be only partially successful in improving remyelination.

Anticholinergic drugs, like benztropine and clemastine, provide some of the best improvement predicted in the model for remyelination. Anticholinergics influence the activity of several pathways including the expression of several other receptors (Model 5). The use of a low dose anticholinergic would be favorable not only because of the success of a lower dose partial treatment predicted by this model, but also due to the possibility in avoiding certain side effects. Overall, the improvement in remyelination, and particularly OPC migration, presented by anticholinergics makes them an important target for consideration.

Despite some evidence that use of statin drugs may improve overall remyelination, this model predicts little success in use of a statin. Partial treatment demonstrated no significant change from baseline, while high dose usage was predicted to encourage demyelination. Statin drugs block the HMG-CoA reductase enzyme, important in production of cholesterol, a vital part of myelin. This model predicts any benefit gained from limiting these lipids in their use for modifying proteins is outweighed by the harm this does in shrinking the pool of lipids for myelin production.

Smoothed receptor agonists, including halcinonide and clobetasol, improve overall expression of $\text{RXR}\gamma$. There was clear effectiveness of these agonists in overall improvement of remyelination. In particular, this treatment strategy showed some of the greatest success in partial treatment states. This success marks SMO agonists as a key target for future examination of remyelination in MS.

Use of the integrin receptor subunit antibody rHlgM22 in the model predicts sustained successful remyelination compared to baseline. rHlgM22 exerts its effects by leading to downstream phosphorylation of the Lyn kinase, which suppresses apoptosis through inactivation of caspases. The results point to a use of low dose antibody being more effective than higher dose, but with both providing improved remyelination and reduced levels of apoptosis. In addition, the use of the antibody in a partial treatment state also predicts more successful remyelination and lowered apoptosis compared to baseline, presenting this antibody as another target for consideration in improving remyelination in MS.

The model predicts that use of the sphingosine receptor agonist fingolimod improves remyelination in all treatment states considered. Fingolimod's action at this receptor leads to downstream activation of major kinase pathways, including the p38 MAPK and ERK pathways, and resulting in OPC differentiation. The success of fingolimod in both full and partial treatment states implicates it as yet another strong target for consideration in the treatment of MS.

However, the use of a higher dose in the partial treatment state is less effective than that of a lower dose, providing unclear evidence of the efficacy of a particular dose in the more realistic partial treatment model.

Modulators of Wnt/ β -catenin signaling provide some evidence for successful improvement of remyelination. Indomethacin, an inhibitor of this signaling pathway improves remyelination in full treatment states, with a higher dose proving more successful than a lower dose. A stimulator of this pathway, treatment with lithium leads to improved protein kinase B signaling and increased remyelination. However, higher doses of lithium can cause the opposite effect, resulting in decreased remyelination. In addition, neither treatment impacted remyelination in partial treatment states. This implies the action of the Wnt/ β -catenin pathway is exerted early in

OPC differentiation, and may not make this pathway an ideal aim for examining potential remyelination treatments. Furthermore, because of lithium's potential to decrease remyelination in high doses, it is unclear whether this efficacy at low doses will correlate with success in the form of an actual treatment.

Use of the LINGO-1 antibody BIIB003 resulted in lower levels of apoptosis and improved remyelination in full treatment states. The LINGO-1 receptor is involved in a number of cell surface interactions, most of which are implicated in inhibiting important cell signals (Model 4). However, while full treatment with LINGO-1 antibody was successful, there was no significant change predicted in partial treatment states. As LINGO-1 is involved in an OPC-neuron interaction, it is likely to take place soon after demyelination. Therefore, it may be difficult to act on LINGO-1 prior to it exerting its effects on the first set of OPC's to respond. However, the antibody could act on any subsequent demyelination, and for this reason BIIB003 may be a valuable target for improving remyelination.

Several combined treatment states were analyzed for potential success of drug cocktails in increasing remyelination. The first cocktail combined the effects of glatiramer acetate, to improve immune signals, and anticholinergics, to improve receptor expression. This cocktail lowered levels of apoptosis in a full treatment state, and improved remyelination overall in a full treatment state, though not at the level of an anticholinergic alone. However, unlike the anticholinergic alone, partial treatment with the first cocktail improved remyelination more efficiently. This difference may involve stimulation of PDGF expression in the presence of GA, which encourages OPC proliferation over differentiation. This is seen in treatment with GA alone, which saw a delay in remyelination for high dose full treatments before becoming the most successful trial for GA. Furthermore, it may implicate GA as a treatment which exerts some

negative effects on remyelination, but has an overall net positive effect. Success in the partial treatment model for the GA and anticholinergic, the most accurate reflection of treating a patient, implicates this cocktail as one for consideration in remyelination. The second cocktail used a smoothened receptor agonist and fingolimod, to upregulate active kinase levels. This second cocktail did recover remyelination in a full treatment state, but was not very effective in the partial treatment state. In addition, this partial treatment surprisingly increased levels of apoptosis, implying the second cocktail is not an ideal mixture of treatments for remyelination. The final cocktail combined glatiramer acetate and rHIgM22, to increase anti-apoptotic Lyn kinase. This cocktail was successful in lowering levels of apoptosis, but failed at improving remyelination in a full treatment state. This effect is likely similar to the actions of GA mentioned previously. However, it slightly recovered remyelination in a partial treatment state. Therefore, the efficacy of this final cocktail is likely mixed, with some potential for treatment of remyelination.

Two new targets for remyelination were examined using the model designed here (Table 3). The first, hyaluronic acid signaling was modulated with inhibition of hyaluronidase and inhibition of TLR2. Inhibition of hyaluronidase resulted in increased remyelination in all treatment states, but with increased apoptosis in a full treatment at high dose. Therefore, there is promise for inhibition of hyaluronidase in some low dose capacity. TLR2 antagonism also resulted in recovery of remyelination, but this time in all treatment states. In addition, levels of apoptosis were significantly reduced in all treatment states. This implicates TLR2 as a target for consideration in improvement of remyelination in MS. Finally, the use of a BMPR antagonist improved expression of MBP in the mathematical model and led to improved levels of remyelination. However, partial treatment states showed no significant improvement, implying

that any targeting of BMPR would need to be early in pathology. This result does provide promise for the targeting of signaling related to BMPR, as its mechanisms of action to modulate MBP expression become more clear. Overall, the model successfully predicts the actions of potential MS treatments for remyelination, and is useful in exploring future targets for examination of remyelination.

5. Conclusion

This paper describes the production of a testable, mathematical model of remyelination in multiple sclerosis. Models of this nature provide a convenient and efficient method for examining potential efficacy of pharmaceutical treatments for multiple sclerosis. The model consists primarily of two distinct, but related, processes: OPC differentiation and the production of myelin components. The former process is upregulated by the presence of certain transcription factors, and inhibited by OPC proliferation. Remyelination overall is then considered based on the successful production of myelin components, while also taking into account the roles of OPC migration and apoptosis. The baseline model comparing a disease and healthy state accurately reflects a course of relapsing-remitting multiple sclerosis, with occasional spikes of remyelination which fail over time. Overall, the model examines the effectiveness of multiple treatments aimed at stimulating and promoting remyelination in multiple sclerosis. These treatments include those already in use, some in clinical trial, some in consideration for clinical trial, and drug cocktails. Furthermore, this model is also able to suggest targets for future evaluation in their efficacy in improving remyelination. Treatment results reinforce ideas of early diagnosis and treatment, as delayed treatment scenarios most often show lower predicted remyelination than full treatment states. Several of these drugs represent approaches which could

improve the failing remyelination pathway present in multiple sclerosis, and should be seriously considered for clinical trial.

Acknowledgements:

This work was supported by grants from The College of William and Mary and by The Roy R. Charles Center for Academic Excellence at The College of William and Mary.

I would like to thank Sarah Day and Christy Porter for being a part of my thesis committee, and especially Randy Coleman for being so supportive of me and this project throughout my time at William & Mary.

The qualitative models used in this work were developed with the program CellDesigner version 4.2, which can be found at <http://www.celldesigner.org/>.

The relative protein species concentrations used in this work were obtained via the PaxDB Protein Abundance Database operated by the University of Zurich, which can be found at <http://www.pax-db.org/>.

The mathematical models used in this work were developed with MATLAB R2016b, which can be found at: <http://www.mathworks.com/products/matlab/>.

Abbreviations:

MS, Multiple Sclerosis; CNS, Central Nervous System; OL, Oligodendrocyte; OPC, Oligodendrocyte Progenitor Cell; BST, Biochemical Systems Theory; ODE, Ordinary Differential Equation; PDGF, Platelet Derived Growth Factor; PDGFR α , Platelet Derived Growth Factor Receptor Alpha; Olig2, Oligodendrocyte Transcription Factor 2; NG2, Neural/Glial Antigen 2; O1, Oligodendrocyte Marker 1; O4, Oligodendrocyte Marker; ECM, Extracellular Matrix; ITGAV, Integrin Alpha V Receptor; p38 MAPK, Protein 38 Mitogen Activated Protein Kinase; UDP, Uridine Diphosphate; GPR17, Cysteinyl Leukotriene Receptor; ET-1, Endothelin-1; CNTF, Ciliary Neurotrophic Factor; IL-1 β , Interleukin-1 beta; FGF-2, Fibroblast Growth Factor 2; FGFR1, Fibroblast Growth Factor Receptor 1; gp130, Glycoprotein 130; JAK2, Janus Kinase 2; STAT, Signal Transducer and Activator of Transcription; TnC, Tenascin C; Akt, Protein Kinase B; TNF α , Tumor Necrosis Factor Alpha; NF- κ B, Nuclear Factor Kappa-Light-Chain-Enhancer of Activated B Cells; CXCL12, C-X-C motif chemokine 12; LIF, Leukemia Inhibitor Factor; CXCR4, C-X-C motif chemokine receptor 4; BDNF, Brain Derived Neurotrophic Factor; TrkB, Tropomyosin Receptor Kinase B; IGF-1, Insulin-like Growth Factor 1; IGFR1, Insulin-like Growth Factor Receptor 1; PI3K, Phosphoinoside-3 Kinase; LINGO-1, Immunoglobulin-like Domain-containing Protein 1; RhoA, Ras homolog gene family member A; ROCK, Rho-associated protein kinase; PTEN, phosphatase and tensin homolog; Erb, Receptor Tyrosine-protein Kinase Erb; MBP, Myelin Basic Protein; cAMP,

Cyclic Adenosine Monophosphate; PKA, Protein Kinase A; ERK, Extracellular Signal-Regulated Kinase; NRG1, Neuregulin 1; LRP, Low-density Lipoprotein Related Receptor Protein; GSK3 β , Glycogen Synthase Kinase 3 Beta; SIP1, Zing Finger E-box-binding Homeobox 2; MYRF, Myelin Regulatory Factor; YY1, Yin-Yang 1; Tcf4, Transcription Factor 4; sIL-6R, Soluble Interleukin 6 Receptor; mTOR, Molecular Target of Rapamycin; PDK1, 3-phosphoinositide Dependent Protein Kinase-1; S6K, Ribosomal Protein S6 Kinase Beta-1; CREB, cAMP Response Element-Binding Protein; MNK, MAP kinase-interacting serine/threonine-protein kinase; 9cRA, 9-cis-retinoic Acid; RXR γ , Retinoid X Receptor Gamma; DR6, Death Receptor 6; CytC, Cytochrome C; BAD, Bcl-2-associated Death Promoter; Bcl-2, B-cell Lymphoma 2; SOX2, Sex Determining Region Y-box 2; TGF α , Transforming Growth Factor Alpha; HB-EGF, Heparin-Binding Epidermal Growth Factor; EGFR, Epidermal Growth Factor Receptor; ILK, Integrin-Linked Kinase; Cdk5, Cyclin-dependent Kinase 5; WAVE2, Wiskott-Alrich Syndrome Protein Family Member 2; NMDA, N-methyl-D-aspartic acid; Tiam1, T lymphoma invasion and metastasis 1; Rac1, Ras-related C3 botulinum toxin substrate 1; HA, hyaluronic acid; HMW, high molecular weight; p21, Cyclin-dependent kinase inhibitor 1; p27, Cyclin-dependent kinase inhibitor 1B; Egr2, Early Growth Response Gene 2; Sp5, Trans-acting Transcription Factor Sp5; BMP, Bone Morphogenic Protein; HDAC, Histone Deacetylase; mSin3a, Paired Amphipathic Helix Protein Sin3a; hnRNP A2, heterogeneous nuclear ribonucleoprotein A2; eIF4e, Eukaryotic Initiation Factor 4e; 4EBP1, 4e Binding Protein 1; NT-3, Neurotrophin-3; S6RP, Ribosomal Protein S6; S6K, S6 Kinase; PLP, Proteolipid Protein; CNPase, 2', 3' – Cyclic-nucleotide 3' phosphodiesterase; MAG, Myelin-Associated Glycoprotein; MPZ, Myelin Protein Zero; MOG, Myelin Oligodendrocyte Glycoprotein; GA, Glatiramer Acetate; S1PR, Sphingosine 1-Phosphate Receptor; LiCl, Lithium Chloride; TLR2, Toll-like Receptor 2; SMO, Smoothed Receptor

References:

- Aguirre, A., Dupree, J.L., Mangin, J.M., & Gallo, V. (2007). A functional role for EGFR signaling in myelination and remyelination. *Nature Neuroscience*, 10(8), 990-1002.
- Ahmad, T.K., Acosta, C., Cortes, C., Lakowski, T.M., Gangadaran, S., & Namaka, M. (2016). Transcriptional Regulation of Brain-Derived Neurotrophic Factor (BDNF) by Methyl CpG Binding Protein 2 (MeCP2): a Novel Mechanism for Re-Myelination and/or Myelin Repair Involved in the Treatment of Multiple Sclerosis (MS). *Molecular Neurobiology*, 53, 1092-1107.
- Albrecht, P.J., Murtie, J.C., Ness, J.K., Redwine, J.M., Enterline, J.R., Armstrong, R.C., & Levison, S.W. (2003). Astrocytes produce CNTF during the remyelination phase of viral-induced spinal cord demyelination to stimulate FGF-2 production. *Neurobiology of Disease*, 13, 89-101.

- Amur-Umarjee, S., Schonmann, V., & Campagnoni, A.T. (1997). Neuronal Regulation of Myelin Basic Protein mRNA Translocation in Oligodendrocytes Is Mediated by Platelet-Derived Growth Factor. *Developmental Neuroscience*, 19, 143-151.
- Arnett, H.A., Wang, Y., Matsushima, G.K., Suzuki, K., & Ting, J.P. (2003). Functional Genomic Analysis of Remyelination Reveals Importance of Inflammation in Oligodendrocyte Regeneration. *Journal of Neuroscience*, 23(30), 9824-9832.
- Ascherio, A., Munger, K.L., & Simon, K.C. (2010). Vitamin D and multiple sclerosis. *Lancet Neurology*, 9, 599-612.
- Back, S.A., Tuohy, T.M., Chen, H., Wallingford, N., Craig, A., Struve, J., ... Sherman, L.S. (2005). Hyaluronan accumulates in demyelinated lesions and inhibits oligodendrocyte progenitor maturation. *Nature Medicine*, 11(9), 966-972.
- Baer, A.S., Syed, Y.A., Kang, S.U., Mitteregger, D., Vig, R., ffrench-Constant, C., ... Kotter, M.R. (2009). Myelin-mediated inhibition of oligodendrocyte precursor differentiation can be overcome by pharmacological modulation of Fyn-RhoA and protein kinase C signalling. *Brain*, 132, 465-481.
- Bankston, A.N., Li, W., Zhang, H., Ku, L., Liu, G., Papa, F., ... Feng, Y. (2013). p39, the Primary Activator for Cyclin-dependent Kinase 5 (Cdk5) in Oligodendroglia, Is Essential for Oligodendroglia Differentiation and Myelin Repair. *Journal of Biological Chemistry*, 288, 18047-18057.
- Bauer, N.M., Moos, C., van Horssen, J., Witte, M., van der Valk, P., Altenhein, B., ... White, R. (2012). Myelin Basic Protein synthesis is regulated by small non-coding RNA 715. *EMBO Reports*, 13(9), 827-834.
- Berndt, J.A., Kim, J.G., Tasic, M., Kim, C., & Hudson, L.D. (2001). The transcriptional regulator Yin Yang 1 activates the myelin PLP gene. *Journal of Neurochemistry*, 77, 935-942.
- Braatz, E.M. & Coleman, R.A. (2015). A mathematical model of insulin resistance in Parkinson's Disease. *Computational Biology and Chemistry*, 56, 84-97.
- Broome, T.M. & Coleman, R.A. (2011). A mathematical model of cell death in multiple sclerosis. *Journal of Neuroscience Methods*, 201, 420-425.
- Brosnan, C.F. & John, G.R. (2009). Revisiting Notch in remyelination of multiple sclerosis lesions. *Journal of Clinical Investigation*, 119(1), 10-13.
- Bujalka, H., Koenning, M., Jackson, S., Perreau, V.M., Pope, B., Hay, C.M., ... Emery, B. (2013). MYRF Is a Membrane-Associated Transcription Factor That Autoproteolytically Cleaves to Directly Activate Myelin Genes. *PLoS Biology*, 11(8).

- Calzá., L., Fernandez, M., & Giardino, L. (2010). Cellular approaches to central nervous system remyelination stimulation: thyroid hormone to promote myelin repair via endogenous stem and precursor cells. *Journal of Molecular Endocrinology*, 44, 13-23.
- Cannoll, P.D., Musacchio, J.M., Hardy, R., Reynolds, R., Marchionni, M.A., & Salzer, J.L. (1996). GGF/Neuregulin Is a Neuronal Signal That Promotes the Proliferation and Survival and Inhibits the Differentiation of Oligodendrocyte Progenitors. *Neuron*, 17, 229-243.
- Cervellini, I., Annenkov, A., Brenton, T., Chernajovsky, Y., Ghezzi, P., & Mengozzi, M. (2013). Erythropoietin (EPO) Increases Myelin Gene Expression in CG4 Oligodendrocyte Cells through the Classical EPO Receptor. *Molecular Medicine*, 19, 223-229.
- Choo, A.Y., Roux, P.P., & Blenis, J. (2006). Mind the GAP: Wnt Steps onto the mTORC1 Train. *Cell*, 126, 834-836.
- Coelho, R.P., Yuelling, L.M., Fuss, B., & Sato-Bigbee, C. (2009). Neurotrophin-3 Targets the Translational Initiation Machinery in Oligodendrocytes. *Glia*, 57, 1754-1764.
- Cohen, R.I. & Almazan, G. (1994). Rat Oligodendrocytes Express Muscarinic Receptors Coupled to Phosphoinositide Hydrolysis and Adenylyl Cyclase. *European Journal of Neuroscience*, 6, 1213-1224.
- Compston, A. & Coles, A. (2002). Multiple Sclerosis. *Lancet*, 360(9333). 648.
- Constantinescu, C.S., Farooqi, N., O'Brien, K., & Gran, B. (2011). Experimental autoimmune encephalomyelitis (EAE) as a model for multiple sclerosis (MS). *British Journal of Pharmacology*, 164, 1079-1106.
- Cui, Q.L., Fang, J., Kennedy, T.E., Almazan, G., & Antel, J.P. (2014). Role of p38 MAPK in S1P Receptor-Mediated Differentiation of Human Oligodendrocyte Progenitors. *Glia*, 62, 1361-1375.
- De Angelis, F., Bernardo, A., Magnaghi, V., Minghetti, L., & Tata, A.M. (2011). Muscarinic Receptor Subtypes as Potential Targets to Modulate Oligodendrocyte Progenitor Survival, Proliferation, and Differentiation. *Developmental Neurobiology*, 72, 713-728.
- Deshmukh, V.A., Tardif, V., Lyssiotis, C.A., Green, C.C., Kerman, B., Kim, H.J., ... Lairson, L.L. (2013). A regenerative approach to the treatment of multiple sclerosis. *Nature*, 502, 327-332.
- Deverman, B.E. & Patterson, P.H. (2012). Exogenous Leukemia Inhibitory Factor Stimulates Oligodendrocyte Progenitor Cell Proliferation and Enhances Hippocampal Remyelination. *Journal of Neuroscience*, 32(6), 2100-2109.

- Emery, B., Agalliu, D., Cahoy, J.D., Watkins, T.A., Dugas, J.C., Mulinyawe, S.B., ... Barres, B.A. (2009). Myelin Gene Regulatory Factor Is a Critical Transcriptional Regulator Required for CNS Myelination. *Cell*, 138, 172-185.
- Espinosa-Jefferey, A., Kumar, S., Zhao, P.M., Awosika, O., Agbo, C., Huang, A., ... de Vellis, J. (2002). Transferrin Regulates Transcription of the MBP Gene and Its Action Synergizes with IGF-1 to Enhance Myelinogenesis in the md Rat. *Developmental Neuroscience*, 24, 227-241.
- Fancy, S.P., Chan, J.R., Baranzini, S.E., Franklin, R.J., & Rowitch, D.H. (2011). Myelin Regeneration: A Recapitulation of Development?. *Annual Review of Neuroscience*, 34, 21-43.
- Fancy, S.P., Harrington, E.P., Yuen, T.J., Silbereis, J.C., Zhao, C., Varanzini, S.E., ... Rowitch, D.H. (2011). Axin2 as regulatory and therapeutic target in newborn brain injury and remyelination. *Nature Neuroscience*, 14(8), 1009-1016.
- Fischer, R., Wajant, H., Kontermann, R., Pfizenmaier, K., & Maier, O. (2014). Astrocyte-Specific Activation of TNFR2 Promotes Oligodendrocyte Maturation by Secretion of Leukemia Inhibitory Factor. *Glia*, 62, 272-283.
- Francone, V.P., Maggipinto, M.J., Kosturko, L.D., & Barbarese, E. (2007). The Microtubule-Associated Protein Tumor Overexpressed Gene/Cytoskeleton-Associated Protein 5 Is Necessary for Myelin Basic Protein Expression in Oligodendrocytes. *Journal of Neuroscience*, 27(29), 7654-7662.
- Fu, H., Qi, Y., Tan, M., Cai, J., Takebayashi, H., Nakafuku, M., ... Qiu, M. (2002). Dual origin of spinal oligodendrocyte progenitors and evidence for the cooperative role of Olig2 and Nkx2.2 in the control of oligodendrocyte differentiation. *Development*, 129, 681-693.
- Fumagalli, M., Lecca, D., & Abbracchio, M.P. (2016). CNS Remyelination as a novel reparative approach to neurodegenerative diseases: The roles of purinergic signaling and the P2Y-like receptor GPR17. *Neuropharmacology*, 104, 82-93.
- Galvin, J., Eyermann, C., & Colognato, H. (2010). Dystroglycan Modulates the Ability of Insulin-Like Growth Factor-1 To Promote Oligodendrocyte Differentiation. *Journal of Neuroscience Research*, 88, 3295-3307.
- Göttle, P., Sabo, J.K., Heinen, A., Venables, G., Torres, K., Tzekova, N., ... Küry, P. (2015). Oligodendroglial Maturation Is Dependent on Intracellular Protein Shuttling. *Journal of Neuroscience*, 35(3), 906-919.
- Guo, L., Eviatar-Ribak, T., & Miskimins, R. (2010). Sp1 Phosphorylation Is Involved in Myelin Basic Protein Gene Transcription. *Journal of Neuroscience Research*, 88, 3233-3242.

- Hammond, T.R., Gadea, A., Dupree, J., Kerninon, C., Nait-Oumesmar, B., Aguirre, A., & Gallo, V. (2013). Astrocyte-Derived Endothelin-1 Inhibits Remyelination through Notch Activation. *Neuron*, 81, 588-602.
- Harlow, D.E., Saul, K.E., Komuro, H., & Macklin, W.B. (2015). Myelin Proteolipid Protein Complexes with α v Integrin and AMPA Receptors In Vivo and Regulates AMPA-Dependent Oligodendrocyte Progenitor Cell Migration through the Modulation of Cell-Surface GluR2 Expression. *Journal of Neuroscience*, 35(34), 12018-12032.
- Herx, L.M., Rivest, S., & Yong, V.W. (2000). Central Nervous System-Initiated Inflammation and Neurotrophism in Trauma: IL-1 β Is Required for the Production of Ciliary Neurotrophic Factor. *Journal of Immunology*, 165, 2232-2239.
- Hu, B.Y., Du, Z.W., & Zhang, S.C. (2009). Differentiation of human oligodendrocytes from pluripotent stem cells. *Nature Protocols*, 4(11), 1614-1622.
- Huang, J.K., Jarjour, A.A., Oumesmar, B.N., Kerninon, C., Williams, A., Krezel, W., ... Franklin, R.J. (2011). Retinoid X receptor gamma signaling accelerates CNS remyelination. *Nature Neuroscience*, 14(1), 45-53.
- Ingwersen, J., Aktas, O., & Hartung, H.P. (2016). Advances in and Algorithms for the Treatment of Relapsing-Remitting Multiple Sclerosis. *Neurotherapeutics*, 13, 47-57.
- Inoki, K., Ouyang, H., Zhu, T., Lindvall, C., Wang, Y., Zhang, X., ... Guan, K.L. (2006). TSC2 Integrates Wnt and Energy Signals via a Coordinated Phosphorylation by AMPK and GSK3 to Regulate Cell Growth. *Cell*, 126, 955-968.
- Jepson, S., Vought, B., Gross, C.H., Gan, L., Austen, D., Frantz, J.D., ... Krauss, R. (2012). LINGO-1, a Transmembrane Signaling Protein, Inhibits Oligodendrocyte Differentiation and Myelination through Intercellular Self-interactions. *Journal of Biological Chemistry*, 287(26), 22184-22195.
- John, G.R., Shankar, S.L., Shafit-Zagardo, B., Massimi, A., Lee, S.C., Raine, C.S., & Brosnan, C.F. (2002). Multiple sclerosis: Re-expression of a developmental pathway that restricts oligodendrocyte maturation. *Nature Medicine*, 8(10), 1115-1121.
- Juarez, A.L., He, D., & Lu, Q.R. (2016). Oligodendrocyte progenitor programming and reprogramming: Toward myelin regeneration. *Brain Research*, 1638, 209-220.
- Kremer, D., Göttle, P., Hartung, H.P., & Küry, P. (2016). Pushing Forward: Remyelination as the New Frontier in CNS Disease. *Trends in Neuroscience*, 39(4), 246-263.
- Kremer, D., Küry, P., & Dutta, R. (2015). Promoting remyelination in multiple sclerosis: Current drugs and future prospects. *Multiple Sclerosis Journal*, 21(5), 541-549.

Kremer, D., Schiechel, T., Förster, M., Tzekova, N., Bernard, C., van der Valk, P., ... Küry, P. (2013). *Annals of Neuroscience*, 74, 721-732.

Kruger, G.M., Diemel, L.T., Copelman, C.A., & Cuzner, M.L. (1999). Myelin Basic Protein Isoforms in Myelinating and Remyelinating Rat Brain Aggregate Cultures. *Journal of Neuroscience Research*, 56, 241-247.

Kuboyama, K., Fujikawa, A., Masumura, M., Suzuki, R., Matsumoto, M., & Noda, M. (2012). Protein Tyrosine Phosphatase Receptor Type Z Negatively Regulates Oligodendrocyte Differentiation and Myelination. *PLoS One*, 7(11).

Kuboyama, K., Fujikawa, A., Suzuki, R., & Noda, M. (2015). Inactivation of Protein Tyrosine Phosphatase Receptor Type Z by Pleiotrophin Promotes Remyelination through Activation of Differentiation of Oligodendrocyte Precursor Cells. *Journal of Neuroscience*, 35(35), 12162-12171.

Lehotzky, A., Lau, P., Tőkési, N., Muja, N., Hudson, L.D., & Ovádi, J. (2010). Tubulin Polymerization-Promoting Protein (TPPP/p25) is Critical for Oligodendrocyte Differentiation. *Glia*, 58, 157-168.

Li, C., Xiao, L., Liu, X., Yang, W., Shen, W., Hu, C., ... He, C. (2013). A Functional Role of NMDA Receptor in Regulating the Differentiation of Oligodendrocyte Precursor Cells and Remyelination. *Glia*, 61, 732-749.

Li, H., Lu, Y., Smith, H.K., & Richardson, W.D. (2007). Olig1 and Sox10 Interact Synergistically to Drive Myelin Basic Protein Transcription in Oligodendrocytes. *Journal of Neuroscience*, 27(52), 14375-14382.

Liang, X., Draghi, N.A., & Resh, M.D. (2004). Signaling from Integrins to Fyn to Rho Family GTPases Regulates Morphologic Differentiation of Oligodendrocytes. *Journal of Neuroscience*, 24(32), 7140-7149.

Lin, S.T., Huang, Y., Zhang, L., Heng, M.Y., Ptáček, L.J., & Fu, Y.H. (2013). MicroRNA-23a promotes myelination in the central nervous system. *Proceedings of the National Academy of Science*, 110(43), 17468-17473.

Lindner, M., Heine, S., Haastert, K., Garde, N., Fokuhl, J., Linsmeier, F., ... Stangel, M. (2008). Sequential myelin protein expression during remyelination reveals fast and efficient repair after central nervous system demyelination. *Neuropathology and Applied Neurobiology*, 34, 105-114.

Liu, G.C., Ahrens, E.H., Schreibman, P.H., & Crouse, J.R. (1976). Measurement of squalene in human tissues and plasma: validation and application. *Journal of Lipid Research*, 17, 38-45.

- Lundgaard, I., Luzhynskaya, A., Stockley, J.H., Wang, Z., Evans, K.A., Swire, M., ... Káradóttir, R.T. (2013). Neuregulin and BDNF Induce a Switch to NMDA Receptor-Dependent Myelination by Oligodendrocytes. *PLoS Biology*, 11(12).
- Luo, F., Burke, K., Kantor, C., Miller, R.H., & Yang, Y. (2014). Cyclin-Dependent Kinase 5 Mediates Adult OPC Maturation and Myelin Repair through Modulation of Akt and GSK-3 β Signaling. *Journal of Neuroscience*, 34(11), 10415-10429.
- Lyons, D.A., Naylor, S.G., Scholze, A., & Talbot, W.S. (2009). Kif1b is essential for mRNA localization in oligodendrocytes and development of myelinated axons. *Nature Genetics*, 41(7), 854-858.
- Mason, J.L., Xuan, S., Dragatsis, I., Efstratiadis, A., & Goldman, J.E. (2003). Insulin-Like Growth Factor (IGF) Signaling through Type 1 IGF Receptor Plays an Important Role in Remyelination. *Journal of Neuroscience*, 23(20), 7710-7718.
- Matthieu, J.M., Comte, V., Tosic, M., & Honegger, P. (1992). Myelin gene expression during demyelination and remyelination in aggregating brain cell cultures. *Journal of Neuroimmunology*, 40, 231-234.
- McKinnon, R.D., Waldron, S., & Kiel, M.E. (2005). PDGF α -Receptor Signal Strength Controls an RTK Rheostat That Integrates Phosphoinositol 3'-Kinase and Phospholipase C γ Pathways during Oligodendrocyte Maturation. *Journal of Neuroscience*, 25(14), 3499-3508.
- Medina-Rodríguez, E.M., Arenzana, F.J., Pastor, J., Redondo, M., Palomo, V., García de Sola, R., ... de Castro, F. (2013). Inhibition of endogenous phosphodiesterase 7 promotes oligodendrocyte precursor differentiation and survival. *Cellular and Molecular Life Sciences*, 70, 3449-3462.
- Meffre, D., Massaad, C., & Grenier, J. (2015). Lithium chloride stimulates PLP and MBP expression in oligodendrocytes via Wnt/ β -catenin and Akt/CREB pathways. *Neuroscience*, 284, 962-971.
- Mei, F., Fancy, S.P., Shen, Y.A., Niu, J., Zhao, C., Presley, B., ... Chan, J.R. (2014). Micropillar arrays as a high-throughput screening platform for therapeutics in multiple sclerosis. *Nature Medicine*, 20(8), 954-960.
- Mi, S., Lee, X., Yinghui, H., Ji, B., Shao, Z., Yang, W., ... Pepinsky, R.B. (2011). Death receptor 6 negatively regulates oligodendrocyte survival, maturation and myelination. *Nature Medicine*, 17(7), 816-821.
- Mi, S., Miller, R.H., Tang, W., Lee, X., Hu, B., Wu, W., ... Pepinsky, B. (2009). Promotion of Central Nervous System Remyelination by Induced Differentiation of Oligodendrocyte Precursor Cells. *Annals of Neurology*, 65, 304-315.

- Mi, S., Pepinsky, R.B., & Cadavid, D. (2013). Blocking LINGO-1 as a Therapy to Promote CNS Repair: From Concept to the Clinic. *CNS Drugs*, 27, 493-503.
- Michel, K., Zhao, T., Karl, M., Lewis, K., & Fyffe-Maricich, S.L. (2015). Translational Control of Myelin Basic Protein Expression by ERK2 MAP Kinase Regulates Timely Remyelination in the Adult Brain. *Journal of Neuroscience*, 35(20), 7850-7865.
- Miller, R.H. & Mi, S. (2007). Dissecting demyelination. *Nature Neuroscience*, 10(11), 1351-1354.
- Miyamoto, Y., Yamauchi, J., & Tanoue, A. (2008). Cdk5 Phosphorylation of WAVE2 Regulates Oligodendrocyte Precursor Cell Migration through Nonreceptor Tyrosine Kinase Fyn. *Journal of Neuroscience*, 28(33), 8326-8337.
- Moll, N.M., Hong, E., Fauveau, M., Naruse, M., Kerninon, C., Tepavcevic, V., ... Oumesmar, B.N. (2013). SOX17 is Expressed in Regenerating Oligodendrocytes in Experimental Models of Demyelination and in Multiple Sclerosis. *Glia*, 61, 1659-1672.
- Moore, C.S., Abdullah, S.L., Brown, A., Arulpragasam, A., & Crocker, S.J. (2011). How Factors Secreted from Astrocytes Impact Myelin Repair. *Journal of Neuroscience Research*, 89, 13-21.
- Müller, C., Bauer, N.M., Schäfer, I., & White, R. (2013). Making myelin basic protein – from mRNA transport to localized translation. *Frontiers in Cellular Neuroscience*, 7(169).
- Murtie, J.C., Zhou, Y.X., Le, T.Q., Vana, A.C., & Armstrong, R.C. (2005). PDGF and FGF2 pathways regulate distinct oligodendrocyte lineage responses in experimental demyelination with spontaneous remyelination. *Neurobiology of Disease*, 19, 171-182.
- Nakahara, J., Tan-Takeuchi, K., Seiwa, C., Gotoh, M., Kaifu, T., Ujike, A., ... Asou, H. (2003). Signaling via Immunoglobulin Fc Receptors Induces Oligodendrocyte Precursor Cell Differentiation. *Developmental Cell*, 4, 841-852.
- Nakatani, H., Martin, E., Hassani, H., Clavairoly, A., Maire, C.L., Viadieu, A., ... Parras, C. (2013). Ascl1/Mash1 Promotes Brain Oligodendrogenesis during Myelination and Remyelination. *Journal of Neuroscience*, 33(23), 9752-9768.
- O'Meara, R.W., Cummings, S.E., Michalski, J.P., & Kothary, R. (2016). A new in vitro mouse oligodendrocyte precursor cell migration assay reveals a role for integrin-linked kinase in cell motility. *BMC Neuroscience*, 17(7).
- O'Meara, R.W., Michalski, J.P., & Kothary, R. (2011). Integrin Signaling in Oligodendrocytes and Its Importance in CNS Myelination. *Journal of Signal Transduction*.

- Ozes, O.N., Mayo, L.D., Gustin, J.A., Pfeffer, S.R., Pfeffer, L.M., & Donner, D.B. (1999). NF- κ B activation by tumour necrosis factor requires the Akt serine-threonine kinase. *Nature*, *401*, 82-85.
- Paintlia, A.S., Paintlia, M.K., Singh, A.K., Orak, J.K., & Singh, I. (2010). Activation of PPAR- γ and PTEN Cascade Participates in Lovastatin-Mediated Accelerated Differentiation of Oligodendrocyte Progenitor Cells. *Glia*, *58*, 1669-1685.
- Pang, Y., Zheng, B., Fan, L.W., Rhodes, P.G., & Cai, Z. (2007). IGF-1 Protects Oligodendrocyte Progenitors Against TNF α -Induced Damage by Activation of PI3K/Akt and Interruption of the Mitochondrial Apoptotic Pathway. *Glia*, *55*, 1099-1107.
- Patel, J.R., Williams, J.L., Muccigrosso, M.M., Liu, L., Sun, T., Rubin, J.B., & Klein, R.S. (2012). Astrocyte TNFR2 is required for CXCL12-mediated regulation of oligodendrocyte progenitor proliferation and differentiation within the adult CNS. *Acta Neuropathologica*, *124*, 847-860.
- Peckham, H., Giuffrida, L., Wood, R., Gonsalvez, D., Ferner, A., Kilpatrick, T.J., ... Xiao, J. (2016). Fyn is an Intermediate Kinase that BDNF Utilizes to Promote Oligodendrocyte Myelination. *Glia*, *64*, 255-269.
- Piao, J.H., Wang, Y., & Duncan, I.D. (2013). CD44 Is Required for the Migration of Transplanted Oligodendrocyte Progenitor Cells to Focal Inflammatory Demyelinating Lesions in the Spinal Cord. *Glia*, *61*, 361-367.
- Podbielska, M., Banik, N.L., Kurowska, E., & Hogan, E.L. (2013). Myelin Recovery in Multiple Sclerosis: The Challenge of Remyelination. *Brain Sciences*, *3*, 1282-1324.9
- Porcu, G., Serone, E., De Nardis, V., Di Giandomenico, D., Lucisano, G., Scardapane, M., ... Ragnini-Wilson, A. (2015). Clobetasol and Halcinonide Act as Smoothed Agonists to Promote Myelin Gene Expression and RxR γ Receptor Activation. *PLoS ONE*, *10*(12).
- Preisner, A., Albrecht, S., Cui, Q.L., Hucke, S., Ghelman, J., Hartmann, C., ... Kuhlmann, T. (2015). Non-steroidal anti-inflammatory drug indomethacin enhances endogenous remyelination. *Acta Neuropathologica*, *130*, 247-261.
- Redwine, J.M. & Armstrong, R.C. (1998). In Vivo Proliferation of Oligodendrocyte Progenitors Expressing PDGF α R during Early Remyelination. *Journal of Neurobiology*, *37*(3), 413-428.
- Rodgers, J.M., Robinson, A.P., Rosler, E.S., Lariosa-Willingham, K., Persons, R.E., Dugas, J.C., & Miller, S.D. (2015). IL-17A Activates ERK1/2 and Enhances Differentiation of Oligodendrocyte Progenitor Cells. *Glia*, *63*, 768-779.
- Scarlato, M., Beesley, J., & Pleasure, D. (2000). Analysis of Oligodendroglial Differentiation Using cDNA Arrays. *Journal of Neuroscience Research*, *59*, 430-435.

- Seiberlich, V., Bauer, N.G., Schwarz, L., Ffrench-Constant, C., Goldbaum, O., & Richter-Landsberg, C. (2015). Downregulation of the Microtubule Associated Protein Tau Impairs Process Outgrowth and Myelin Basic Protein mRNA Transport in Oligodendrocytes. *Glia*, *63*, 1621-1635.
- Seiwa, C., Yamamoto, M., Tanaka, K., Fukutake, M., Ueki, T., Takeda, S., ... Asou, H. (2007). Restoration of FcR γ /Fyn Signaling Repairs Central Nervous System Demyelination. *Journal of Neuroscience Research*, *85*, 954-966.
- Shirani, A., Okuda, D.T., & Stüve, O. (2016). Therapeutic Advances and Future Prospects in Progressive Forms of Multiple Sclerosis. *Neurotherapeutics*, *13*, 58-69.
- Sim, F.J., Hinks, G.L., & Franklin, R.J. (2000). The re-expression of the homeodomain transcription factor Gtx during remyelination of experimentally induced demyelinating lesions in young and old rat brain. *Neuroscience*, *100*(1), 131-139.
- Skihar, V., Silva, C., Chojnaki, A., Döring, A., Stallcup, W.B., Weiss, S., & Yong, V. W. (2009). Promoting oligodendrogenesis and myelin repair using the multiple sclerosis medication glatiramer acetate. *Proceedings of the National Academy of Science*, *106*(42), 17992-17997.
- Sloane, J.A., Batt, C., Ma, Y., Harris, M., Trapp, B., & Vartanian, T. (2010). Hyaluronan blocks oligodendrocyte progenitor maturation and remyelination through TLR2. *Proceedings of the National Academy of Science*, *107*(25), 11555-11560.
- Stadelmann, C. (2011). Multiple sclerosis as a neurodegenerative disease: pathology, mechanisms and therapeutic implications. *Current Opinion in Neurology*, *24*, 224-229.
- Steelman, A.J., Zhou, Y., Koito, H., Kim, S., Payne, H.R., Lu, Q.R., & Li, J. (2016). Activation of oligodendroglial Stat3 is required for efficient remyelination. *Neurobiology of Disease*, *91*, 336-346.
- Stoffels, J.M., Hoekstra, D., Franklin, R.J., Baron, W., & Zhao, C. (2015). The EIIIA Domain from Astrocyte-Derived Fibronectin Mediates Proliferation of Oligodendrocyte Progenitor Cells Following CNS Demyelination. *Glia*, *63*, 242-256.
- Syed, Y.A., Baer, A., Hofer, M.P., González, G.A., Rundle, J., Myrta, S., ... Kotter, M.R. (2013). Inhibition of phosphodiesterase-4 promotes oligodendrocyte precursor cell differentiation and enhances CNS remyelination. *EMBO Molecular Medicine*, *5*, 1918-1934.
- Talbott, J.F., Cao, Q., Bertram, J., Nkansah, M., Benton, R.L., Lavik, E., & Whittemore, S.R. (2007). CNTF promotes the survival and differentiation of adult spinal cord-derived oligodendrocyte precursor cells *in vitro* but fails to promote remyelination *in vivo*. *Experimental Neurology*, *204*, 485-489.
- Tanaka, T., Murakami, K., Bando, Y., & Yoshida, S. (2013). Minocycline reduces remyelination by suppressing ciliary neurotrophic factor expression after cuprizone-induced demyelination. *Journal of Neurochemistry*, *127*, 259-270.

- Taveggia, C., Feltri, M.L., & Wrabetz, L. (2010). Signals to promote myelin formation and repair. *Nature Reviews Neurology*, 6(5), 276-287.
- Taveggia, C., Thaker, P., Petrylak, A., Caporaso, G.L., Toews, A., Falls, D.L., ... Salzer, J.L. (2008). Type III Neuregulin-1 Promotes Oligodendrocyte Myelination. *Glia*, 56, 284-293.
- Thorton, T.M., Pedraza-Alva, G., Deng, B., Wood, C.D., Aronshtam, A., Clements, J.L., ... Rincon, M. (2008). Phosphorylation by p38 MAPK as an Alternative Pathway for GSK3 β Inactivation. *Science*, 320, 667-670.
- Tran, J.Q., Rana, J., Barkhof, F., Melamed, I., Gevorkyan, H., Wattjes, M.P., ... Cadavid, D. (2014). Randomized phase I trials of the safety/tolerability of anti-LINGO-1 monoclonal antibody BIIB033. *Neurology: Neuroimmunology & Neuroinflammation*, 1, 1-8.
- Tzakos, A.G., Trojanis, A., Theodorou, V., Tselios, T., Svarnas, C., Matsoukas, J., ... Gerothanassis, I.P. (2005). Structure and Function of the Myelin Proteins: Current Status and Perspectives in Relation to Multiple Sclerosis. *Current Medicinal Chemistry*, 12, 1569-1587.
- Valerio, A., Ferrario, M., Dreano, M., Garotta, G., Spano, P., & Pizzi, M. (2002). Soluble Interleukin-6 (IL-6) Receptor/IL-6 Fusion Protein Enhances in Vitro Differentiation of Purified Rat Oligodendroglial Lineage Cells. *Molecular and Cellular Neuroscience*, 21, 602-615.
- Wang, E., Dimova, N., & Cambi, F. (2007). PLP/DM20 ratio is regulated by hnRNPH and F and a novel G-rich enhancer in oligodendrocytes. *Nucleic Acids Research*, 35(12), 4164-4178.
- Wang M., Herrmann, C.J., Simonovic, M., Szklarczyk, D., & von Mering, C. (2015). Version 4.0 of PaxDb: Protein abundance data, integrated across model organisms, tissues, and cell-lines. *Proteomics*, 15(18), 3163-3168.
- Wang, P.S., Wang, J., Xiao, Z.C., & Pallen, C.J. (2009). Protein-tyrosine Phosphatase α Acts as an Upstream Regulator of Fyn Signaling to Promote Oligodendrocyte Differentiation and Myelination. *Journal of Biological Chemistry*, 284(48), 33692-33702.
- Watzlawik, J., Holicky, E., Edberg, D.D., Marks, D.L., Warrington, A.E., Wright, B.R., ... Rodriguez, M. (2010). Human Remyelination Promoting Antibody Inhibits Apoptotic Signaling and Differentiation Through Lyn Kinase in Primary Rat Oligodendrocytes. *Glia*, 58, 1782-1793.
- Watzlawik, J., Warrington, A.E., & Rodriguez, M. (2013). PDGF is Required for Remyelination-Promoting IgM Stimulation of Oligodendrocyte Progenitor Cell Proliferation. *PLoS One*, 8(2).
- Wegener, A., Deboux, C., Bachelin, C., Frah, M., Kerninon, C., Seilhean, D., ... Nait-Oumesmar, B. (2015). Gain of Olig2 function in oligodendrocyte progenitors promotes remyelination. *Brain*, 138, 120-135.
- Wei, Q., Miskimins, W.K., & Miskimins, R. (2005). Stage-specific Expression of Myelin Basic Protein in Oligodendrocyte Involves Nkx2.2-mediated Repression That is Relieved by the Sp1 Transcription Factor. *Journal of Biological Chemistry*, 280(16), 16284-16294.

- Weng, Q., Chen, Y., Wang, H., Xu, X., Yang, B., He, Q., ... Lu, Q.R. (2012). Dual-Mode Modulation of Smad Signaling by Smad-Interacting Protein Sip1 Is Required for Myelination in the Central Nervous System. *Neuron*, 73, 713-728.
- Wheeler, D., Bandaru, V.V., Calabresi, P.A., Nath, A., & Haughey, N.J. (2008). A defect of sphingolipid metabolism modifies the properties of normal appearing white matter in multiple sclerosis. *Brain*, 131(11), 3092-3102.
- White, R., Gonsior, C., Krämer-Albers, E.M., Stöhr, N., Hüttelmaier, S., & Trotter, J. (2008). Activation of oligodendroglial Fyn kinase enhances translation of mRNAs transported in hnRNP A2-dependent RNA granules. *Journal of Cell Biology*, 181(4), 579-586.
- Wolf, R.M., Wilkes, J.J., Chao, M.V., & Resh, M.D. (2001). Tyrosine Phosphorylation of p190 RhoGAP by Fyn Regulates Oligodendrocyte Differentiation. *Journal of Neurobiology*, 49(1), 62-78.
- Woodruff, R.H. & Franklin, R.J. (1999). The expression of myelin protein mRNAs during remyelination and lysolecithin-induced demyelination. *Neuropathology and Applied Neurobiology*, 25, 226-235.
- Woodruff, R.H., Fruttiger, M., Richardson, W.D., Franklin, R.J. (2003). Platelet-derived growth factor regulates oligodendrocyte progenitor numbers in adult CNS and their response following CNS demyelination. *Molecular and Cellular Neuroscience*, 25, 252-262.
- Xiao, L., Hu, C., Yang, W., Guo, D., Li, C., Shen, W., ... He, C. (2013). NMDA Receptor Couples Rac1-GEF Tiam1 to Direct Oligodendrocyte Precursor Cell Migration. *Glia*, 61, 2078-2099.
- Xie, C., Li, Z., Zhang, G.X., & Guan, Y. (2014). Wnt Signaling in Remyelination in Multiple Sclerosis: Friend or Foe?. *Molecular Neurobiology*, 49, 1117-1125.
- Zhao, C., Fancy, S.P., Franklin, R.J., & ffrench-Constant, C. (2009). Up-Regulation of Oligodendrocyte Precursor Cell α V Integrin and Its Extracellular Ligands During Central Nervous System Remyelination. *Journal of Neuroscience Research*, 87, 3447-3455.
- Zhao, C., Ma, D., Zawadzka, M., Fancy, S.P., Elis-Williams, L., Bouvier, G., ... Franklin, R.J. (2015). Sox2 Sustains Recruitment of Oligodendrocyte Progenitor Cells following CNS Demyelination and Primes Them for Differentiation during Remyeliantion. *Journal of Neuroscience*, 35(33), 11482-11499.
- Zhou, L., Shao, C.Y., Xu, S., Ma, J., Xie, Y.J., Zhou, L., ... Shen, Y. (2014). GSK3 β Promotes the Differentiation of Oligodendrocyte Precursor Cells via β -Catenin-Mediated Transcriptional Regulation. *Molecular Neurobiology*, 50, 507-519.

Appendix – MATLAB Code

Equations and Initial Conditions

(example shown is for partial treatment state where $G = 0.01$ at $t=75$)

```
function [dx] = RemyelinationBackupHalfTreat_eq(t,X)

% Make rate constants and independent variables global variables
global k Xind B C D E F G I K W Y Z A1 A2

tTreat = 75;

if t < tTreat
    G = 0;
else
    G = 0.01;
end

X0 = zeros(412,1);

k = zeros(153,1);

Xind = zeros (140,1);

tspan= 0:0.01:120;

% Write initial concentrations for the dependent variables (in CellDesigner
% any species that has an arrow pointing toward it). Use comments to keep
% track of species identities.

%KEEP IN nM concentrations, 10 used as placeholder
%Program used on calculator to convert PPM from PaxDB to nM
%Keep in scientific notation to two decimal places

%ASSUMPTION CODE A = Must decide if concentration of phosphorylated protein
%is zero or not
%ASSUMPTION CODE B = Vague concept given placeholder value
%ASSUMPTION CODE C = Complex given placeholder of 10

X0(135) = 1.41e3; %Contactin2
X0(136) = 6.81; %NT-3
X0(137) = 10; %Hyaluronic Acid (PLACEHOLDER)
X0(138) = 3.16e2; %TNFa (averaged several whole organism values)
X0(139) = 7.44e3; %PTN
X0(140) = 4.34e-1; %HB-EGF
X0(141) = 4.34e2; % TGFa
X0(142) = 10; % TGF Complex (%ASSUMPTION CODE C)
X0(143) = 6.28e1; % Jagged1
X0(144) = 10; % Tnfa/Tnfr2 Complex (ASSUMPTION CODE C)
X0(145) = 6.63e1; % CNTF
X0(146) = 4.5e1; % ET-1 (averaged several whole organism values)
```

```

X0(147) = 2.36e2; % TnC (used Brain integrated value)
X0(148) = 1.54e3; % FGF2
X0(149) = 10; % PDGF (astro) (sort of assuming there is none being produced, no
brain measurements were available, average whole organism value is 1.4e2)
X0(150) = 10; % p85-P (ASSUMPTION CODE A)
X0(151) = 10; % PIP3 (astro)
X0(152) = 10; % Pdk1 active (astro)
X0(153) = 1.03e1; % Nf-kB (astro)
X0(154) = 1.03e2; % Ikb (astro)
X0(155) = 10; % Akt -P (astro) (ASSUMPTION CODE A)
X0(156) = 3.83e3; % CXCL12 (USED SPINAL CORD DATA)
X0(157) = 5.00; % LIF
X0(158) = 10; % HA/CD44 Complex (%ASSUMPTION CODE C)
X0(159) = 10; % OPC Proliferation (ASSUMPTION CODE B)
X0(160) = 10; % OPC Differentiation (ASSUMPTION CODE B)
X0(161) = 10; % Laminin/aV Complex (%ASSUMPTION CODE C)
X0(162) = 10; % TnC/aV Complex (%ASSUMPTION CODE C)
X0(163) = 10; % FGF2/R Complex (%ASSUMPTION CODE C)
X0(164) = 10; % PDGF/R Complex (%ASSUMPTION CODE C)
X0(165) = 10; % CXCL12/R4 Complex (%ASSUMPTION CODE C)
X0(166) = 10; % LIF/gp130 Complex (%ASSUMPTION CODE C)
X0(167) = 10; % CNTF/gp130 Complex (%ASSUMPTION CODE C)
X0(168) = 10; % TNFa/DR6 Complex (%ASSUMPTION CODE C)
X0(169) = 10; % TLR2/MyD88 Complex (%ASSUMPTION CODE C)
X0(170) = 10; % TLR2/MyD88/HA Complex (%ASSUMPTION CODE C)
X0(171) = 5.61e-2; % Laminin (Assumed laminin 1 trimer of alpha, beta, gamma subunits,
used lowest ppm of three subunits and full total mass)
X0(172) = 10; % Contactin 1 (PLACEHOLDER)
X0(173) = 10; % L1 (PLACEHOLDER)
X0(174) = 10; % Laminin/a6B1 Complex (%ASSUMPTION CODE C)
X0(175) = 10; % TnR/aV integrin Complex (%ASSUMPTION CODE C)
X0(176) = 3.49e3; % TnR
X0(177) = 10; % PDGFR-P (PLACEHOLDER)
X0(178) = 10; % gp130-P (PLACEHOLDER)
X0(179) = 10; % JAK2 active
X0(180) = 10; % IL6/IL6R Chimera
X0(181) = 1e10; % OPC Migration (ASSUMPTION CODE B)
X0(182) = 10; % EGFR-P
X0(183) = 10; % PDGF (Th2) (See assumption in X149)
X0(184) = 10; % BDNF (Th2) (Being given placeholder of 10 because of confusion
with X301)
X0(185) = 10; % ILK/Parvin Complex (%ASSUMPTION CODE C)
X0(186) = 10; % Akt-P (OPC) (%ASSUMPTION CODE A)
X0(187) = 10; % Fyn-P (OPC) (%ASSUMPTION CODE A)
X0(188) = 1.70e3; % Fyn (OPC)
X0(189) = 10; % Wave2-P (%ASSUMPTION CODE A)
X0(190) = 10; % p38 MAPK-P
X0(191) = 10; % p39/Cdk5 Complex (%ASSUMPTION CODE C)
X0(192) = 10; % Cdk5-P (%ASSUMPTION CODE A)
X0(193) = 10; % p25/CDK Complex (%ASSUMPTION CODE C)
X0(194) = 10; % STAT3-P
X0(195) = 10; % STAT1-P
X0(196) = 0.18; % Caspase 8
X0(197) = 0.1; % Caspase 3

```



```

X0(198) = 10;      % Apoptosis (ASSUMPTION CODE B) (10)
X0(199) = 10;      % Tiam1-P (%ASSUMPTION CODE A)
X0(200) = 10;      % Rac1 GTP (%ASSUMPTION CODE A)
X0(201) = 10;      % HMW-HA (PLACEHOLDER)
X0(202) = 10;      % Jagged1/Notch1 Complex (%ASSUMPTION CODE C)
X0(203) = 10;      % PTPRZ inactive (PLACEHOLDER)
X0(204) = 10;      % CSL active (ASSUMPTION CODE A)
X0(205) = 10;      % contactin1/Notch1 Complex (ASSUMPTION CODE C)
X0(206) = 10;      % miRNA/Rik complex (ASSUMPTION CODE C)
X0(207) = 5.98e2;   % Bcl-2 (Used spinal cord data)
X0(208) = 10;      % Bcl-2/BAD complex (ASSUMPTION CODE C)
X0(209) = 10;      % Deltex active (ASSUMPTION CODE A)
X0(210) = 4.44e3;   % IGF-1 (Th2 cell)
X0(211) = 1.62e1;   % IGF/R Complex
X0(212) = 10;      % PI3K Active (OPC) (ASSUMPTION CODE A)
X0(213) = 10;      % RXRy Complex (ASSUMPTION CODE C)
X0(214) = 1.97e1;   % FGFR1
X0(215) = 10;      % Wnt/LRP Complex (ASSUMPTION CODE C)
X0(216) = 10;      % Tcf4/B-catenin complex (ASSUMPTION CODE C)
X0(217) = 10;      % TSC2-P (ASSUMPTION CODE A)
X0(218) = 1.58e4;   % Rheb GDP
X0(219) = 10;      % Rheb GTP (ASSUMPTION CODE A)
X0(220) = 1.87e2;   % TrkC
X0(221) = 10;      % PDK1 active (OPC) (ASSUMPTION CODE C)
X0(222) = 10;      % Rik siRNA (PLACEHOLDER)
X0(223) = 10;      % Ascl1 (PLACEHOLDER)
X0(224) = 10;      % BAD-P (ASSUMPTION CODE A)
X0(225) = 10;      % Cyt C in Cyto
X0(226) = 10;      % Caspase 9 (PLACEHOLDER)
X0(227) = 10;      % Cdc42 GTP (ASSUMPTION CODE A)
X0(228) = 10;      % IgG/FcRy complex (ASSUMPTION CODE C)
X0(229) = 10;      % BDNF/TrkB complex (ASSUMPTION CODE C)
X0(230) = 10;      % Laminin/Dystroglycan complex (ASSUMPTION CODE C)
X0(231) = 10;      % MNK-P (ASSUMPTION CODE A)
X0(232) = 10;      % GSK3B inactive (ASSUMPTION CODE A)
X0(233) = 10;      % b-catenin degraded (ASSUMPTION CODE A)
X0(234) = 1.85e1;   % Olig2
X0(235) = 10;      % mTOR1 -P (ASSUMPTION CODE A)
X0(236) = 10;      % S6K - P (ASSUMPTION CODE A)
X0(237) = 3.54e2;   % p190RhoGAP
X0(238) = 10;      % p190RhoGAP-P (ASSUMPTION CODE A)
X0(239) = 5.36e4;   % RhoA GDP
X0(240) = 10;      % RhoA GTP (ASSUMPTION CODE A)
X0(241) = 10;      % Caspase 9-P (ASSUMPTION CODE A)
X0(242) = 10;      % CREB-P (ASSUMPTION CODE A)
X0(243) = 7.27e2;   % aV integrin
X0(244) = 2.35;     % Axin2
X0(245) = 1.63e1;   % Sipl
X0(246) = 6.03;     % MRF
X0(247) = 3.16e2;   % Akt (astro)
X0(248) = 10;      % IL-17 complex (ASSUMPTION CODE C)
X0(249) = 10;      % ERK1/2-P (ASSUMPTION CODE A)
X0(250) = 8.74e1;   % YY1
X0(251) = 1;        % O4 (can't find data)

```

```

X0(252) = 1;          % O1 (can't find data)
X0(253) = 5.10e2;     % Cdk4
X0(254) = 1.62e2;     % p21 (whole organism data)
X0(255) = 3.23e3;     % p27
X0(256) = 7.31e2;     % PTEN
X0(257) = 10;         % PLP/AMPA/integrin complex (ASSUMPTION CODE C)
X0(258) = 10;         % PKA active (ASSUMPTION CODE A)
X0(259) = 10;         % cAMP
X0(260) = 10;         % AMP
X0(261) = 10;         % AMPK active (ASSUMPTION CODE C)
X0(262) = 10;         % PPARy Free
X0(263) = 10;         % cPLA2-P (ASSUMPTION CODE C)
X0(264) = 10;         % RhoA/ROCK Complex (ASSUMPTION CODE C)
X0(265) = 10;         % p75/Ngr1/LINGO complex (ASSUMPTION CODE C)
X0(266) = 1.62e1;     % IGFR1
X0(267) = 1e4;        % Mevalonate
X0(268) = 1e4;        % Mevalonate Phosphate
X0(269) = 1e4;        % Mevalonate PP
X0(270) = 1e4;        % Isopentyl PP
X0(271) = 1e4;        % Farnesyl PP
X0(272) = 1e4;        % geranylgeranyl PP
X0(273) = 1e4;        % Squalene
X0(274) = 10;         % NRG1/ErB3 complex (ASSUMPTION CODE C)
X0(275) = 10;         % NRG1/ErB4 complex (ASSUMPTION CODE C)
X0(276) = 5.49e-1;    % HES5
X0(277) = 1.03e1;     % NF-kB (OPC)
X0(278) = 1.03e2;     % Ikb (OPC)
X0(279) = 10;         % ENV/TLR4 complex (ASSUMPTION CODE C)
X0(280) = 7.08;       % RXRy (used spinal cord data)
X0(281) = 0;          % Clobetasol/Smoothened complex
X0(282) = 0;          % Halcinonide/Smoothened complex
X0(283) = 7.22;       % ErB3
X0(284) = 5.59;       % ErB4
X0(285) = 3.66e1;     % PDGFRa
X0(286) = 10;         % Adenylate Cyclase active (ASSUMPTION CODE A)
X0(287) = 10;         % MBP mRNA
X0(288) = 1.48e1;     % Notch1
X0(289) = 10;         % M1/Ach complex (ASSUMPTION CODE C)
X0(290) = 10;         % M3/Ach complex (ASSUMPTION CODE C)
X0(291) = 10;         % M2/Ach complex (ASSUMPTION CODE C)
X0(292) = 10;         % M4/Ach complex (ASSUMPTION CODE C)
X0(293) = 10;         % S1P complex (ASSUMPTION CODE C)
X0(294) = 0;          % FTY720 complex
X0(295) = 0;          % FTY720-P
X0(296) = 0;          % rHIgM22 antibody compkex
X0(297) = 10;         % Lyn-P (ASSUMPTION CODE A)
X0(298) = 10;         % MYRF-N terminus
X0(299) = 10;         % Nkx2.2/HDAC1/Sin3a (ASSUMPTION CODE C)
X0(300) = 10;         % MeCP2/HDAC1/sin3a (ASSUMPTION CODE C)
X0(301) = 10;         % BDNF (OPC) (Being given placeholder of 10 because of confusion
with X184)
X0(302) = 2.62;       % Sp5
X0(303) = 10;         % MAG mRNA
X0(304) = 7e3;        % MAG

```

```

X0(305) = 8e2;      % MPZ
X0(306) = 10;      % Spl-P (ASSUMPTION CODE A)
X0(307) = 10;      % 4EBP1-P (ASSUMPTION CODE A)
X0(308) = 10;      % 4eEBP1/eIF4E complex (ASSUMPTION CODE C)
X0(309) = 10;      % eIF4E-P (ASSUMPTION CODE A)
X0(310) = 10;      % BMP4/R complex (ASSUMPTION CODE C)
X0(311) = 10;      % Smad1-P (ASSUMPTION CODE C)
X0(312) = 10;      % Egr2 (COULD NOT FIND DATA, 2.07e1 IS WHOLE ORGANISM VALUE)
X0(313) = 10;      % EPO/R complex (ASSUMPTION CODE C)
X0(314) = 10;      % MOG mRNA
X0(315) = 8e4;      % MOG
X0(316) = 5e5;      % PLP
X0(317) = 10;      % Smad7 (COULD NOT FIND DATA, 4.52 IS WHOLE ORGANISM VALUE)
X0(318) = 10;      % Olig1/Sox10 complex (ASSUMPTION CODE C)
X0(319) = 0;       % MBP mRNA translocated
X0(320) = 2.54E2;   % SOX 10
X0(321) = 10;      % MEK-P (ASSUMPTION CODE A)
X0(322) = 10;      % glutamate/NMDA complex (ASSUMPTION CODE C)
X0(323) = 10;      % Raf/Ras GTP complex (ASSUMPTION CODE C)
X0(324) = 10;      % Ras GTP (ASSUMPTION CODE A)
X0(325) = 6e5;      % MBP
X0(326) = 10;      % SR6P-P (ASSUMPTION CODE A)
X0(327) = 10;      % Olig1 (USED RETINA DATA)
X0(328) = 10;      % Smad7/Smurf1 complex (ASSUMPTION CODE C)
X0(329) = 1e5;      % CNPase
X0(330) = 10;      % PLP mRNA
X0(331) = 2.88e4;   % hnRNP A2
X0(332) = 10;      % L1/contactin2 complex (ASSUMPTION CODE C)
X0(333) = 10;      % NT-3/TrkC complex (ASSUMPTION CODE C)
X0(334) = 0;       % Remyelination
X0(335) = 10;      % Ikb degraded (astro)
X0(336) = 10;      % Ikb degraded (OPC)
X0(337) = 10;      % TNFR2 (astro) (no data found, whole organism 7.06e1)
X0(338) = 10;      % CXCR4 (no data found, 1.12e2 whole organism)
X0(339) = 1.53e2;   % a6B1 integrin
X0(340) = 9.91e2;   % ILK
X0(341) = 9.18e1;   % Parvin (used parvin beta)
X0(342) = 1.85e1;   % gp130
X0(343) = 4.18;     % DR6
X0(344) = 1.31e3;   % CD44
X0(345) = 4.45e1;   % TLR2
X0(346) = 6.02e2;   % MyD88 (spinal cord data)
X0(347) = 10;      % NMDAR (data not found)
X0(348) = 10;      % Glutamate
X0(349) = 4.81e2;   % IgG
X0(350) = 1.28e1;   % FcRy
X0(351) = 2.3e3;    % PKA
X0(352) = 10;      % TGFB1 (data not found)
X0(353) = 10;      % TGFB2 (astro) (data not found)
X0(354) = 8.75e2;   % TrkB
X0(355) = 10;      % p39 (whole organism value is 1.02e2)
X0(356) = 2.50e2;   % p25 (used value for CDKR1)
X0(357) = 7.34;     % miRNA-23A
X0(358) = 8.37e3;   % BAD

```

```

X0(359) = 10;      % AMPA (placeholder)
X0(360) = 10;      % 9cRA (placeholder)
X0(361) = 3.81;    % Wnt-3a
X0(362) = 5.58e-2; % LRP5/6
X0(363) = 4.74e3;  % B-catenin
X0(364) = 1.04e1;  % Tcf4
X0(365) = 3.78e2;  % Dystoglycan
X0(366) = 5.15e5;  % PLP (extracellular)
X0(367) = 2.06e1;  % IL-17A
X0(368) = 1.04;    % IL-17RA
X0(369) = 1.80e3;  % AMPK
X0(370) = 1.11e3;  % ROCK II
X0(371) = 8.40e2;  % LINGO1
X0(372) = 2.01e4;  % Erb2
X0(373) = 0;      % p75
X0(374) = 10;      % NRG1-Type III (no data)
X0(375) = 0;      % ENV (SPECIFIC VIRAL INFECTION)
X0(376) = 1.10e1;  % TLR4
X0(377) = 4.28e2;  % M1
X0(378) = 2.93e2;  % M3
X0(379) = 8.88e1;  % M2
X0(380) = 1.89e-1; % M4
X0(381) = 10;      % Acetylcholine
X0(382) = 10;      % S1P (placeholder)
X0(383) = 4.13e2;  % S1P1
X0(384) = 1.29e1;  % mSin3a
X0(385) = 1.68e2;  % HDAC1
X0(386) = 4.41e3;  % MeCP2
X0(387) = 1.89e1;  % Nkx2.2 (used retina)
X0(388) = 8.35e3;  % 4EBP1
X0(389) = 1.28e5;  % eIF4E
X0(390) = 10;      % BMP4 (whole organism is 3.65)
X0(391) = 6.99e1;  % BMPR
X0(392) = 10;      % EPO (whole organism is 2.32e2)
X0(393) = 2.18;    % EPOR
X0(394) = 1.49e1;  % Smurf1
X0(395) = 1.10e2;  % Raf
X0(396) = 3.16e2;  % Akt (OPC)
X0(397) = 1.77e2;  % p38 MAPK (Used MAPK11)
X0(398) = 4.75e-1; % PI3K inactive
X0(399) = 1.07e3;  % PDK1 inactive (OPC)
X0(400) = 2.18e4;  % ERK1/2 (added sum of ERK1 and ERK 2 aka MAPK3 and MAPK1)
X0(401) = 2.14;    % MNK (used spinal cord)
X0(402) = 7.51e1;  % mTOR1
X0(403) = 1.77e4;  % MEK
X0(404) = 1.07e3;  % PDK1 inactive (astro)
X0(406) = 10;      %Adenosine relased
X0(407) = 16.63;   %P1 receptor (A2A)
X0(408) = 10;      %Adenosine Complex
X0(410) = 10;      %UDP released
X0(411) = 7.81;    %GPR17
X0(412) = 10;      %UDP complex

```

```

% Write initial concentrations for the independent variables (in
% CellDesigner any species that does not have an arrow pointing toward it)
%Placeholder values are at a standard of 1
%Genes were eyeballed more or less using the NCBI Geo profiles graphs
%ASSUMPTION ISSUE D refers to the use of rat profile comparing OPC to Olig
%which is based off of a ratio of 1

Xind(1) = 10;          % Demyelination
Xind(2) = 0.1;         % OPC Not Migrated
Xind(3) = 1;          % Living Cell
Xind(4) = 10;         % Jagged1 gene (astro) (323.5)
Xind(5) = 10;         % TNFR2 (astro) (data not found, whole organism is 7.06e1)
Xind(6) = 10;         % CNTF gene (astro) (14.6)
Xind(7) = 10;         % ET-1 gene (astro) (6.24)
Xind(8) = 10;         % TNC gene (astro) (2234)
Xind(9) = 10;         % FGF2 gene (astro) (123.2)
Xind(10) = 10;        % PDGF gene (astro) (2659)
Xind(11) = 5.96e2;    % p85 (astro)
Xind(12) = 10;        % PIP2 (astro) (placeholder)
Xind(13) = 6.20e2;    % Adenylate cyclase inactive (sum of ADCY1,2, and 8)
Xind(14) = 10;        % NF-kB/IkB complex (astro) (Placeholder)
Xind(15) = 10;        % ErbB4 gene (0.545)
Xind(16) = 10;        % CXCL12 gene (astro) (4046)
Xind(17) = 10;        % LIF gene (astro) (43.9)
Xind(18) = 1;         % OPC Non-Proliferating
Xind(19) = 10;        % PDGFRa gene (4.47)

Xind(20) = 10;        % Olig1 gene (2e4)
Xind(21) = 10;        % Ascl1 gene (1.3e3)
Xind(22) = Z;         % Indometacin
Xind(23) = 1.10e4;    % PTPa
Xind(24) = 0;         % Monocycline
Xind(25) = 1;         % Demyelinated Lesion
Xind(26) = 10;        % IL-1B (data not found whole organism value 1.79e1)
Xind(27) = 10;        % Hyaluronidase (data not found whole organism values 2.61e1)
Xind(28) = G;         % Halcinonide
Xind(29) = 10;        % Laminin blocked (PLACEHOLDER)
Xind(30) = 2.77e3;    % L1 blocked
Xind(31) = 1.05e4;    % contactin blocked
Xind(32) = 9.70e2;    % Lamin B
Xind(33) = 10;        % TnR gene (ASSUMPTION ISSUE D) (1)
Xind(34) = 1.61;      % JAK2 inactive
Xind(35) = 1.18e1;    % IL-6
Xind(36) = 10;        % sIL-6R (whole organism value is 2.08e1)
Xind(37) = 2.96e2;    % EGFR
Xind(38) = 10;        % PDGF gene (Th2) (11.9)
Xind(39) = 10;        % BDNF gene (Th2) (4.5)
Xind(40) = 3.70e3;    % HDAC11
Xind(41) = 9.15e3;    % H3 (HIST1H3A was what was used)
Xind(42) = B;         % Glatiramer Acetate
Xind(43) = C;         % Benzotropine
Xind(44) = 5.78e2;    % Wave2
Xind(45) = 3.31e2;    % Sphk2
Xind(46) = 10;        % PLP gene (ASSUMPTION ISSUE D) (3.5)

```

```

Xind(47) = 9.97e3; % Cdk5
Xind(48) = 10; % CNPase gene (ASSUMPTION ISSUE D) (7)
Xind(49) = 6.52e2; % STAT3
Xind(50) = 7.73e2; % STAT1
Xind(51) = 10; % Procaspace8 (PLACEHOLDER)
Xind(52) = 1.99e2; % Procaspace3 (1.99e2)
Xind(53) = 5.04e1; % Tiam1
Xind(54) = 4.04e4; % Rac1 GDP
Xind(55) = 4.93e1; % Sox2
Xind(56) = 1.32e3; % PTPRZ active
Xind(57) = 2.66e1; % CSL inactive
Xind(58) = 10; % Smad7 gene (ASSUMPTION ISSUE D) (1.20)
Xind(59) = 10; % T3 (placeholder)
Xind(60) = 10; % Bcl-2 gene (no real data found, used rat choroid plexus data)
(5.67)
Xind(61) = 1.04; % Deltex inactive (used retinal data)
Xind(62) = 10; % IGF-1 gene (Th2) (31.3)
Xind(63) = Y; % FTY720
Xind(64) = 10; % p57kip2 (whole organism is 4.26e1)
Xind(65) = 10; % FGFR1 gene (ASSUMPTION ISSUE D) (1.11)
Xind(66) = 8.96e3; % S6RP
Xind(67) = 2.88e4; % hnRNPA2
Xind(68) = 5.37e2; % TOG
Xind(69) = 10; % sncRNA715 (placeholder)
Xind(70) = 1.44e2; % TSC2
Xind(71) = 10; % Notch1 gene (astrocyte t antigen inactivation value) (78.2)
Xind(72) = 10; % Rik gene (placeholder)
Xind(73) = 7.94e3; % Ras GDP
Xind(74) = 1.67e5; % Cyt in Mito
Xind(75) = 1.34e3; % Bax
Xind(76) = 10; % Procaspace9 (1.04e2)
Xind(77) = 4.25e4; % Cdc42 GDP
Xind(78) = F; % Clobetasol
Xind(79) = 10; % RXRy gene (ASSUMPTION ISSUE D) (0.98)
Xind(80) = 6.09e3; % Transferrin
Xind(81) = 10; % Sox10 gene (ASSUMPTION ISSUE D) (5.44)
Xind(82) = 1.26e1; % Gtx (used whole organism data because it is oligodendrocyte
specific)
Xind(83) = 2.35e3; % GSK3B
Xind(84) = A1; % LiCl
Xind(85) = 10; % Olig2 gene (ASSUMPTION ISSUE D) (1.456)
Xind(86) = 2.95e4; % Pur-a
Xind(87) = 1.21e2; % S6K
Xind(88) = 6.25; % Dvl-2
Xind(89) = 10; % Dkk1 (whole organism is 3.10e1)
Xind(90) = 2.71e2; % CREB (used CREB1)
Xind(91) = 10; % ITGAV gene (ASSUMPTION ISSUE D) (1.273)
Xind(92) = 2.35; % Axin2
Xind(93) = 10; % Sip1 gene (ASSUMPTION ISSUE D) (1.552)
Xind(94) = 10; % MRF gene (ASSUMPTION ISSUE D) (7)
Xind(95) = 1.18e4; % MAPt
Xind(96) = 4.47e1; % Kif1b
Xind(97) = 10; % MOG gene (ASSUMPTION ISSUE D) (26)
Xind(98) = 10; % Egr2 gene (ASSUMPTION ISSUE D) (0.587_

```

```

Xind(99) = 10;      % MBP gene (73.5)
Xind(100) = 4.72e3; % PKC (used PRKCA)
Xind(101) = 10;    % YY1 gene (ASSUMPTION ISSUE D) (0.867)
Xind(102) = 10;    % O4 gene (DATA NOT FOUND)
Xind(103) = 10;    % O1 gene (DATA NOT FOUND)
Xind(104) = 10;    % Cdk4 gene (ASSUMPTION ISSUE D) (0.97)
Xind(105) = 10;    % p21 gene (ASSUMPTION ISSUE D) (1.416)
Xind(106) = 10;    % p27 gene (ASSUMPTION ISSUE D) (1.086)
Xind(107) = 10;    % PTEN gene (ASSUMPTION ISSUE D) (1.41)
Xind(108) = 7.385; % Smad1
Xind(109) = 10;    % Spl (whole organism is 2.85e2)
Xind(110) = 10;    % MPZ gene (ASSUMPTION ISSUE D) (95.3)
Xind(111) = 10;    % ATP (PLACEHOLDER)
Xind(112) = 7.39e1; % PDE4 (used PDE4A)
Xind(113) = 10;    % PDE7 (whole organism is 4.50)
Xind(114) = 10;    % MAG gene (ASSUMPTION ISSUE D) (20)
Xind(115) = 10;    % PPARy bound (whole organism is 6.42)
Xind(116) = 3.39e1; % cPLA2
Xind(117) = 10;    % Sp5 gene (5.69)

Xind(118) = 10 + A2; % BIIB033
Xind(119) = 10;    % BDNF gene (OPC) (ASSUMPTION ISSUE D) (0.842)
Xind(120) = 10;    % ErB3 gene (0.59)
Xind(121) = 1.16e2; % Lyn
Xind(122) = 10;    % TNFa gene (OPC) (ASSUMPTION ISSUE D) (1)
Xind(123) = D;    % Simvastatin
Xind(124) = E;    % Lovastatin
Xind(125) = 1e9;   % HMG-CoA (placeholder) (1e10)
Xind(126) = 10;    % HMG-CoA reductase (placeholder, estimate was at 0.103)
Xind(127) = 5.47e2; % Mevalonate kinase (5.47e2)
Xind(128) = 2.42e3; % phosphomevalonate kinase
Xind(129) = 1.39e3; % Mevalonate PP decarboxylase
Xind(130) = 6.32e2; % farnesyl PP synthase
Xind(131) = 4.70e2; % geranylgeranylPP synthase
Xind(132) = 4.69e2; % Squalene synthase
Xind(133) = 0.463; % Smoothened
Xind(134) = 10;    %NFkB/IkB complex (OPC) (sort of ASSUMPTION CODE C)
Xind(135) = 10;    % HES5 gene (ASSUMPTION ISSUE D) (0.895)
Xind(136) = K;    % rHlgM22
Xind(137) = 8.37e-1; % avB3 integrin
Xind(138) = W;    % GNBAC1
Xind(139) = 10;   %Adenosine neuron
Xind(140) = 10;   %UDP neuron

```

```

% Write initial rates for flux equations. Any reaction that does not have
% any promoters or inhibitors is assigned a k value. Any reaction that has
% promoters or inhibitors is assigned an X0 value and corresponding
% differential equation.

```

```

%0.01 used as placeholder (especially for vague processes)
%rates kept in nM/s/mg

k(1) = 0.01;    % J1  k1
k(2) = 0.01;    % J2  k2
k(3) = 0.01;    % J3  k3
k(4) = 0.01;    % J4  k4
k(5) = 0.01;    % J5  k5
k(6) = 0.01;    % J6  k6
X0(1) = 0.01;   % J7  X1
k(8) = 0.01;    % J8  k8
X0(2) = 0.01;   % J9  X2
X0(3) = 0.01;   % J10 X3
X0(4) = 0.01;   % J11 X4
X0(5) = 0.01;   % J12 X5
X0(6) = 0.01;   % J13 X6
X0(7) = 0.01;   % J14 X7
X0(8) = 0.01;   % J15 X8 SABIO reference 4221 (REALLY REALLY FAST) (11.67)
X0(9) = 0.01;   % J16 X9
X0(10) = 0.01;  % J17 X10
X0(11) = 0.01;  % J18 X11
X0(12) = 0.01;  % J19 X12
X0(13) = 0.01;  % J20 X13
k(9) = 0.01;    % J21 k9
k(10) = 0.01;   % J22 k10
X0(14) = 0.01;  % J23 X14
k(12) = 0.01;   % J24 k12
k(13) = 0.01;   % J25 k13
k(14) = 0.01;   % J26 k14
k(15) = 0.01;   % J27 k15
k(16) = 0.01;   % J28 k16
k(17) = 0.01;   % J29 k17
k(18) = 0.01;   % J30 k18
X0(15) = 0.01;  % J31 X15
k(11) = 0.01;   % J32 k11
k(19) = 0.01;   % J33 k19
k(20) = 0.01;   % J34 k20
k(21) = 0.01;   % J35 k21
k(22) = 0.0001; % J36 k22
X0(16) = 0.01;  % J37 X16
X0(17) = 0.01;  % J38 X17
X0(18) = 0.01;  % J39 X18
k(23) = 0.01;   % J40 k23
k(24) = 0.01;   % J41 k24
X0(19) = 0.01;  % J42 X19
X0(20) = 0.01;  % J43 X20
X0(21) = 0.01;  % J44 X21
X0(22) = 0.01;  % J45 X22 SABIO entry ID 3525 (REALLY REALLY SLOW 0.00002)
k(25) = 0.01;   % J46 k25
k(26) = 0.01;   % J47 k26
k(27) = 0.01;   % J48 k27
X0(23) = 0.01;  % J49 X23
X0(24) = 0.01;  % J50 X24

```



```

X0(25) = 0.01; % J51 X25
X0(26) = 0.01; % J52 X26
k(28) = 0.01; % J53 k28
k(30) = 0.01; % J54 k30
X0(27) = 0.01; % J55 X27
X0(28) = 0.01; % J56 X28
X0(29) = 0.01; % J57 X29
X0(30) = 0.01; % J58 X30
X0(31) = 0.01; % J59 X31
k(31) = 0.01; % J60 k31
X0(32) = 0.01; % J61 X32
k(32) = 0.01; % J62 k32
X0(33) = 0.01; % J63 X33
X0(34) = 0.01; % J64 X34
X0(35) = 0.01; % J65 X35
X0(36) = 0.01; % J66 X36
k(33) = 0.01; % J67 k33
k(34) = 0.01; % J68 k34
X0(37) = 0.01; % J69 X37
X0(38) = 0.01; % J70 X38
X0(39) = 0.01; % J71 X39
k(35) = 0.01; % J72 k35
k(36) = 0.01; % J73 k36
k(37) = 0.01; % J74 k37
k(38) = 0.01; % J75 k38
k(39) = 0.01; % J76 k39
k(40) = 0.01; % J77 k40
k(41) = 0.01; % J78 k41
k(42) = 0.01; % J79 k42
k(89) = 0.01; % J80 k89
k(44) = 0.01; % J81 k44
k(45) = 0.01; % J82 k45
X0(40) = 0.01; % J83 X40
X0(41) = 0.01; % J84 X41
k(46) = 0.01; % J85 k46
k(47) = 0.01; % J86 k47
k(48) = 0.01; % J87 k48
X0(42) = 0.01; % J88 X42
k(49) = 0.01; % J89 k49
k(50) = 0.01; % J90 k50
X0(43) = 0.01; % J91 X43
X0(44) = 0.01; % J92 X44
k(51) = 0.01; % J93 k51
X0(45) = 0.01; % J94 X45
k(52) = 0.01; % J95 k52
X0(46) = 0.01; % J96 X46
k(53) = 0.01; % J97 k53
k(54) = 0.01; % J98 k54
k(55) = 0.01; % J99 k55
k(56) = 0.01; % J100 k56
X0(47) = 0.01; % J101 X47
k(57) = 0.01; % J102 k57
X0(48) = 0.01; % J103 X48
X0(49) = 0.01; % J104 X49

```

```

X0(50) = 0.01; % J105 X50
k(58) = 0.01; % J106 k58
X0(51) = 0.01; % J107 X51
X0(52) = 0.01; % J108 X52
X0(53) = 0.01; % J109 X53
X0(54) = 0.01; % J110 X54
k(59) = 0.01; % J111 k59
X0(55) = 0.01; % J112 X55
k(60) = 0.01; % J113 k60
k(61) = 0.01; % J114 k61
k(43) = 0.01; % J115 k43
k(62) = 0.01; % J116 k62
X0(57) = 0.01; % J117 X57
X0(58) = 0.01; % J118 X58
X0(59) = 0.01; % J119 X59
X0(60) = 0.01; % J120 X60
X0(61) = 0.01; % J121 X61
X0(62) = 0.01; % J122 X62 SABIO Reaction ID 2490 (0.275)
X0(63) = 0.01; % J123 X63
X0(64) = 0.01; % J124 X64
X0(65) = 0.01; % J125 X65
X0(79) = 0.01; % J126 X79
k(64) = 0.01; % J127 k64
k(65) = 0.01; % J128 k65
X0(66) = 0.01; % J129 X66
X0(67) = 0.01; % J130 X67
X0(68) = 0.01; % J131 X68
X0(69) = 0.01; % J132 X69
X0(70) = 0.01; % J133 X70
X0(71) = 0.01; % J134 X71
k(87) = 0.01; % J135 k87
k(67) = 0.01; % J136 k67
k(68) = 0.01; % J137 k68
k(69) = 0.01; % J138 k69
k(70) = 0.01; % J139 k70
X0(72) = 0.01; % J140 X72
X0(73) = 0.01; % J141 X73
X0(74) = 0.01; % J142 X74
k(71) = 0.01; % J143 k71
X0(76) = 0.01; % J145 X76
X0(75) = 0.01; % J144 X75
X0(77) = 0.01; % J146 X77
X0(78) = 0.01; % J147 X78
k(72) = 0.01; % J148 k72
k(73) = 0.01; % J149 k73
k(74) = 0.01; % J150 k74
k(63) = 0.01; % J151 k63
k(75) = 0.01; % J152 k75
X0(80) = 0.0021; % J153 X80 SABIO Reaction ID 101
X0(81) = 0.0346; % J154 X81 SABIO Reaction ID 292 averaged
k(76) = 0.01; % J155 k76
X0(82) = 0.01; % J156 X82
X0(83) = 0.01; % J157 X83
X0(84) = 0.01; % J158 X84

```

```

X0(85) = 0.01; % J159 X85
X0(86) = 0.01; % J160 X86
X0(87) = 0.01; % J161 X87 SABIO Reaction ID 6923 (THIS SEEMS REALLY REALLY FAST 493.3)
X0(88) = 0.01; % J162 X88 SABIO Reaction ID 6922 (REALLY REALLY FAST 616.7)
X0(89) = 0.02067; % J163 X89 SABIO Reaction ID 3066
X0(90) = 0.01; % J164 X90 SABIO reaction ID 1380 (REALLY REALLY SLOW 0.00001867)
X0(91) = 0.0045; % J165 X91 SABIO reaction ID 2041
X0(92) = 0.01; % J166 X92 SABIO Reaction ID 2078 (REALLY REALLY FAST 211.67)
X0(93) = 0.01; % J167 X93 SABIO REaction ID 5806 (REALLY REALLY FAST 75)
k(78) = 0.01; % J168 k78
k(79) = 0.01; % J169 k79
X0(94) = 0.01; % J170 X94
X0(95) = 0.01; % J171 X95
X0(96) = 0.01; % J172 X96
X0(97) = 0.01; % J173 X97
k(80) = 0.01; % J174 k80
k(81) = 0.01; % J175 k81
X0(98) = 0.01; % J176 X98
X0(99) = 0.01; % J177 X99
X0(100) = 0.01; % J178 X100
X0(101) = 0.01; % J179 X101
X0(102) = 0.01; % J180 X102
X0(103) = 0.01; % J181 X103
X0(104) = 0.01; % J182 X104
X0(105) = 0.01; % J183 X105
k(83) = 0.01; % J184 k83
k(82) = 0.01; % J185 k82
k(85) = 0.01; % J186 k85
k(86) = 0.01; % J187 k86
X0(125) = 0.01; % J188 X125
k(88) = 0.01; % J189 k88
X0(56) = 0.01; % J190 X56
k(90) = 0.01; % J191 k90
k(91) = 0.01; % J192 k91
X0(121) = 0.01; % J193 X121
k(7) = 0.01; % J194 k7
k(29) = 0.01; % J195 k29
k(84) = 0.01; % J196 k84
X0(106) = 0.01; % J197 X106
X0(107) = 0.01; % J198 X107
X0(108) = 0.01; % J199 X108
X0(109) = 0.01; % J200 X109
X0(110) = 0.01; % J201 X110
X0(111) = 0.01; % J202 X111
X0(112) = 0.01; % J203 X112
k(92) = 0.01; % J204 k92
X0(113) = 0.01; % J205 X113
X0(114) = 0.01; % J206 X114
k(93) = 0.01; % J207 k93
X0(115) = 0.01; % J208 X115
k(95) = 0.01; % J209 k95
X0(116) = 0.01; % J210 X116
X0(117) = 0.01; % J211 X117
k(96) = 0.01; % J212 k96

```

```

X0(127) = 0.01; % J213 X127
k(97) = 0.01; % J214 k97
X0(118) = 0.01; % J215 X118
X0(120) = 0.01; % J216 X120
X0(122) = 0.01; % J217 X122
X0(123) = 0.01; % J218 X123
X0(124) = 0.01; % J219 X124
k(94) = 0.01; % J220 k94
X0(126) = 0.01; % J221 X126
X0(128) = 0.01; % J222 X128
X0(129) = 0.01; % J223 X129
X0(130) = 0.01; % J224 X130
X0(131) = 0.01; % J225 X131
k(79) = 0.01; % J226 k79
X0(133) = 0.001; % J227 X133
X0(134) = 0.01; % J228 X134
X0(132) = 0.01; % J229 X132
X0(119) = 0.01; % J230 X119
k(98) = 0.01; % J231 k98
k(99) = 0.01; % J232 k99
k(100) = 0.01; % J233 k100
k(101) = 0.01; % J234 k101
k(102) = 0.01; % J235 k102
k(103) = 0.01; % J236 k103
k(104) = 0.01; % J237 k104
k(105) = 0.01; % J238 k105
k(106) = 0.01; % J239 k106
k(107) = 0.01; % J240 k107
k(108) = 0.01; % J241 k108
k(109) = 0.01; % J242 k109
k(110) = 0.01; % J243 k110
k(111) = 0.01; % J244 k111
k(112) = 0.01; % J245 k112
k(113) = 0.01; % J246 k113
k(114) = 0.01; % J247 k114
k(115) = 0.01; % J248 k115
k(116) = 0.01; % J249 k116
k(117) = 0.01; % J250 k117
k(118) = 0.01; % J251 k118
k(119) = 0.01; % J252 k119
k(120) = 0.01; % J253 k120
k(121) = 0.01; % J254 k121
k(122) = 0.01; % J255 k122
k(123) = 0.01; % J256 k123
k(124) = 0.01; % J257 k124
k(125) = 0.01; % J258 k125
k(126) = 0.01; % J259 k126
k(127) = 0.01; % J260 k127
k(128) = 0.01; % J261 k128
k(129) = 0.01; % J262 k129
k(130) = 0.01; % J263 k130
k(131) = 0.01; % J264 k131
k(132) = 0.01; % J265 k132
k(133) = 0.01; % J266 k133

```

```

k(134) = 0.01;    % J267 k134
k(135) = 0.01;    % J268 k135
k(136) = 0.01;    % J269 k136
k(137) = 0.01;    % J270 k137
k(139) = 0.01;    % J271 k139
k(66) = 0.01;     % J272 k66
k(140) = 0.01;    % J273 k140
k(141) = 0.01;    % J274 k141
k(142) = 0.01;    % J275 k142
k(143) = 0.01;    % J276 k143
k(144) = 0.01;    % J277 k144 (0.01)
k(145) = 0.01;    % J278 k145 (0.01)
k(146) = 0.01;    % J279 k146
k(147) = 0.01;    % J280 k147
k(148) = 0.01;    % J281 k148 (0.01)
X0(406) = 0.01;
X0(409) = 0.01;
k(149) = 0.01;
k(150) = 0.01;
k(151) = 0.01;
k(152) = 0.01;
k(153) = 0.01;

% Create initial output array of zeros containing as many entries as
% dependent variables.
dx = zeros(404,1);
% Systems equations consist of flux equations for the reactions increasing
% the species concentration minus the flux equations for reactions
% decreasing the species concentration. Each dependent variable receives a
% systems equation.
% RATE EQUATIONS
dx(1) = 0.01 * (X(142) + X(146));
dx(2) = 0.01 * Xind(26);
dx(3) = 0.01 * Xind(1);
dx(4) = 0.01 * Xind(1);
dx(5) = 0.01 * (Xind(1) + X(145));
dx(6) = 0.01 * Xind(1);
dx(7) = 0.01 * X(144);

```

```

dx(8) = 0.01 * X(150);
dx(9) = 0.01 * X(151);
dx(10) = 0.01 * X(155);
dx(11) = 0.01 * X(152);
dx(12) = 0.01 * X(153);
dx(13) = 0.01 * X(153);
dx(14) = 0.01 * -X(163);
dx(15) = 0.01 * -Xind(64);
dx(16) = 0.01 * Xind(1);
dx(17) = 0.01 * Xind(1);
dx(18) = 0.01 * Xind(1);
dx(19) = 0.01 * Xind(1);
dx(20) = 0.01 * X(164);
dx(21) = 0.01 * (X(179) + X(180));
dx(22) = 0.01 * (X(166) + X(167));
dx(23) = 0.01 * (X(140) + X(141));
dx(24) = 0.01 * Xind(42);
dx(25) = 0.01 * Xind(42);
dx(26) = 0.01 * Xind(42);
dx(27) = 0.01 * (X(161) + X(175) + X(162) + X(229) + Xind(84) + X(221) + X(191) +
X(212));
dx(28) = 0.01 * (X(175) + X(161) + X(162) + X(177) + Xind(23) + X(229) + X(332));
dx(29) = 0.01 * X(228);
dx(30) = 0.01 * X(193);
dx(31) = 0.01 * (X(162) + X(161) + X(175) + X(258) + X(200) + X(211) + X(230) + X(293)
+ X(294) + X(321) - X(264));
dx(32) = 0.01 * X(187);
dx(33) = 0.01 * X(178);
dx(34) = 0.01 * X(180);
dx(35) = 0.01 * X(168);
dx(36) = 0.01 * X(196);
dx(37) = 0.01 * X(322);
dx(38) = 0.01 * (X(187) + X(199));
dx(39) = 0.01 * Xind(27);
dx(40) = 0.01 * X(139);
dx(41) = 0.01 * X(202);
dx(42) = 0.01 * X(194);
dx(43) = 0.01 * X(205);
dx(44) = 0.01 * Xind(42);
dx(45) = 0.01 * (X(211) + X(206) + X(177) + X(357) + X(274) + X(275) + X(322) + X(333)
- X(256));
dx(46) = 0.01 * X(145);
dx(47) = 0.01 * (X(261) + Xind(83) - X(215));
dx(48) = 0.01 * X(217);
dx(49) = 0.01 * X(212);
dx(50) = 0.01 * (X(250) + X(387));
dx(51) = 0.01 * X(186);
dx(52) = 0.01 * (Xind(75) - X(207));
dx(53) = 0.01 * (X(225) - X(297));
dx(54) = 0.01 * X(187);
dx(55) = 0.01 * -X(265);
dx(56) = 0.01 * X(296);
dx(57) = 0.01 * X(190);
dx(58) = 0.01 * (X(190) + X(191) + X(215));

```

```

dx(59) = 0.01 * (Xind(83) + Xind(92) - Xind(84) + Xind(22));
dx(60) = 0.01 * -X(363);
dx(61) = 0.01 * (X(186) + X(219));
dx(62) = 0.01 * (X(235) + X(249) + Xind(88) - Xind(89));
dx(63) = 0.01 * X(187);
dx(64) = 0.01 * Xind(56);
dx(65) = 0.01 * X(238);
dx(66) = 0.01 * X(186);
dx(67) = 0.01 * (X(249) + X(186) + X(231));
dx(68) = 0.01 * Xind(1);
dx(69) = 0.01 * -X(216);
dx(70) = 0.01 * (X(234) + X(327) - X(363));
dx(71) = 0.01 * (X(250) - X(363));
dx(72) = 0.01 * (X(248) + X(258) + X(200) + X(293) + X(294) + X(297) + Xind(100));
dx(73) = 0.01 * -X(68);
dx(74) = 0.01 * X(190);
dx(75) = 0.01 * X(186);
dx(76) = 0.01 * X(253);
dx(77) = 0.01 * X(253);
dx(78) = 0.01 * X(262);
dx(79) = 0.01 * X(265);
dx(80) = 0.01 * (X(286) - X(291) - X(292));
dx(81) = 0.01 * (Xind(112) + Xind(113));
dx(82) = 0.01 * (X(263) - X(264));
dx(83) = 0.01 * X(190);
dx(84) = 0.01 * X(272);
dx(85) = 0.01 * -Xind(118);
dx(86) = 0.01 * X(277);
dx(87) = 0.01 * (Xind(126) - Xind(123) - Xind(124));
dx(88) = 0.01 * Xind(127);
dx(89) = 0.01 * Xind(128);
dx(90) = 0.01 * Xind(129);
dx(91) = 0.01 * Xind(130);
dx(92) = 0.01 * Xind(131);
dx(93) = 0.01 * Xind(132);
dx(94) = 0.01 * X(202);
dx(95) = 0.01 * X(279);
dx(96) = 0.01 * -Xind(138);
dx(97) = 0.01 * (X(281) + X(282));
dx(98) = 0.01 * (-X(289) - X(290) - X(292));
dx(99) = 0.01 * (-X(289) - X(290) - X(292));
dx(100) = 0.01 * (X(289) + X(290) + X(292));
dx(101) = 0.01 * (X(289) - X(412));
dx(102) = 0.01 * (X(289) + X(290) + X(292) + X(255) + X(194) + X(246) + X(160) +
X(298) + X(254) + X(312) + Xind(82) + Xind(86) + Xind(80) + X(210) + X(306) - X(310)
- X(302) - X(299));
dx(103) = 0.01 * (X(289) + X(290) + X(292));
dx(104) = 0.01 * -Xind(43);
dx(105) = 0.01 * -Xind(43);
dx(106) = 0.01 * (X(386) - X(300));
dx(107) = 0.01 * X(216);
dx(108) = 0.01 * (X(160) + X(298));
dx(109) = 0.01 * (X(309) - X(308));
dx(110) = 0.01 * X(160);

```

```

dx(111) = 0.01 * X(249);
dx(112) = 0.01 * (X(190) + X(235));
dx(113) = 0.01 * (X(235) + X(186) + X(231));
dx(114) = 0.01 * (X(311) - X(328) - X(245) - Xind(24));
dx(115) = 0.01 * X(313);
dx(116) = 0.01 * (X(160) + X(298) + X(312));
dx(117) = 0.01 * (X(309) - X(308));
dx(118) = 0.01 * (X(177) + Xind(95) + Xind(96) + X(331));
dx(119) = 0.01 * X(187);
dx(120) = 0.01 * Xind(83);
dx(121) = 0.01 * (X(185) + X(189) + X(158) + X(200) + X(204) + X(257));
dx(122) = 0.01 * X(323);
dx(123) = 0.01 * X(182);
dx(124) = 0.01 * (X(165) + X(177) + Xind(55) + X(182) + X(297) - X(408)); %OPC
Proliferation
dx(125) = 0.01 * Xind(45);
dx(126) = 0.01 * X(333);
dx(127) = 0.01 * (X(181) + X(304) + X(305) + X(315) + X(316) + X(325) + X(329) +
X(273) - X(198));
dx(128) = 0.01 * (Xind(68) + X(326) + X(309) - Xind(67) - Xind(69));
dx(129) = 0.01 * X(249);
dx(130) = 0.01 * Xind(59);
dx(131) = 0.01 * X(245);
dx(132) = 0.01 * (X(358) + X(241) + X(197));
dx(133) = 0.01 * X(160);
dx(134) = 0.01 * (X(250) + X(234) + X(298) + X(160) + Xind(40) + Xind(82) + X(387) -
Xind(41) - Xind(32));
dx(405) = 0.01 * Xind(1);
dx(409) = 0.01 * Xind(1);

% SYSTEMS EQUATIONS, Currently everything pointing toward OPC
% Differentiation has had it's subtracted statement deleted
dx(135) = k(89) * X(332) - k(98) * X(135) * X(173);
dx(136) = k(90) * X(333) - k(99) * X(136) * X(220);
dx(137) = X(39) * X(201) + k(101) * X(158) + k(103) * X(170) - k(9) * X(137) - k(22) *
X(137);
dx(138) = Xind(1) * k(2) + X(86) * Xind(122) + k(39) * X(144) + k(73) * X(168) - k(8)
* X(138) * X(337) - k(20) * X(138) * X(343);
dx(139) = Xind(1) * k(3);
dx(140) = Xind(1) * k(4);
dx(141) = Xind(1) * k(5);
dx(142) = X(352) * X(353) * k(6) - k(107) * X(142);
dx(143) = X(1) * Xind(4) + k(112) * X(202) - X(143) * X(288) * k(40);
dx(144) = k(8) * X(138) * X(337) - k(39) * X(144);
dx(145) = X(2) * Xind(6) + k(100) * X(167) - k(19) * X(145) * X(342);
dx(146) = X(3) * Xind(7);
dx(147) = X(4) * Xind(8) + k(26) * X(162) - k(15) * X(147) * X(243);
dx(148) = X(5) * Xind(9) + k(38) * X(163) - k(16) * X(148) * X(214);
dx(149) = X(6) * Xind(10) + k(72) * X(164) - k(17) * X(149) * X(285);
dx(150) = X(7) * Xind(11);
dx(151) = X(8) * Xind(12);

```



```

dx(152) = X(9) * X(404) - k(33) * X(152);
dx(153) = X(10) * Xind(14);
dx(154) = X(10) * Xind(14) - k(12) * X(154);
dx(155) = X(11) * X(247) - k(148) * X(155);
dx(156) = X(12) * Xind(16) - k(18) * X(156) * X(338) + k(50) * X(165);
dx(157) = X(13) * Xind(17) + k(30) * X(166) - k(11) * X(157) * X(342);
dx(158) = k(9) * X(137) * X(344) - k(101) * X(158);
dx(159) = X(124) * Xind(18); %OPC Proliferation
dx(160) = k(65) * X(194) + k(64) * X(195) + k(69) * X(251) + k(68) * X(252) + X(14) *
X(177) + k(13) * X(165) + X(15) * X(223) + k(54) * X(213) + k(43) * X(235) + k(62) *
X(234) + k(61) * X(242) + k(36) * X(182) + k(44) * X(227) + k(45) * X(209) - k(41) *
X(204) - k(42) * Xind(55) - k(37) * X(297) - k(35) * X(170) - k(67) * X(240) - k(27) *
X(159) - k(55) * X(216) - k(91) * X(277) - k(63) * X(276) + k(151) * X(408); %OPC
Differentiation
dx(161) = k(14) * X(171) * X(243) - k(108) * X(161);
dx(162) = k(15) * X(147) * X(243) - k(26) * X(162);
dx(163) = k(16) * X(148) * X(214) - k(38) * X(163);
dx(164) = k(17) * X(149) * X(285) + k(17) * X(183) * X(285) - k(72) * X(164);
dx(165) = k(18) * X(156) * X(338) - k(50) * X(165);
dx(166) = k(11) * X(342) * X(157) - k(30) * X(166);
dx(167) = k(19) * X(342) * X(145) - k(100) * X(167);
dx(168) = k(20) * X(138) * X(343) - k(73) * X(168);
dx(169) = k(21) * X(345) * X(346) + k(103) * X(170) - k(102) * X(169);
dx(170) = k(22) * X(169) * X(137) - k(103) * X(170);
dx(171) = X(16) * X(29) + k(34) * X(174) + k(108) * X(161) + k(26) * X(162) + k(47) *
X(175) - k(60) * X(171) * X(365) - k(23) * X(169) * X(339) - k(14) * X(171) * X(243);
dx(172) = X(18) * Xind(31) - k(46) * X(172) * X(288);
dx(173) = X(17) * Xind(30) + k(89) * X(332) - k(98) * X(173) * X(26);
dx(174) = k(23) * X(171) * X(339) - k(34) * X(174);
dx(175) = k(24) * X(243) * X(176) - k(47) * X(175);
dx(176) = X(19) * X(33) + k(47) * X(175) - k(24) * X(243) * X(176);
dx(177) = X(20) * X(285);
dx(178) = X(21) * X(342);
dx(179) = X(22) * Xind(34);
dx(180) = k(25) * Xind(35) * Xind(36);
dx(181) = X(121) * Xind(2);
dx(182) = X(23) * Xind(37);
dx(183) = Xind(38) * X(24) + k(72) * X(164) - k(17) * X(285) * X(183);
dx(184) = k(109) * X(229) + X(25) * Xind(39) - X(55) * X(184) * X(354);
dx(185) = X(26) * X(341) * X(340) - k(28) * X(185);
dx(186) = X(27) * X(396) - k(140) * X(186);
dx(187) = X(28) * X(188) - X(29) * X(187);
dx(188) = X(29) * X(187) - X(28) * X(188);
dx(189) = X(30) * Xind(44);
dx(190) = X(31) * X(397) - k(145) * X(190);
dx(191) = k(31) * X(355) * X(192) - k(110) * X(191);
dx(192) = X(32) * Xind(47) + k(110) * X(191) + k(111) * X(193) - k(31) * X(355) *
X(192) - k(32) * X(192) * X(356);
dx(193) = k(32) * X(192) * X(356) - k(111) * X(193);
dx(194) = X(33) * Xind(49);
dx(195) = X(34) * Xind(50);
dx(196) = X(35) * Xind(51);
dx(197) = X(36) * Xind(52);
dx(198) = X(132) * Xind(3);

```

```

dx(199) = X(37) * Xind(53);
dx(200) = X(38) * Xind(54);
dx(201) = k(1) * Xind(1);
dx(202) = k(40) * X(143) * X(288) - k(112) * X(202);
dx(203) = X(40) * Xind(56);
dx(204) = X(41) * Xind(57);
dx(205) = k(46) * X(172) * X(288) - k(113) * X(205);
dx(206) = k(48) * X(357) * X(222) - k(114) * X(206);
dx(207) = X(42) * Xind(60) + k(115) * X(208) - k(49) * X(207) * X(358);
dx(208) = k(49) * X(207) * X(358) - k(115) * X(208);
dx(209) = X(43) * Xind(61);
dx(210) = X(44) * Xind(62) + k(116) * X(211) - k(51) * X(210) * X(266);
dx(211) = k(51) * X(210) * X(266) - k(116) * X(211);
dx(212) = X(45) * X(398) - k(141) * X(212);
dx(213) = k(52) * X(360) * X(280) - k(117) * X(213);
dx(214) = k(38) * X(163) + X(46) * Xind(65) - k(16) * X(148) * X(214);
dx(215) = k(53) * X(361) * X(362) - k(118) * X(215);
dx(216) = k(56) * X(363) * X(364) - k(119) * X(216);
dx(217) = X(47) * Xind(70);
dx(218) = k(57) * X(219) - X(48) * X(218);
dx(219) = X(48) * X(218) - k(57) * X(219);
dx(220) = k(90) * X(333) - k(99) * X(220) * X(136);
dx(221) = X(49) * X(399) - k(142) * X(221);
dx(222) = X(50) * Xind(72) + k(114) * X(206) - k(48) * X(222) * X(357);
dx(223) = k(58) * Xind(21);
dx(224) = X(51) * X(221);
dx(225) = X(52) * Xind(74);
dx(226) = X(53) * Xind(76) - X(66) * X(226);
dx(227) = X(54) * Xind(77);
dx(228) = k(59) * X(349) * X(350) - k(105) * X(228);
dx(229) = X(55) * X(184) * X(354) + X(55) * X(301) * X(354) - k(109) * X(229);
dx(230) = k(60) * X(171) * X(365) - k(120) * X(230);
dx(231) = X(57) * X(401) - k(144) * X(231);
dx(232) = X(58) * Xind(83);
dx(233) = X(59) * X(363);
dx(234) = X(60) * Xind(85);
dx(235) = X(61) * X(402) - k(143) * X(235);
dx(236) = X(62) * Xind(87);
dx(237) = X(64) * X(238) - X(63) * X(237);
dx(238) = X(63) * X(237) - X(64) * X(238);
dx(239) = X(65) * X(240) - X(79) * X(239);
dx(240) = X(79) * X(239) + k(124) * X(264) - X(65) * X(240) - X(84) * X(240) * X(370);
dx(241) = X(66) * X(226);
dx(242) = X(67) * Xind(90);
dx(243) = X(68) * Xind(91) + k(121) * X(257) + k(108) * X(161) + k(26) * X(162) +
k(47) * X(175) - k(24) * X(243) * X(176) - k(14) * X(243) * X(171) - k(15) * X(243) *
X(147) - k(74) * X(243) * X(359) * X(366);
dx(244) = X(69) * Xind(92);
dx(245) = X(70) * Xind(93);
dx(246) = X(71) * Xind(94);
dx(247) = k(148) * X(155) - X(11) * X(247);
dx(248) = k(70) * X(367) * X(368) - k(122) * X(248);
dx(249) = X(72) * X(400) - k(146) * X(249);
dx(250) = X(73) * Xind(101);

```

```

dx(251) = X(74) * Xind(102);
dx(252) = k(71) * Xind(103);
dx(253) = X(75) * Xind(104);
dx(254) = X(76) * Xind(105);
dx(255) = X(77) * Xind(106);
dx(256) = X(78) * Xind(107);
dx(257) = k(74) * X(366) * X(359) * X(243) - k(121) * X(257);
dx(258) = k(75) * X(351) * X(259) - k(106) * X(258);
dx(259) = X(80) * Xind(111) + k(106) * X(258) - k(75) * X(259) * X(351);
dx(260) = k(123) * X(261) + X(81) * X(259) - k(76) * X(260) * X(369);
dx(261) = k(76) * X(260) * X(369) - k(123) * X(261);
dx(262) = X(82) * Xind(115);
dx(263) = X(83) * Xind(116);
dx(264) = X(84) * X(240) * X(370) - k(124) * X(264);
dx(265) = X(85) * X(371) * X(372) - k(125) * X(265);
dx(266) = k(116) * X(211) - k(51) * X(266) * X(210);
dx(267) = X(87) * Xind(125) - X(88) * X(267);
dx(268) = X(88) * X(267) - X(89) * X(268);
dx(269) = X(89) * X(268) - X(90) * X(269);
dx(270) = X(90) * X(269) - X(91) * X(270);
dx(271) = X(91) * X(270) - X(93) * X(271) - X(92) * X(271);
dx(272) = X(92) * X(271);
dx(273) = X(93) * X(271);
dx(274) = k(78) * X(374) * X(283) - k(126) * X(274);
dx(275) = k(77) * X(374) * X(284) - k(127) * X(275);
dx(276) = X(94) * Xind(135);
dx(277) = X(95) * Xind(134);
dx(278) = X(95) * Xind(134) - k(10) * X(278);
dx(279) = X(96) * X(375) * X(376) - k(128) * X(279);
dx(280) = X(97) * Xind(79) + k(117) * X(213) - k(52) * X(280) * X(360);
dx(281) = k(80) * Xind(78) * Xind(133);
dx(282) = k(81) * Xind(28) * Xind(133);
dx(283) = X(98) * Xind(120) + k(126) * X(274) - k(78) * X(283) * X(374);
dx(284) = X(99) * Xind(15) + k(127) * X(275) - k(77) * X(284) * X(374);
dx(285) = X(100) * Xind(19) + k(72) * X(164) - k(17) * X(285) * X(185) - k(17) *
X(285) * X(149);
dx(286) = X(101) * Xind(13);
dx(287) = X(102) * Xind(99) - X(118) * X(287);
dx(288) = X(103) * Xind(71) + k(112) * X(202) + k(113) * X(205) - k(40) * X(288) *
X(143) - k(46) * X(288) * X(172);
dx(289) = X(104) * X(377) * X(381) - k(129) * X(289);
dx(290) = X(105) * X(378) * X(381) - k(130) * X(290);
dx(291) = k(83) * X(381) * X(379) - k(131) * X(291);
dx(292) = k(82) * X(381) * X(380) - k(132) * X(292);
dx(293) = k(85) * X(382) * X(383) - k(133) * X(293);
dx(294) = k(86) * X(383) * X(295);
dx(295) = X(125) * Xind(63);
dx(296) = k(88) * Xind(136) * Xind(137);
dx(297) = X(56) * Xind(121);
dx(298) = k(7) * X(246);
dx(299) = k(29) * X(384) * X(385) * X(387) - k(135) * X(300);
dx(300) = k(84) * X(384) * X(385) * X(386) - k(134) * X(299);
dx(301) = X(106) * Xind(119) + k(109) * X(229) - X(55) * X(301) * X(354);
dx(302) = X(107) * Xind(117);

```

```

dx(303) = X(108) * Xind(114) - 0.5 * X(109) * X(303);
dx(304) = X(109) * X(303);
dx(305) = X(110) * Xind(110);
dx(306) = X(111) * Xind(109);
dx(307) = X(112) * X(388);
dx(308) = k(92) * X(388) * X(389) - k(136) * X(308);
dx(309) = X(113) * X(389);
dx(310) = X(114) * X(390) * X(391) - k(137) * X(310);
dx(311) = k(93) * Xind(108);
dx(312) = X(115) * Xind(98);
dx(313) = k(95) * X(392) * X(393) - k(138) * X(313);
dx(314) = X(116) * Xind(97) - 0.5 * X(117) * X(314);
dx(315) = X(117) * X(314);
dx(316) = k(96) * X(330);
dx(317) = X(131) * Xind(58) + k(139) * X(328) - k(79) * X(394) * X(317);
dx(318) = k(97) * X(320) * X(327) - k(66) * X(318);
dx(319) = X(118) * X(287) - 0.5 * X(128) * X(319);
dx(320) = X(120) * Xind(81) + k(66) * X(318) - k(97) * X(320) * X(327);
dx(321) = X(122) * X(403) - k(147) * X(321);
dx(322) = X(123) * X(347) * X(348) - k(104) * X(322);
dx(323) = k(94) * X(395) * X(324) - k(87) * X(323);
dx(324) = X(126) * Xind(73) + k(87) * X(323) - k(94) * X(395) * X(324);
dx(325) = X(128) * X(319);
dx(326) = X(129) * Xind(66);
dx(327) = X(130) * Xind(20) + k(66) * X(318) - k(97) * X(320) * X(327);
dx(328) = k(79) * X(394) * X(317) - k(139) * X(328);
dx(329) = X(133) * Xind(48);
dx(330) = X(134) * Xind(46) - 0.5 * k(96) * X(330);
dx(331) = X(135) * Xind(67);
dx(332) = k(98) * X(173) * X(135) - k(89) * X(332);
dx(333) = k(99) * X(136) * X(220) - k(90) * X(333);
dx(334) = X(127) * Xind(25);
dx(335) = k(12) * X(154);
dx(336) = k(10) * X(278);
dx(337) = k(39) * X(144) - k(8) * X(337) * X(138);
dx(338) = k(50) * X(165) - k(18) * X(338) * X(156);
dx(339) = k(34) * X(174) - k(23) * X(339) * X(171);
dx(340) = k(28) * X(185) - X(26) * X(340) * X(341);
dx(341) = k(28) * X(185) - X(26) * X(340) * X(341);
dx(342) = k(30) * X(166) + k(100) * X(167) - k(11) * X(342) * X(157) - k(19) * X(342)
* X(145) - X(21) * X(342);
dx(343) = k(73) * X(168) - k(20) * X(343) * X(138);
dx(344) = k(101) * X(158) - k(9) * X(344) * X(137);
dx(345) = k(102) * X(169) - k(21) * X(345) * X(346);
dx(346) = k(102) * X(169) - k(21) * X(345) * X(346);
dx(347) = k(104) * X(322) - X(123) * X(347) * X(348);
dx(348) = k(104) * X(322) - X(123) * X(347) * X(348);
dx(349) = k(105) * X(228) - k(59) * X(349) * X(350);
dx(350) = k(105) * X(228) - k(59) * X(349) * X(350);
dx(351) = k(106) * X(258) - k(75) * X(351) * X(259);
dx(352) = k(107) * X(142) - k(6) * X(352) * X(353);
dx(353) = k(107) * X(142) - k(6) * X(352) * X(353);
dx(354) = k(109) * X(229) - X(55) * X(184) * X(354) - X(55) * X(301) * X(354);
dx(355) = k(110) * X(191) - k(31) * X(355) * X(192);

```

```

dx(356) = k(111) * X(193) - k(32) * X(192) * X(356);
dx(357) = k(114) * X(206) - k(48) * X(222) * X(357);
dx(358) = k(115) * X(208) - k(49) * X(207) * X(358) - X(51) * X(358);
dx(359) = k(121) * X(257) - k(74) * X(366) * X(359) * X(243);
dx(360) = k(117) * X(213) - k(52) * X(360) * X(280);
dx(361) = k(118) * X(215) - k(53) * X(361) * X(362);
dx(362) = k(118) * X(215) - k(53) * X(361) * X(362);
dx(363) = k(119) * X(216) - k(56) * X(363) * X(364) - k(56) * Xind(22) * X(363) +
k(56) * Xind(84) * X(363);
dx(364) = k(119) * X(216) - k(56) * X(363) * X(364);
dx(365) = k(120) * X(230) - k(60) * X(171) * X(365);
dx(366) = k(121) * X(257) - k(74) * X(366) * X(359) * X(243);
dx(367) = k(122) * X(248) - k(70) * X(367) * X(368);
dx(368) = k(122) * X(248) - k(70) * X(367) * X(368);
dx(369) = k(123) * X(261) - k(76) * X(260) * X(369);
dx(370) = k(124) * X(264) - X(84) * X(240) * X(370);
dx(371) = k(125) * X(265) - X(85) * X(372) * X(371);
dx(372) = k(125) * X(265) - X(85) * X(372) * X(371);
dx(373) = 0;
dx(374) = k(126) * X(274) + k(127) * X(275) - k(77) * X(374) * X(284) - k(78) * X(374)
* X(283);
dx(375) = k(128) * X(279) - X(96) * X(375) * X(376);
dx(376) = k(128) * X(279) - X(96) * X(375) * X(376);
dx(377) = k(129) * X(289) - X(104) * X(381) * X(377);
dx(378) = k(130) * X(290) - X(105) * X(378) * X(381);
dx(379) = k(131) * X(291) - k(83) * X(379) * X(381);
dx(380) = k(132) * X(292) - k(82) * X(380) * X(381);
dx(381) = k(129) * X(289) + k(130) * X(290) + k(131) * X(291) + k(132) * X(292) -
X(104) * X(381) * X(377) - X(105) * X(378) * X(381) - k(83) * X(379) * X(381) - k(82)
* X(380) * X(381);
dx(382) = k(133) * X(293) - k(85) * X(382) * X(383);
dx(383) = k(133) * X(293) - k(85) * X(382) * X(383);
dx(384) = k(134) * X(300) + k(135) * X(299) - k(84) * X(385) * X(384) * X(386) - k(29)
* X(384) * X(387) * X(385);
dx(385) = k(134) * X(300) + k(135) * X(299) - k(84) * X(385) * X(384) * X(386) - k(29)
* X(384) * X(387) * X(385);
dx(386) = k(134) * X(300) - k(84) * X(385) * X(384) * X(386);
dx(387) = k(135) * X(299) - k(29) * X(384) * X(387) * X(385);
dx(388) = k(136) * X(308) - k(92) * X(389) * X(388) - X(112) * X(388);
dx(389) = k(136) * X(308) - k(92) * X(389) * X(388) - X(113) * X(389);
dx(390) = k(137) * X(310) - X(114) * X(390) * X(391);
dx(391) = k(137) * X(310) - X(114) * X(390) * X(391);
dx(392) = k(138) * X(313) - k(95) * X(392) * X(393);
dx(393) = k(138) * X(313) - k(95) * X(392) * X(393);
dx(394) = k(139) * X(328) - k(79) * X(394) * X(317);
dx(395) = k(87) * X(323) - k(94) * X(395) * X(324);
dx(396) = k(140) * X(186) - X(27) * X(396);
dx(397) = k(145) * X(190) - X(31) * X(397);
dx(398) = k(141) * X(212) - X(45) * X(398);
dx(399) = k(142) * X(221) - X(49) * X(399);
dx(400) = k(146) * X(249) - X(72) * X(400);
dx(401) = k(144) * X(231) - X(57) * X(401);
dx(402) = k(143) * X(235) - X(61) * X(402);
dx(403) = k(147) * X(321) - X(122) * X(403);

```

```

dx(404) = k(33) * X(152) - X(9) * X(404);
dx(406) = X(405) * Xind(139) + k(150) * X(408) - k(149) * X(406) * X(407);
dx(407) = k(150) * X(408) - k(149) * X(406) * X(407);
dx(408) = k(149) * X(407) * X(406) - k(150) * X(408);
dx(410) = Xind(140) * X(409) + k(153) * X(412) - k(152) * X(410) * X(411);
dx(411) = k(153) * X(412) - k(152) * X(410) * X(411);
dx(412) = k(152) * X(410) * X(411) - k(153) * X(412);
end

```

Run Document

```

options = odeset('NonNegative',1:412);
% options = odeset('JPattern',S,'Vectorized','on');
disp('in run')
[t,X] = ode15s(@RemyelinationBackupHalfTreat_eq, tspan, X0, options);
plot(t,X)

```

Analysis Document

```

% Make the species concentrations or rate constants you wish to change
% global variables.

```

```

global B C D E F G I K W Z Y A1 A2

```

```

B = 0; % Glatiramer Acetate
C = 0; % Benztropine
D = 0; % Simvastatin
E = 0; % Lovastatin
F = 0; % Clobetasol
G = 0; % Halcinonide
I = 0; % Experimental Treatment
K = 0; % rHIgM22
W = 0; % GNbAC1
Y = 0; % FTY720
Z = 0; % Indometacin
A1 = 0; % LiCl
A2 = 0; % BIIB033

```

```

RemyelinationBackupHealthy_run
dataHealthy = X;

```

```

RemyelinationBackupDisease_run
dataDisease = X;

```

```

RemyelinationBackupHalfTreat_run
dataTreatment = X;

```

```
RemyelinationBackupHalfTreatDose2_run
dataHalfTreatDose2 = X;
```

```
% RemyelinationCombinedHalfTreat_run
% dataCombinedPart = X;
```

```
B = 0;
C = 0;
D = 0;
E = 0;
F = 0;
G = 0.01;
I = 0;
K = 0;
W = 0;
Y = 0;
Z = 0;
A1 = 0;
A2 = 0;
```

```
RemyelinationBackupDisease_run
dataFullTreat = X;
```

```
B = 0;
C = 0;
D = 0;
E = 0;
F = 0;
G = 0.1;
I = 0;
K = 0;
W = 0;
Y = 0;
Z = 0;
A1 = 0;
A2 = 0;
```

```
RemyelinationBackupDisease_run
dataDose2 = X;
```

```
% B = 0.1;
% C = 0;
% D = 0;
% E = 0;
% F = 0;
% G = 0;
% I = 0;
% K = 0.1;
```

```

% W = 0;
% Y = 0;
% Z = 0;
% A1 = 0;
% A2 = 0;
%
% RemyelinationBackupDisease_run
% dataCombined = X;

difference = dataDisease - dataHealthy;
differencePartTreat = dataTreatment - dataHealthy;
differenceFullTreat = dataFullTreat - dataHealthy;
differenceDose2 = dataDose2 - dataHealthy;
differenceHalfDose2 = dataHalfTreatDose2 - dataHealthy;
% differenceCombined = dataCombined - dataHealthy;
% differenceCombinedPart = dataCombinedPart - dataHealthy;

RemyelinationBackup_plots2

species = {'X1','X2','X3','X4','X5','X6','X7','X8','X9','X10','X11',...
          'X12','X13','X14','X15','X16','X17','X18','X19','X20','X21',...
          'X22','X23','X24','X25','X26','X27','X28','X29','X30',...
          'X31','X32','X33','X34','X35','X36','X37','X38','X39',...
          'X40','X41','X42','X43','X44','X45','X46','X47','X48',...
          'X49','X50','X51','X52','X53','X54','X55','X56','X57',...
          'X58','X59','X60','X61','X62','X63','X64','X65','X66',...
          'X67','X68','X69','X70','X71','X72','X73','X74','X75',...
          'X76','X77','X78','X79','X80','X81','X82','X83','X84',...
          'X85','X86','X87','X88','X89','X90','X91','X92','X93',...
          'X94','X95','X96','X97','X98','X99','X100','X101','X102',...
          'X103','X104','X105','X106','X107','X108','X109','X110',...
          'X111','X112','X113','X114','X115','X116','X117','X118',...
          'X119','X120','X121','X122','X123','X124','X125','X126',...
          'X127','X128','X129','X130','X131','X132','X133','X134',...
          'X135','X136','X137','X138','X139','X140','X141','X142',...
          'X143','X144','X145','X146','X147','X148','X149','X150',...
          'X151','X152','X153','X154','X155','X156','X157','X158',...
          'X159','X160','X161','X162','X163','X164','X165','X166',...
          'X167','X168','X169','X170','X171','X172','X173','X174',...
          'X175','X176','X177','X178','X179','X180','X181','X182',...
          'X183','X184','X185','X186','X187','X188','X189','X190',...
          'X191','X192','X193','X194','X195','X196','X197','X198',...
          'X199','X200','X201','X202','X203','X204','X205','X206',...
          'X207','X208','X209','X210','X211','X212','X213','X214',...
          'X215','X216','X217','X218','X219','X220','X221','X222',...
          'X223','X224','X225','X226','X227','X228','X229','X230',...

```



```

'X231', 'X232', 'X233', 'X234', 'X235', 'X236', 'X237', 'X238', ...
'X239', 'X240', 'X241', 'X242', 'X243', 'X244', 'X245', 'X246', ...
'X247', 'X248', 'X249', 'X250', 'X251', 'X252', 'X253', 'X254', ...
'X255', 'X256', 'X257', 'X258', 'X259', 'X260', 'X261', 'X262', ...
'X263', 'X264', 'X265', 'X266', 'X267', 'X268', 'X269', 'X270', ...
'X271', 'X272', 'X273', 'X274', 'X275', 'X276', 'X277', 'X278', ...
'X279', 'X280', 'X281', 'X282', 'X283', 'X284', 'X285', 'X286', ...
'X287', 'X288', 'X289', 'X290', 'X291', 'X292', 'X293', 'X294', ...
'X295', 'X296', 'X297', 'X298', 'X299', 'X300', 'X301', 'X302', ...
'X303', 'X304', 'X305', 'X306', 'X307', 'X308', 'X309', 'X310', ...
'X311', 'X312', 'X313', 'X314', 'X315', 'X316', 'X317', 'X318', ...
'X319', 'X320', 'X321', 'X322', 'X323', 'X324', 'X325', 'X326', ...
'X327', 'X328', 'X329', 'X330', 'X331', 'X332', 'X333', 'X334', ...
'X335', 'X336', 'X337', 'X338', 'X339', 'X340', 'X341', 'X342', ...
'X343', 'X344', 'X345', 'X346', 'X347', 'X348', 'X349', 'X350', ...
'X351', 'X352', 'X353', 'X354', 'X355', 'X356', 'X357', 'X358', ...
'X359', 'X360', 'X361', 'X362', 'X363', 'X364', 'X365', 'X366', ...
'X367', 'X368', 'X369', 'X370', 'X371', 'X372', 'X373', 'X374', ...
'X375', 'X376', 'X377', 'X378', 'X379', 'X380', 'X381', 'X382', ...
'X383', 'X384', 'X385', 'X386', 'X387', 'X388', 'X389', 'X390', ...
'X391', 'X392', 'X393', 'X394', 'X395', 'X396', 'X397', 'X398', ...
'X399', 'X400', 'X401', 'X402', 'X403', 'X404',
'X405', 'X406', 'X407', 'X408', 'X409', 'X410', 'X411', 'X412'};

cellDiff = cell(412,1);

% Add the values of the difference, one at a time, into the cell.
for i = 1:412
    cellDiff(i) = {difference(:,i)};
end

% Create tables with the maximum and minimum values of each species. Change
% the variable name of the cell (in this case cellDiff) and array length
% (in this case 18) to fit your model.
maxDiff = sortrows(stack(varfun(@max, struct2table(cell2struct(cellDiff, ...
    species,1))),1:412, 'NewDataVariableName', 'Relative_Value', ...
    'IndexVariableName', 'Variable'),2, 'descend');
minDiff = sortrows(stack(varfun(@min, struct2table(cell2struct(cellDiff, ...
    species,1))),1:412, 'NewDataVariableName', 'Relative_Value', ...
    'IndexVariableName', 'Variable'),2);

maxDiff(1:10,:)
minDiff(1:10,:)

```

Example of Plots Document

```

% Create an array the same size as tspan in Example_run.
t = 0:0.01:120;

```

```

figure(2)
% Plot specific columns of the matrix.
plot(tspan,difference(:,325),tspan,differenceFullTreat(:,325),tspan,differencePartTreat(:,325),tspan,differenceDose2(:,325),tspan,differenceHalfDose2(:,325),'LineWidth',2)
% Create a legend in the bottom left corner.
legend('MBP - Baseline','MBP Full Treat - Low Dose', 'MBP Part Way Treat - Low Dose','MBP Full Treat - High Dose','MBP Part Treat - High Dose','Location','SouthWest')
% Label the axes, set font sizes, and title the plot.
xlabel('time', 'FontSize', 8)
ylabel('relative difference', 'FontSize', 8)
set(gca, 'FontSize', 8)
title('BMPR Antagonist - Effect on MBP Expression','FontSize',12)

figure(3)
% Plot specific columns of the matrix.
plot(tspan,difference(:,329),tspan,differenceFullTreat(:,329),tspan,differencePartTreat(:,329),tspan,differenceDose2(:,329),tspan,differenceHalfDose2(:,329),'LineWidth',2)
% Create a legend in the bottom left corner.
legend('CNPase - Baseline','CNPase Full Treat - Low Dose', 'CNPase Part Way Treat - Low Dose','CNPase Full Treat - High Dose','CNPase Part Treat - High Dose','Location','SouthWest')
% Label the axes, set font sizes, and title the plot.
xlabel('time', 'FontSize', 8)
ylabel('relative difference', 'FontSize', 8)
set(gca, 'FontSize', 8)
title('CNPase','FontSize',12)

figure(4)
% Plot specific columns of the matrix.
plot(tspan,difference(:,316),tspan,differenceFullTreat(:,316),tspan,differencePartTreat(:,316),tspan,differenceDose2(:,316),tspan,differenceHalfDose2(:,316),'LineWidth',2)
% Create a legend in the bottom left corner.
legend('PLP - Baseline','PLP Full Treat - Low Dose', 'PLP Part Way Treat - Low Dose','PLP Full Treat - High Dose','PLP Part Treat - High Dose','Location','SouthWest')
% Label the axes, set font sizes, and title the plot.
xlabel('time', 'FontSize', 8)
ylabel('relative difference', 'FontSize', 8)
set(gca, 'FontSize', 8)
title('PLP','FontSize',12)

figure(5)
% Plot specific columns of the matrix.
plot(tspan,difference(:,334),tspan,differenceFullTreat(:,334),tspan,differencePartTreat(:,334),tspan,differenceDose2(:,334),tspan,differenceHalfDose2(:,334),'LineWidth',2)
% Create a legend in the bottom left corner.
legend('Remyelination - Baseline','Remyelination Full Treat - Low Dose', 'Remyelination Part Treat - Low Dose','Remyelination Full Treat - High Dose','Remyelination Part Treat - High Dose','Location','SouthWest')
% Label the axes, set font sizes, and title the plot.
xlabel('time', 'FontSize', 8)
ylabel('relative difference', 'FontSize', 8)
set(gca, 'FontSize', 8)

```

```

title('SMO Receptor Agonist - Effect on Remyelination','FontSize',12)

figure(6)
% Plot specific columns of the matrix.
plot(tspan,difference(:,363),tspan,differenceFullTreat(:,363),tspan,differencePartTreat(:,363),tspan,differenceDose2(:,363),tspan,differenceHalfDose2(:,363),'LineWidth',2)
% Create a legend in the bottom left corner.
legend('Beta Catenin - Baseline','Beta Catenin Full Treat - Low Dose', 'Beta Catenin Part Way Treat - Low Dose','Beta Catenin Full Treat - High Dose','Beta Catenin Part Treat - High Dose','Location','SouthWest')
% Label the axes, set font sizes, and title the plot.
xlabel('time', 'FontSize', 8)
ylabel('relative difference', 'FontSize', 8)
set(gca, 'FontSize', 8)
title('Lithium Effect on Beta Catenin Levels','FontSize',12)

figure(7)
% Plot specific columns of the matrix.
plot(tspan,difference(:,213),tspan,differenceFullTreat(:,213),tspan,differencePartTreat(:,213),tspan,differenceDose2(:,213),tspan,differenceHalfDose2(:,213),'LineWidth',2)
% Create a legend in the bottom left corner.
legend('RXRy Complexes - Baseline','RXRy Complexes Full Treat - Low Dose', 'RXRy Complexes Part Treat - Low Dose','RXRy Complexes Full Treat - High Dose','RXRy Complexes Part Treat - High Dose','Location','SouthWest')
% Label the axes, set font sizes, and title the plot.
xlabel('time', 'FontSize', 8)
ylabel('relative difference', 'FontSize', 8)
set(gca, 'FontSize', 8)
title('RXRy Complex Formation','FontSize',12)

figure(8)
% Plot specific columns of the matrix.
plot(tspan,difference(:,272),tspan,differenceFullTreat(:,272),tspan,differencePartTreat(:,272),tspan,differenceDose2(:,272),tspan,differenceHalfDose2(:,272),'LineWidth',2)
% Create a legend in the bottom left corner.
legend('Gernaylgeranyl PP - Baseline','Gernaylgeranyl PP - Low Dose', 'Gernaylgeranyl PP - Low Dose','Gernaylgeranyl PP - High Dose','Gernaylgeranyl PP - High Dose','Location','SouthWest')
% Label the axes, set font sizes, and title the plot.
xlabel('time', 'FontSize', 8)
ylabel('relative difference', 'FontSize', 8)
set(gca, 'FontSize', 8)
title('Geranylgeranyl Pyrophosphate Formation','FontSize',12)

figure(9)
% Plot specific columns of the matrix.
plot(tspan,difference(:,181),tspan,differenceFullTreat(:,198),tspan,differencePartTreat(:,198),tspan,differenceDose2(:,198),tspan,differenceHalfDose2(:,198),'LineWidth',2)
% Create a legend in the bottom left corner.
legend('OPC Migration - Baseline','OPC Migration Full Treat - Low Dose', 'OPC Migration Part Way Treat - Low Dose','OPC Migration Full Treat - High Dose','OPC Migration Part Treat - High Dose','Location','SouthWest')
% Label the axes, set font sizes, and title the plot.
xlabel('time', 'FontSize', 8)

```

```

ylabel('relative difference', 'FontSize', 8)
set(gca, 'FontSize', 8)
title('Anticholinergic Effects on OPC Migration','FontSize',12)

figure(10)
% Plot specific columns of the matrix.
plot(tspan,difference(:,160),tspan,differenceFullTreat(:,160),tspan,differencePartTreat(:,160),tspan,differenceDose2(:,160),tspan,differenceHalfDose2(:,160),'LineWidth',2)
% Create a legend in the bottom left corner.
legend('OPC Differentiation - Baseline','OPC Differentiation Full Treat - Low Dose','OPC Differentiation Part Way Treat - Low Dose','OPC Differentiation Full Treat - High Dose','OPC Differentiation Part Treat - High Dose','Location','SouthWest')
% Label the axes, set font sizes, and title the plot.
xlabel('time', 'FontSize', 8)
ylabel('relative difference', 'FontSize', 8)
set(gca, 'FontSize', 8)

title('OPC Differentiation','FontSize',12)

figure(11)
% Plot specific columns of the matrix.
plot(tspan,difference(:,198),tspan,differenceFullTreat(:,181),tspan,differencePartTreat(:,181),tspan,differenceDose2(:,181),tspan,differenceHalfDose2(:,181),'LineWidth',2)
% Create a legend in the bottom left corner.
legend('Apoptosis - Baseline','Apoptosis Full Treat - Low Dose','Apoptosis Part Way Treat - Low Dose','Apoptosis Full Treat - High Dose','Apoptosis Part Treat - High Dose','Location','SouthWest')
% Label the axes, set font sizes, and title the plot.
xlabel('time', 'FontSize', 8)
ylabel('relative difference', 'FontSize', 8)
set(gca, 'FontSize', 8)
title('TLR2 Antagonist - Effect on Apoptosis','FontSize',12)

figure(12)
% Plot specific columns of the matrix.
plot(tspan,difference(:,334),tspan,differenceFullTreat(:,334),'LineWidth',2)
% Create a legend in the bottom left corner.
legend('Remyelination - Baseline','Remyelination - High Dose Lithium','Location','SouthWest')
% Label the axes, set font sizes, and title the plot.
xlabel('time', 'FontSize', 8)
ylabel('relative difference', 'FontSize', 8)
set(gca, 'FontSize', 8)
title('High Dose Lithium Effect on Remyelination','FontSize',12)

```

